Chapter 3

Decarboxylative Asymmetric Ni-Catalyzed Cross-Coupling of Benzylic N-Hydroxyphthalimide Esters and Alkenyl Bromides‡

3.1 INTRODUCTION

Nickel catalyzed cross-coupling reactions have emerged as powerful methods to form $C(sp^3)$–$C(sp^2)$ and $C(sp^3)$–$C(sp^3)$ bonds.[1–5] Whereas pioneering investigations focused on the canonical cross-coupling of $C(sp^3)$ electrophiles with organometallic reagents—variants of the venerable Negishi,[6–13] Kumada,[14–18] and Suzuki,[19–23] reactions, among others—additional modes of alkyl cross-coupling using nickel catalysis have recently been disclosed. These include cross-electrophile "reductive" couplings that use an

‡Portions of this chapter have been reproduced from the following communication: Suzuki, N.†; Hofstra, J. L.†; Poremba, K. E.; Reisman, S. E. *Org. Lett.* **2017**, *19*, 2150–2153, DOI: 10.1021/acs.orglett.7b00793, copyright 2017 American Chemical Society. The research presented in this chapter was completed in collaboration with Naoyuki Suzuki (postdoctoral scholar) and Kelsey E. Poremba (graduate student) in the Reisman group.

exogenous, stoichiometric reductant to shuttle electrons to the nickel catalyst,[24–32] as well as cross-coupling reactions that rely on synergistic reactivity between nickel and photoredox co-catalysts.[33–40] Taken together, these reactions enable the cross-coupling of a broad range of C(sp^3) substrates, providing access to a variety of products.

Ni-catalyzed reductive cross-coupling reactions have proven particularly useful for the cross-coupling of secondary alkyl electrophiles, often affording chiral products as racemic mixtures.[24–30,32] Recognizing that the ability to render these transformations enantioselective would enhance their utility,[41,42] our laboratory has recently developed enantioselective Ni-catalyzed reductive cross-coupling reactions of both benzylic chlorides[43–45] and α-chloronitriles.[46] An important objective for further improving the synthetic usefulness of asymmetric reductive cross-coupling reactions is to develop reactions of new electrophile classes. Just as in conventional cross-coupling reactions, where different organometallic reagents (e.g. organozinc, organomagnesium, organoboron reagents, etc.) bring unique advantages to a specific synthetic scenario, the ability to cross-couple new electrophile classes broadens the tool box for strategic C–C bond formation. However, it can be challenging to apply conditions from previously developed reductive cross-coupling reactions to new electrophile classes, especially if there are changes to the mechanism by which the coupling partner undergoes oxidative addition. In particular, it can require tuning of either the ligand structure or the stoichiometric reductant (or both) in order to develop reactions that proceed both in good yield and enantioselectivity.

As part of our efforts to develop asymmetric cross-coupling reactions that employ a variety of C(sp^3) electrophiles, we became interested in the coupling of redox-active *N*-

hydroxyphthalimide (NHP) esters (**124**) which are readily prepared from the corresponding carboxylic acids.[47,48] In 1988, Okada and Oda demonstrated that NHP esters could undergo fragmentation to afford alkyl radicals via a photosensitized electron transfer mechanism (Figure 3.1). Irradiation of an alkyl NHP ester (**124**) with light (>350 nm) in the presence of 1,6-bis(dimethylamino)pyrene (BDMAP, **127**) provided the corresponding alkane (**125**) in good yield (88%). The reaction was proposed to proceed via excitation of BDMAP to the excited singlet state, followed by electron transfer to **124** to afford the NHP ester radical anion (**125**). Protonation of **125**, cleavage of the N–O bond, and extrusion of CO_2 produced alkyl radical **129**, which terminated via H atom abstraction. While an alternative sequence could occur via N–O bond cleavage prior to protonation, both operative mechanisms produce alkyl radical **129**, which could potentially engage in a variety of radical reactions.

Figure 3.1 *Mechanism of NHP ester fragmentation.*

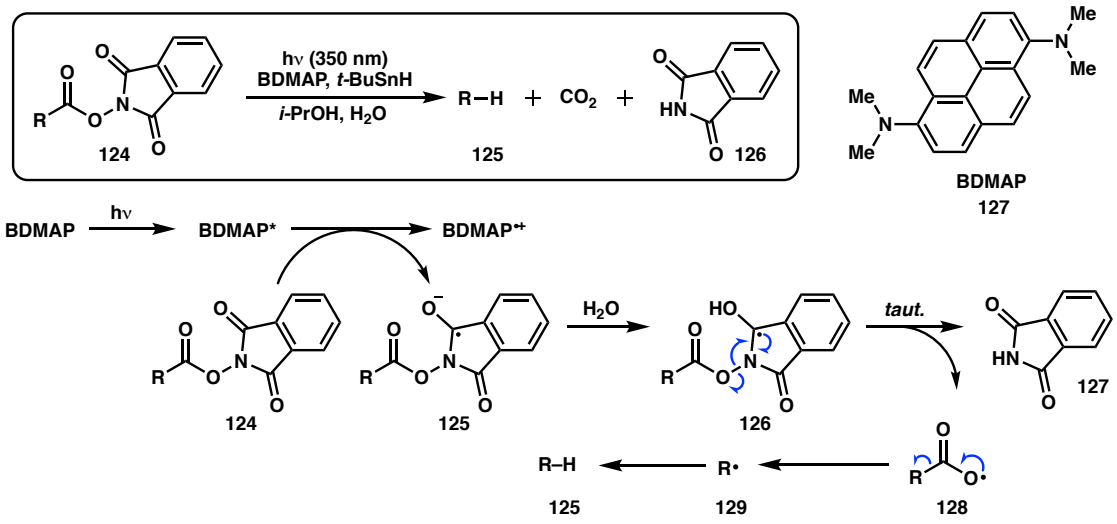

Alkyl radicals generated from NHP esters can be intercepted by metal catalysts and have recently been used in a variety of cross-coupling reactions.[49,50] For example, NHP esters have been demonstrated as C(sp^3) substrates for Ni-catalyzed Negishi,[51–57]

Suzuki,[55,58] and reductive[59–62] cross-coupling reactions to generate racemic products (Scheme 3.1a–c). Furthermore, NHP esters have also been shown to undergo other Ni-catalyzed reactions such as Giese additions,[63] radical additions to sulfinimies,[64] hydroalkylations,[65] and borylations[66]. Despite a breadth of reactivity, NHP esters have not been demonstrated as competent coupling partners in Ni-catalyzed *enantioselective* cross-coupling reactions. We recognized that the use of NHP esters might be advantageous for substrates in which the corresponding alkyl chlorides are unstable or challenging to prepare. Herein, we report the first Ni-catalyzed asymmetric cross-coupling reactions of NHP esters (Scheme 3.1d). These alkenylation reactions proceed under mild conditions using tetrakis(*N*,*N*-dimethylamino)ethylene (TDAE) as a homogenous reductant.

Scheme 3.1 *Selected examples of NHP esters in cross-coupling.*

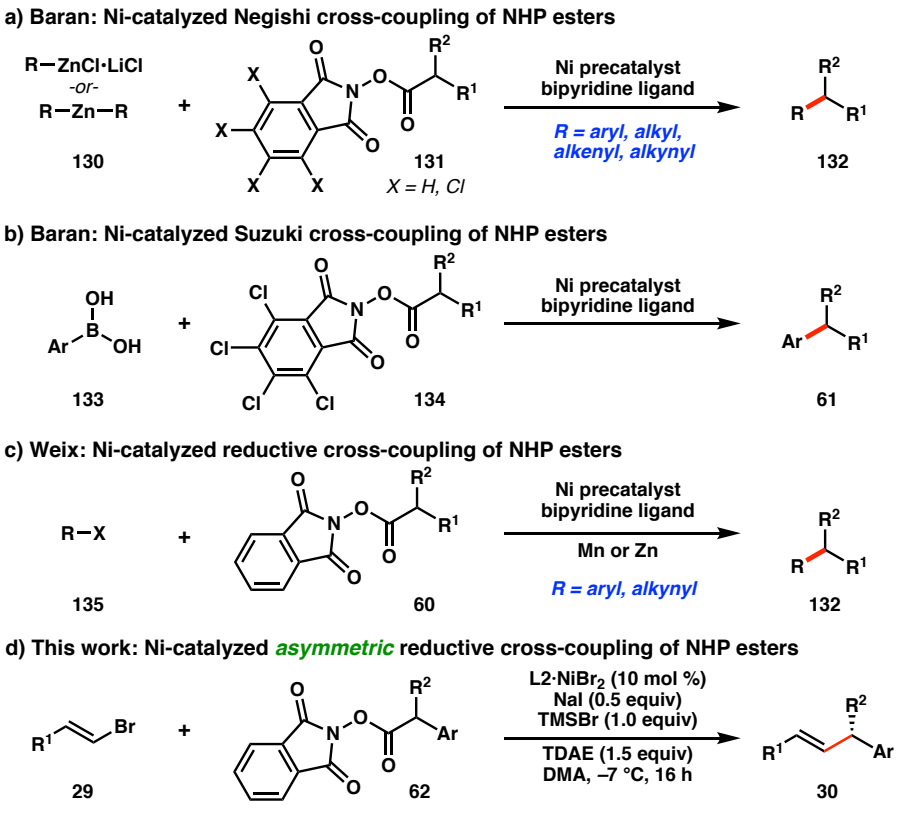

3.2 REACTION OPTIMIZATION

3.2.1 Initial Hit with Additives

Our efforts began with NHP ester **136**, which was prepared in one step from commercially available 2-phenylpropanoic acid. Subjection of NHP ester **136** and alkenyl bromide **86** to our optimal conditions developed for the reductive cross-coupling of alkenyl bromides and benzyl chlorides provided only trace quantities of product (Table 3.1, entry 1).[44] The use of Zn as a reductant did not improve the reaction (entry 2). We were pleased to find, however, that the addition of stoichiometric TMSCl, which has previously been used as a substoichiometric additive in Ni-catalyzed reductive cross-couplings,[46,67–69] provided the desired product **137** in low yield but with good enantioselectivity (90% ee) when Mn was used as the reductant (entries 3). It has been proposed that the role of TMSCl in reductive cross-couplings may activate the surface of the heterogeneous metal reductant, which is typically either Mn powder or Zn dust. The addition of 1,2-dibromoethane (DBE), which is typically used to activate Mg turnings in Grignard reagent formations,

Table 3.1. *Evaluation of reaction additives.*

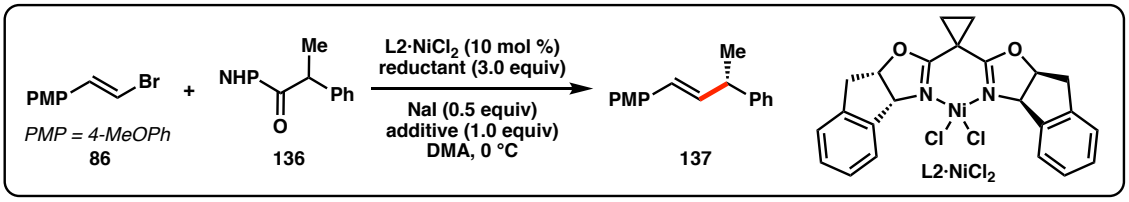

Entry	Reductant	Additive	yield (%)	ee (%)
1	Mn	—	trace	—
2	Zn	—	trace	—
3	Mn	TMSCl	27	90
4	Zn	TMSCl	38	64
5	Zn	DBE	trace	—

failed to provide **137** (entry 5). Given these results, we propose that alternatively, TMSCl may be used to sequester phthalimide anions, which would prevent recombination with Ni in the catalytic cycle if such a process is deleterious to the cross-coupling reaction.[52]

3.2.2 Activating Groups

A variety of other activated esters have previously been studied in decarboxylative cross-couplings.[52] Unfortunately, both the tetrachloro-*N*-hydroxyphthalimide ester (**138a**) and 1-hydroxy-7-azabenzotriazole (HOAt) ester (**138b**) failed to yield any cross-coupling product under the reaction conditions (Figure 3.2). Further optimization of the cross-coupling reaction was investigated with NHP ester **136**.

Figure 3.2 *Evaluation of activating groups.*

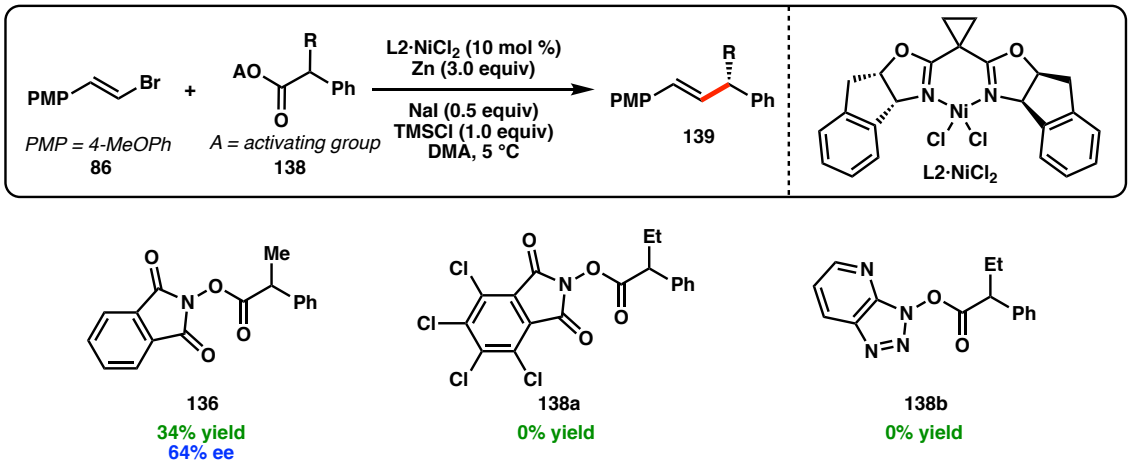

3.2.3 Reductants

While Zn and Mn reductants both showed reactivity to produce **137** when TMSCl was used as an additive, the enantioselectivity was diminished (64% and 90% ee, Table 3.2 entries 1–2) compared to the optimal conditions developed for the cross-coupling of alkenyl bromides and benzylic chlorides (96% ee with **L2**·$NiCl_2$).[44] During our

mechanistic investigations between alkenyl bromides and benzylic chlorides (*see Chapter 4*), we investigated the addition of TMSCl to activate Mn or Zn. While this led to increased reaction rates it also decreased the enantioselectivity of the cross-coupling product.[70] Therefore, we became interested in non-metal reductants to see if the combination of Mn/Zn and TMSCl was deleterious to ee; if so, this could allow us to still employ TDAE as an additive without diminishing enantioselectivity. As our previous reaction between alkenyl bromides and benzylic chlorides could be conducted using the organic reductant TDAE in 23% yield, an investigation of alternative homogenous reductants revealed that TDAE was a competent reductant and delivered **137** in 95% ee.[44,71,72] More notably, the use of TDAE also substantially increased the reactivity, thus providing **137** in 61% yield (entry 3).

Table 3.2. *Evaluation of reductants.*

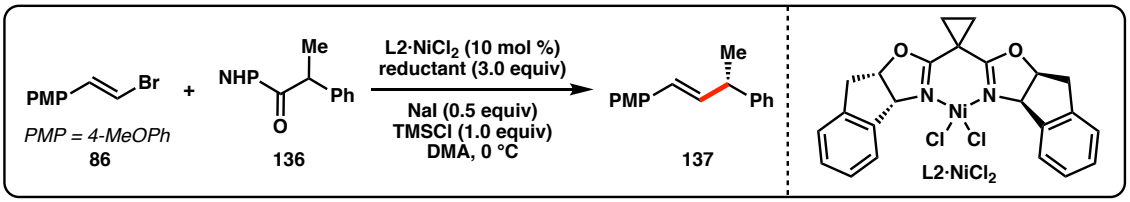

Entry	Reductant	yield (%)	ee (%)
1	Zn	38	64
2	Mn	27	90
3	TDAE	61	95

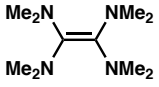

TDAE

3.2.4 Halide Exchange

Monitoring the reaction progress at room temperature determined that (*E*)-1-(2-chlorovinyl)-4-methoxybenzene (**140**) was forming and accumulating under the reaction conditions, presumably through a Ni-catalyzed halide exchange process.[73,74] Since alkenyl

chloride **140** does not readily engage in the cross-coupling reaction, we hypothesized that the yield of **137** could be improved by removing chloride from the reaction and thus preventing formation of this unproductive side product. Indeed, the use of TMSBr instead of TMSCl, and the use of **L2**·$NiBr_2$ as the catalyst, furnished product **137** in 75% yield and 92% ee (Table 3.3, entry 2).

Table 3.3. *Evaluation of halide exchange.*

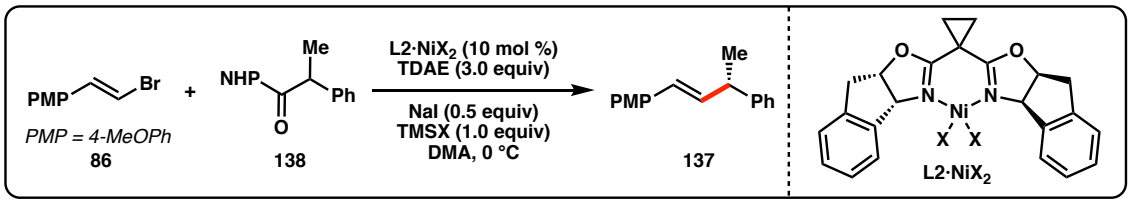

PMP = 4-MeOPh
86 **138** **137**

Entry	X	yield (%)	ee (%)
1	Cl	61	95
2	Br	75	92

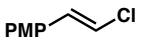

PMP = 4-MeOPh
140

3.2.5 Temperature

The reaction temperature was then evaluated (Table 3.4). By decreasing the reaction temperature to –7 °C, the yield was slightly improved, providing **137** in 79% yield and 93% ee (entry 3). We note that the melting point of TDAE is reported as 0 °C, however,

Table 3.4. *Evaluation of temperature.*

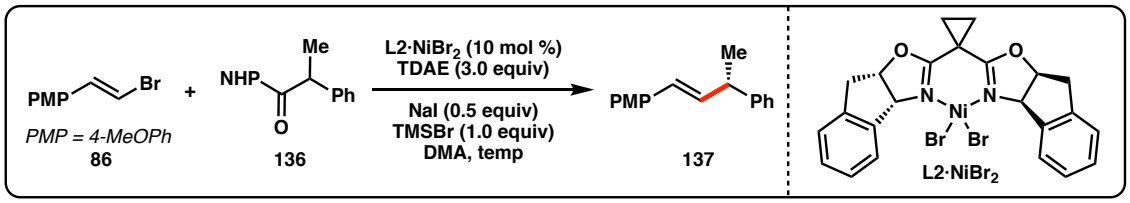

PMP = 4-MeOPh
86 **136** **137**

Entry	Temperature	yield (%)	ee (%)
1	5 °C	58	91
2	0 °C	75	92
3	–7 °C	79	93

the reaction remains homogenous down to a temperature of –7 °C. When the reaction was conducted at temperatures below –7 °C, solidification of TDAE was observed in the reaction mixture.

3.2.6 Reductant Equivalents

The quantity of reductant was then evaluated (Table 3.5). Typically, Mn reductants are used in extreme excess (2.0–3.0 equiv) in asymmetric Ni-catalyzed cross-coupling reactions, possibly due to the heterogenous nature of the reaction where the addition of Mn increases the reaction rate.[43,44,46,69,75] Excess reductant is needed in order to obtain good conversion. In this case, TDAE is a homogenous reductant, and we were pleased to find that lowering the amount to 1.5 equivalents provided **137** in comparable yield and ee (entries 1–2).[72]

Table 3.5. *Evaluation of reductant equivalents.*

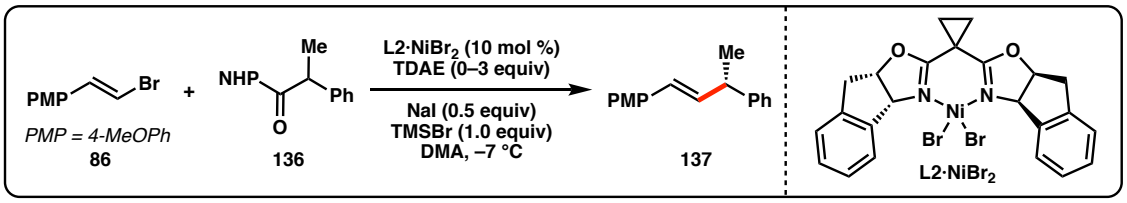

Entry	TDAE (equiv)	yield (%)	ee (%)
1	3.0	79	93
2	1.5	80	96

3.2.7 Solvents

Although *N*,*N'*-dimethylacetamide (DMA) as a solvent showed good levels of reactivity and enantioselectivity under the optimal conditions, other solvents were evaluated (Table 3.6). Weix and coworkers found that compared to Zn reductants, cross-coupling reactions of aryl iodides with benzylic chlorides with TDAE were more generally

robust in a variety of solvents.[72] For this alkenylation reaction, both acetonitrile (MeCN) and propylene carbonate were found to provide cross-coupled product **137** with excellent enantioselectivity, though in moderate yield (entries 2–3). Since the coordination sphere of these solvents are different, given these results we hypothesize that it is unlikely DMA is coordinated to Ni during the enantiodetermining step.

Table 3.6. *Evaluation of solvents.*

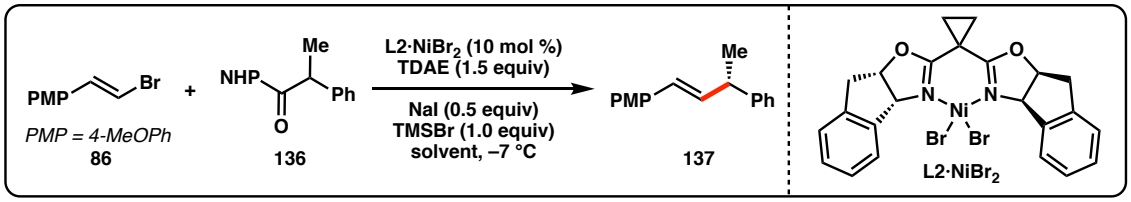

Entry	Solvent	yield (%)	ee (%)
1	DMA	80	96
2	MeCN	30	99
3	propylene carbonate	43	95

3.2.8 Optimization Controls

A variety of control reactions were conducted by running the optimal conditions but omitting various components of the reaction (Table 3.7). Without NaI, the yield of **137** was slightly reduced. In contrast to Ni-catalyzed cross-coupling of alkenyl bromides and benzyl chlorides where NaI additives may play a role in halide exchange and prevent the formation of alkenyl chloride,[44,73,74] the NaI additive in this transformation plays a different, yet unknown role. Without either TDAE or **L2**·$NiBr_2$ catalyst, no product was formed (entries 2–3). Running the reaction but omitting TMSBr confirmed that this additive remains crucial for obtaining high yields of **137** (entry 5).

Table 3.7. *Control reactions.*

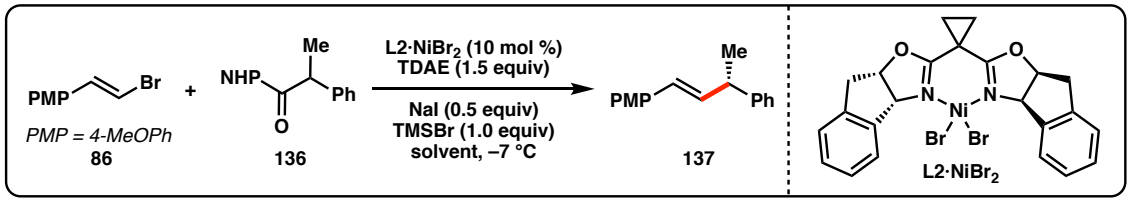

Entry	Deviation	yield (%)	ee (%)
1	—	80	96
2	no NaI	68	95
3	no TDAE	0	—
4	no L2·$NiBr_2$	0	—
5	no TMSBr	19	88

3.3 SUBSTRATE SCOPE

To demonstrate the scope of the reaction, a series of (*E*)-alkenyl bromides was cross-coupled with NHP ester **136**, providing the corresponding products (**140**) in uniformly good yield and high ee (Figure 3.3). The reaction exhibits good tolerance of Lewis basic functional groups: for example, dimethyl anilines (**140b**), nitriles (**140d**), and esters (**140e**, **140i**) could be incorporated into the substrate without detriment to the yield or enantioselectivity. A pyridine-containing alkenyl bromide also performed well, providing **140h** in 67% yield and 95% ee. In addition, alkyl-substituted alkenyl bromides reacted smoothly, providing the corresponding products in good yield and ee (**140i**–**140n**). An alkenyl bromide possessing a free alcohol coupled efficiently, although silylation occurred under the reaction conditions to give silyl ether **140l**. In order to obtain complete conversion for this substrate, 2 equivalents of TMSBr are used in the reaction. The silyl ether can easily be cleaved with a mild acid workup; in this case it was preserved in order

to facilitate purification. It is notable that alkenyl MIDA boronate **140m** and alkenyl silane **140n** could be prepared in 97% ee from commercially available vinyl bromides, which could be used as cross-coupling handles for further derivatization. To demonstrate that this method can be used preparatively, the coupling was conducted on 5.0 mmol scale, which delivered 918 mg (77% yield) of **137** in 91% ee.

Figure 3.3 *Scope of the alkenyl bromide coupling partner.*

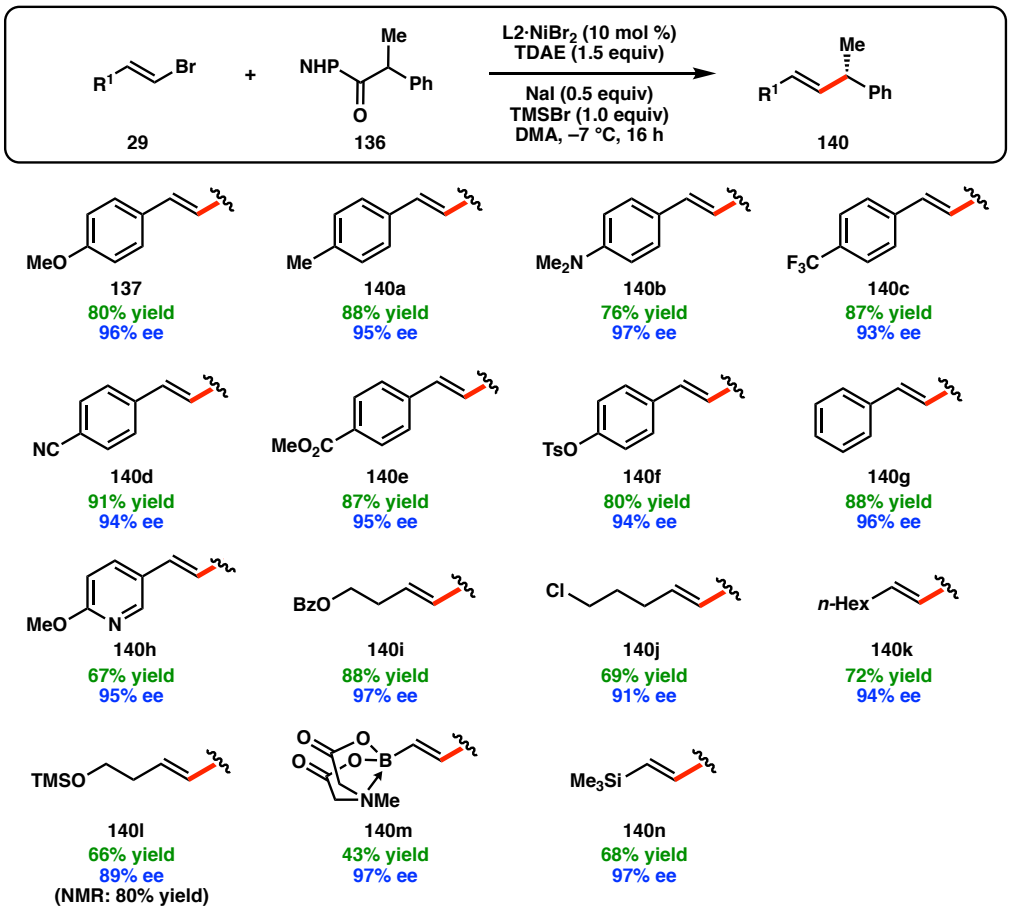

Reactions are conducted on 0.2 mmol scale under N_2. Isolated yields are provided; ee is determined by SFC using a chiral stationary phase. For **140f**, 1.5 equiv NHP ester was used. For **140l**, 2.0 equiv TMSBr was used; the alcohol is silylated under the reaction conditions. NMR yield of **140l** versus an internal standard is provided in parenthesis.

The reaction also exhibits broad scope for the NHP ester coupling partner, delivering good yields and high enantioselectivities for a range of substrates bearing substitution on

the arene or at the benzylic position (Figure 3.4). In certain cases (e.g. **141e–141f**), the NHP esters cross-coupled with improved yield relative to the corresponding benzyl chlorides (under the previously reported conditions).[44] For example, aryl dichloride **141f** could be prepared in 77% yield and 82% ee with the corresponding NHP ester; use of the benzyl chloride electrophile provided **141f** in 21% yield and 75% ee. Moreover, dimethyl aniline **141e** could be prepared in 66% yield and 94% ee; this compound could not be accessed via our previously reported benzylic chloride coupling due challenges in preparing and handling 4-(chloro(phenyl)methyl)-*N*,*N*-dimethylaniline under standard

Figure 3.4 *Scope of the NHP ester coupling partner.*

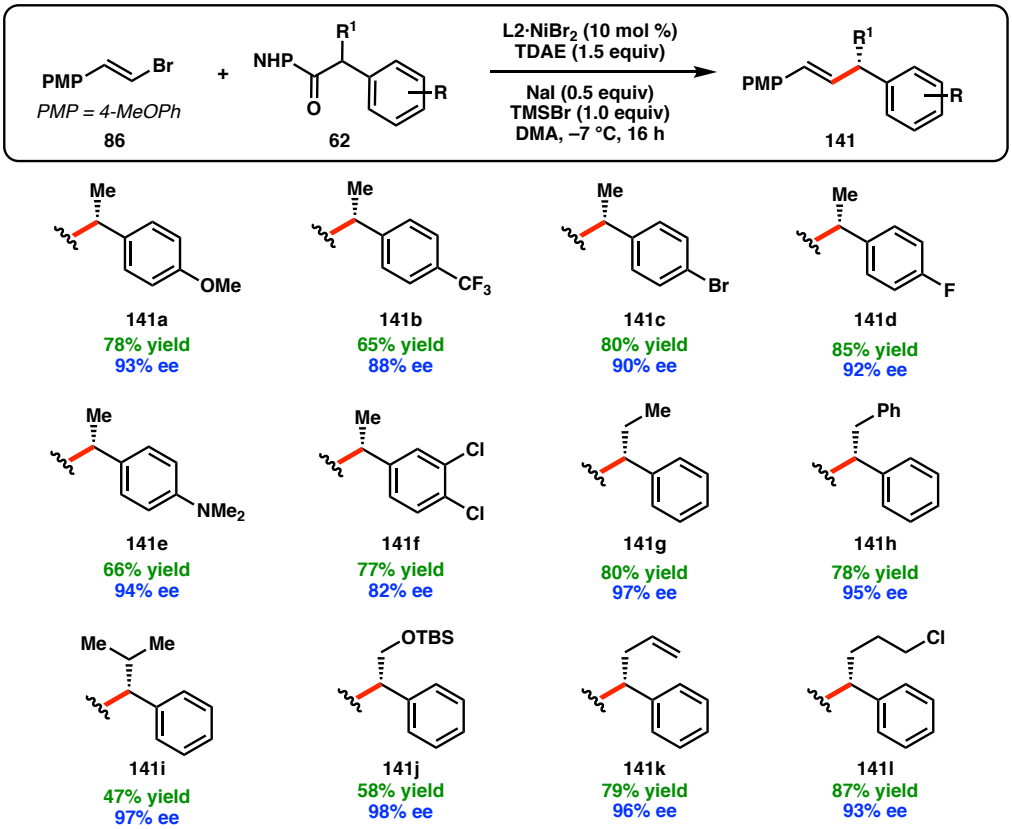

Reactions are conducted on 0.2 mmol scale under N_2. Isolated yields are provided; ee is determined by SFC using a chiral stationary phase.

conditions. Chlorination of the corresponding benzyl alcohol using either $SOCl_2$ or PPh_3/CCl_4 provided the desired benzyl chloride product, however the reaction profile was messy, and purification was ultimately unsuccessful. Higher substitution at the benzylic position was also tolerated (**141g–141l**), although the yield began to decrease with larger groups (e.g. *i*-Pr, **141i**). Notable products include those containing pendant functional groups at the benzylic position including a siloxy group (**141j**), alkene (**141k**), and alkyl chloride (**141l**). Perfect chemoselectivity for cross-coupling of the NHP ester over the primary alkyl chloride is observed.

Nevertheless, a few substrates were evaluated that provided the desired cross-coupling products in moderate to good yield, but with synthetically intractable ee (Figure 3.5). An alkenyl bromide containing an alkenyl fluoride motif provided **142** in 43% yield and 32% ee. Particular benzylic groups on the NHP ester fragment were also found to decrease enantioselectivity. Both trimethoxy **143** an *N*-methyl indole **144** could be prepared in moderate to good yield, however the products were formed in 71% ee and 75% ee, respectively.

Figure 3.5 *Products with poor enantioselectivity.*

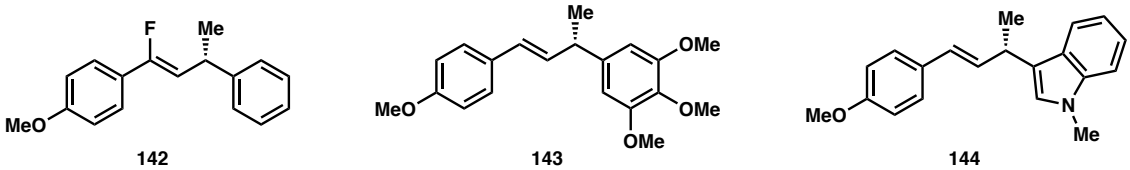

Although the primary focus of this study was the cross-coupling of NHP esters with alkyl substituents at the benzylic position, we also investigated substrates containing heteroatom substitution (Scheme 3.2). Reaction of α-methoxy ester **145** furnished allylic

ether **146** in good yield and ee. This highlights an advantage of the NHP ester for certain C(sp^3) electrophiles, as the corresponding α-chloroether substrate is unstable and difficult to work with.

Scheme 3.2 *Cross-coupling of α-methoxy NHP ester.*

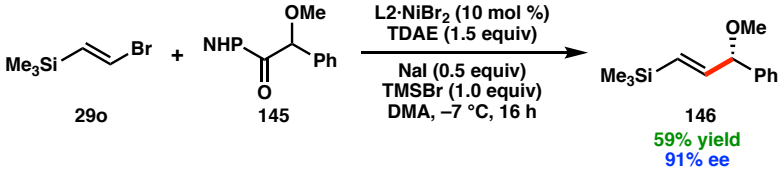

While alkyl benzylic substituents and α-methoxy NHP ester **145** were successful coupling partners, other substrates containing benzylic α-heteroatoms were not tolerated under the reaction conditions (Figure 3.6). For example, NHP esters containing dimethyl amines (**147**) as well as Boc protected amines (**148**, **149**) did not form the desired cross-coupling products. An NHP ester which would provide a tetrasubstituted center also did not form any desired product (**150**). A variety of non-benzylic substrates containing

Figure 3.6 *Unsuccessful chiral products.*

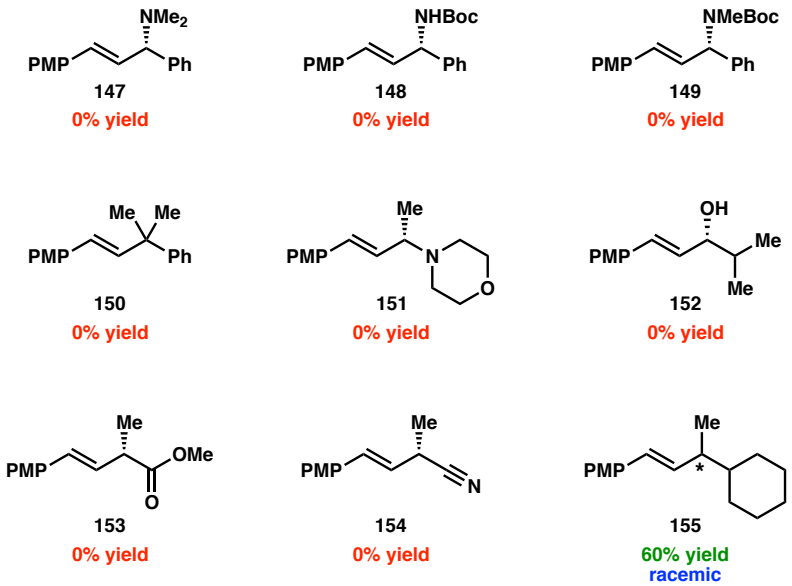

functional groups that could potentially stabilize an α-radical (**151**–**154**) did not form any desired cross-coupling product. However, a simple alkyl NHP ester did react to form the cyclohexyl substituted product **155** in 60% yield, albeit in racemic form.

Further investigations into the Ni-catalyzed cross coupling of cyclohexyl NHP ester **156** were conducted. Since **155** was formed as a racemate, we hypothesized that the cross-coupling reaction was not occurring on Ni, preventing the catalyst from imparting any enantioinduction. Running the reaction in the absence of **L2**·$NiBr_2$ demonstrated that styrenyl bromides successfully reacted to form the desired cross-coupled products (**155** and **157a**), however, alkyl substituted alkenyl bromides failed under these conditions (**157b** and **157d**) (Figure 3.7).

Figure 3.7 *Evaluation of alkenyl bromides in Ni-free cross-coupling.*

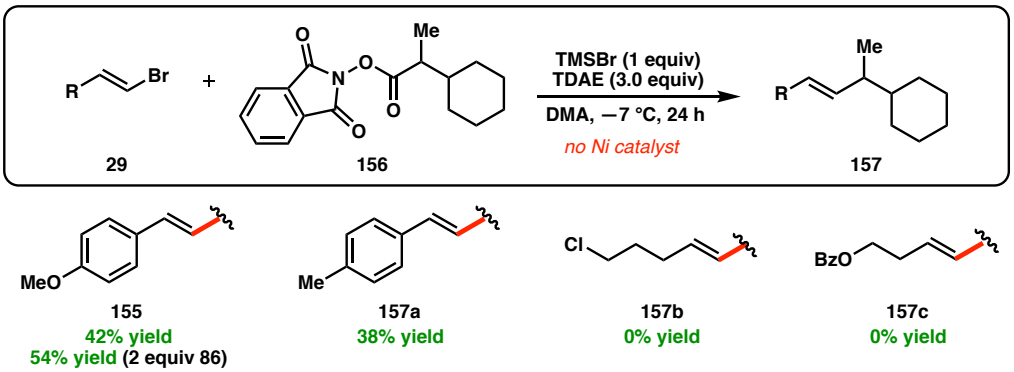

One possible mechanistic explanation for the observed results is depicted in Figure 3.8. Addition of alkyl radical **158** to alkenyl bromide **86** could form stabilized benzylic radical **159** when styrenyl bromides are used in the reaction. In contrast, an unstable alkyl radical would be generated if alkyl substituted alkenyl halides were used in this process. Radical elimination of the bromide could reform the styrene moiety and provide **155** in racemic form. The tuning of the reaction rate and the stability of the alkyl radical may

prove to be important in Ni-catalyzed cross-coupling reactions that proceed through cage escape processes. While additional studies into the reaction mechanism are required, these studies highlight the importance for appropriate substrate selection to avoid inherent background reactivity.

Figure 3.8 *Possible mechanism for Ni-free cross-coupling.*

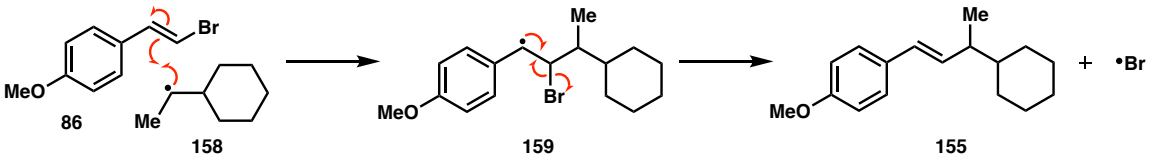

3.4 REACTION MECHANISM

To probe for the intermediacy of a radical species, NHP ester **160** was prepared and subjected to the standard cross-coupling conditions (Table 3.8, 10 mol % **L2**·$NiBr_2$). A 42% combined yield of the coupled products **161a–161c** was obtained. It has been shown that for phenyl substituted cyclopropyl carbonyl radicals, the ring opening is reversible and that the cyclopropane species is favored at lower temperatures (Figure 3.9).[76,77] The fact

Table 3.8. *Evaluation of Ni loading with cyclopropyl ring opening radical clock.*

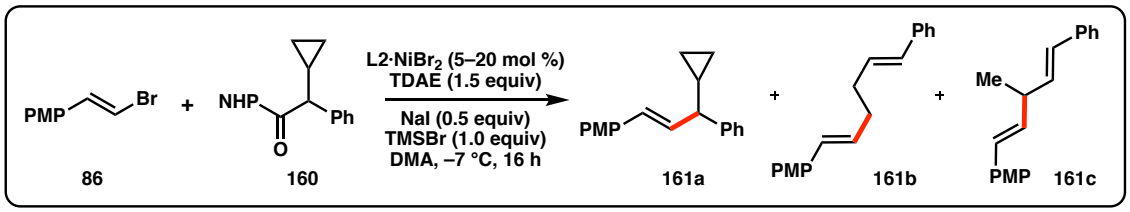

Entry	L2·$NiBr_2$ (mol %)	Total Yield (%)	161a :	161b :	161c
1	5	44	12%	85%	3%
2	10	42	15%	79%	6%
3	20	49	20%	69%	11%

that **161b** predominates, even though it derives from the minor equilibrium species, could indicate that the rate of radical recombination with nickel is sensitive to the steric profile of the radical. When the catalyst loading of **L2**·$NiBr_2$ was varied, the ratio of **161a** to total ring opened product (**161b** + **161c**) was found to increase at higher nickel concentrations (entries 2–3). This Ni-dependent behavior suggests that the mechanism proceeds through a cage-escaped radical, which at higher concentrations of **L2**·$NiBr_2$, can competitively recombine with nickel before undergoing ring scission; a radical-chain mechanism may be in effect.[70]

Figure 3.9 *Rate constants for cyclopropyl carbinyl radicals.*

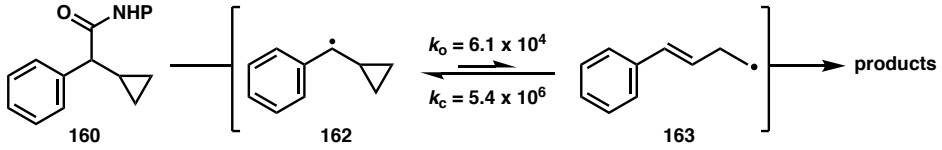

Further studies of the mechanism are ongoing; it is unclear at this time whether the absolute stereochemistry of the cross-coupling product is set during the oxidative addition or reductive elimination steps.[78] We do note, however, that the products are formed in similar ee when using either the NHP esters under the conditions reported here or the benzylic chloride using the conditions reported previously (Figure 3.10).[44] The enantioselectivities of **141** were converted into $\Delta\Delta G^{\ddagger}$ by using the reported er and the reaction temperature. A linear correlation is observed between $\Delta\Delta G^{\ddagger}$ values for the benzyl chlorides (Conditions A) vs. $\Delta\Delta G^{\ddagger}$ values for the NHP esters (Conditions B). This linear trendline ($y = 0.86x + 0.30$, $R^2 = 0.96$) suggests that both reactions proceed through the same stereochemistry-determining step.

Figure 3.10 *Evaluation of enantioselectivity for the benzylic chloride and benzylic NHP ester alkenylation reactions.*

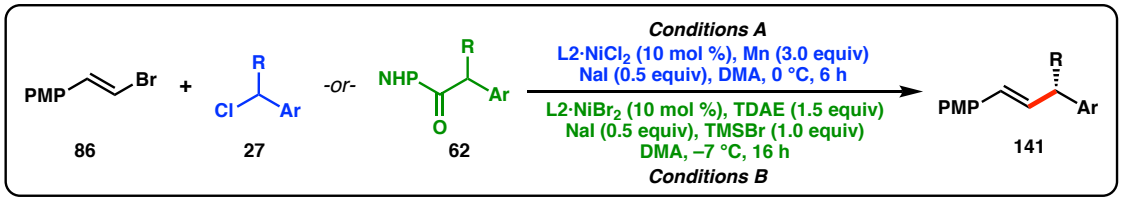

		Conditions:	A	B
Entry	Ar	R	ee(%)	ee(%)
1	Ph	Me	96	96
2	4-OMePh	Me	93	93
3	4-CF_3Ph	Me	87	88
4	4-BrPh	Me	90	90
5	4-FPh	Me	90	92
6	3,4-Cl_2Ph	Me	77	82
7	Ph	Et	97	97
8	Ph	Bn	92	95
9	Ph	*i*-Pr	97	97

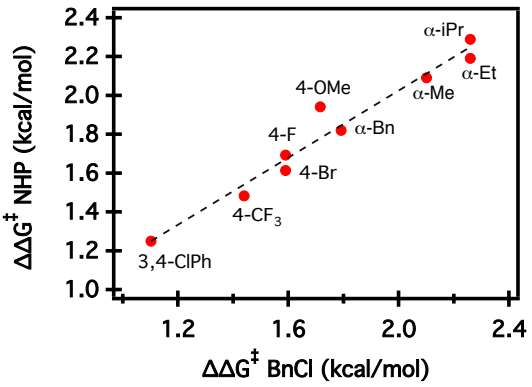

3.5 CONCLUSION

In summary, these results demonstrate that Ni-catalyzed reductive cross-coupling reactions of NHP esters can be rendered highly enantioselective, thus broadening the scope of C(sp^3) electrophiles available for asymmetric C–C bond formation. In contrast to the related reductive cross-couplings of benzyl chlorides,[44] optimal results were obtained when TDAE was used as the terminal reductant. A preliminary result demonstrated that these conditions could be used to cross-couple α-alkoxy NHP esters and other substrates for which the corresponding benzylic chloride could be difficult to prepare or unstable. The ability to use both NHP esters (this study) and benzylic chlorides in asymmetric reductive alkenylation reactions allows users to select from either electrophile depending on factors

such as commercial availability of the corresponding carboxylic acid or benzylic chloride starting material and improves the overall scope of this transformation. The further development of asymmetric cross-electrophile coupling reactions of NHP esters and other $C(sp^3)$ electrophiles is the focus of ongoing work in our laboratory.

3.6 EXPERIMENTAL SECTION

3.6.1 Materials and Methods

Unless otherwise stated, reactions were performed under a nitrogen atmosphere using freshly dried solvents. Tetrahydrofuran (THF), methylene chloride (CH_2Cl_2), diethyl ether (Et_2O), and toluene (PhMe) were dried by passing through activated alumina columns. Trimethylsilyl chloride (TMSCl) was distilled over calcium hydride. Trimethylsilyl bromide (TMSBr) and anhydrous dimethylacetamide (DMA) were purchased from Aldrich and stored in the glovebox. Manganese powder (–325 mesh, 99.3%) was purchased from Alfa Aesar. Zinc dust (97.5%) and nickel(II) chloride ($NiCl_2$) were purchased from Strem. Tetrakis(dimethylamino)ethylene (TDAE) was purchased from TCI and stored in the glovebox. Unless otherwise stated, chemicals were used as received. All reactions were monitored by thin-layer chromatography (TLC) using EMD/Merck silica gel 60 F254 pre-coated plates (0.25 mm) and were visualized by ultraviolet (UV) light or with cerium ammonium molybdate (CAM) staining. Flash column chromatography was performed as described by Still et al.[79] using silica gel (230-400 mesh) purchased from Silicycle or 10% $AgNO_3$ doped silica gel (+230 mesh) purchased from Sigma Aldrich. Optical rotations were measured on a Jasco P-2000 polarimeter using a 100 mm path-length cell at 589 nm.

^{1}H and ^{13}C NMR spectra were recorded on a Bruker Avance III HD with Prodigy cyroprobe (at 400 MHz and 101 MHz, respectively), a Varian 400 MR (at 400 MHz and 101 MHz, respectively), or a Varian Inova 500 (at 500 MHz and 126 MHz, respectively). ^{1}H and ^{19}F NMR spectra were also recorded on a Varian Inova 300 (at 300 MHz and 282 MHz, respectively). NMR data is reported relative to internal $CHCl_3$ (^{1}H, $\delta = 7.26$), $CDCl_3$ (^{13}C, $\delta = 77.1$), C_6F_6 (^{19}F, $\delta = -164.9$), $CH_3C_6D_5$ (^{1}H, $\delta = 2.09$), and $CD_3C_6D_5$ (^{13}C, $\delta = 20.4$). Data for ^{1}H NMR spectra are reported as follows: chemical shift (δ ppm) (multiplicity, coupling constant (Hz), integration). Multiplicity and qualifier abbreviations are as follows: s = singlet, d = doublet, t = triplet, q = quartet, m = multiplet. IR spectra were recorded on a Perkin Elmer Paragon 1000 spectrometer and are reported in frequency of absorption (cm^{-1}). Analytical chiral SFC was performed with a Mettler SFC supercritical CO_2 chromatography system with Chiralcel AD-H, OD-H, AS-H, OB-H, and OJ-H columns (4.6 mm x 25 cm). LRMS were obtained using an Aglient 1290 Infinity/6140 Quadrupole system (LC-MS) or an Agilent 7890A GC/5975C VL MSD system (GC-MS). HRMS were acquired from the Caltech Mass Spectral Facility using fast-atom bombardment (FAB), electrospray ionization (ESI-TOF), or electron impact (EI). X-ray diffraction and elemental analysis (EA) were performed at Caltech X-ray Crystal Facility.

3.6.2 Ni(II) Complex Preparation

For the synthesis of ligand **L2**, see Chapter 2.

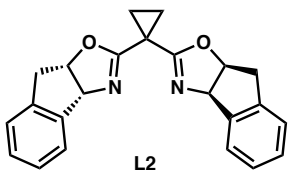

L2

Nickel(II) bis(bromide) (3a*R*,3a'*R*,8a*S*,8a'*S*)-2,2'-(cyclopropane-1,1-diyl)bis(3a,8a-dihydro-8*H*-indeno[1,2-*d*]oxazole) (L2·$NiBr_2$)

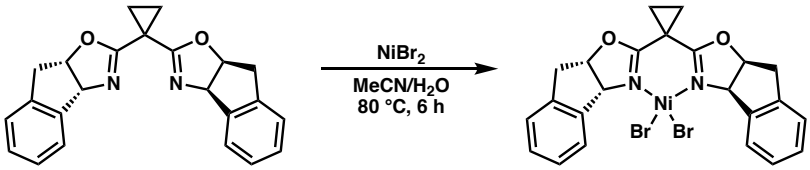

Similar to a procedure reported by Evans and coworkers,[80] the bis(oxazoline) ligand **L2** (1.07 g, 3.0 mmol, 1 equiv) and anhydrous nickel(II) bromide (655 mg, 3.0 mmol, 1 equiv) were added to a round bottom flask equipped with a magnetic stir bar and dissolved in a mixture of acetonitrile (CH_3CN, 65 mL) and water (0.75 mL). The solution was heated to 80 °C for 6 hours to afford a dark purple solution. The reaction was concentrated under reduced pressure and the obtained solid was saturated in CH_2Cl_2, filtered through a plug of cotton, dispensed into four 20 mL scintillation vials, and recrystallized by vapor diffusion (CH_2Cl_2/pentane) to afford dark purple crystals suitable for X-ray diffraction. For the isolation of **L2**·$NiBr_2$, the crystals were washed with hexane, which was added by pipet and subsequently removed. The crystals were removed with a spatula, transferred to a new vial, and crushed to provide a powder. The resulting complex was dried under vacuum to yield 1.6 g (91% yield) of **L2**·$NiBr_2$ as a purple solid. **m.p.** = >300 °C. **^{1}H NMR (400 MHz, $CDCl_3$):** δ 96.48 (s, 2H), 46.46 (s, 2H), 20.16 (d, *J* = 17.1 Hz, 2H), 11.67 – 10.85 (m, 6H), 10.55 (d, *J* = 16.6 Hz, 2H), 6.96 (s, 2H), 5.40 (s, 2H), -0.65 (s, 2H). **FTIR (NaCl, thin film, cm^{-1}):** 3333, 2222, 1660, 1479, 1461, 1444, 1427, 1312, 1247, 1227, 1214, 1120, 1010, 911, 859, 758, 728. **EA:** Anal. Calc'd. for **L2**·$NiBr_2$, $C_{23}H_{20}Br_2N_2NiO_2$ (%): C, 48.05; H, 3.51; N, 4.87. Found: C, 48.38; H, 3.54; N, 4.84.

3.6.3 Large Scale Preparation of TDAE

N,N,N',N'-tetramethylformamidinium chloride (S28)

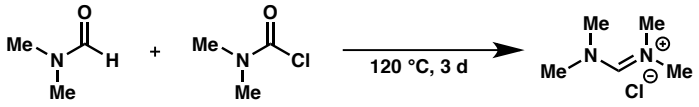

According to a procedure by Bestmann and coworkers,[81] the dimethylcarbamyl chloride (500 mmol, 46 mL, 1 equiv) and anhydrous dimethylformamide (DMF, 1 mol, 77 mL, 2 equiv) were added under an inert atmosphere (N_2) to a flame-dried 500 mL round bottom flask fitted with a reflux condenser and a magnetic stir bar. The solution was heated to 120 °C for 3 days, during which the reaction remained a homogeneous solution and turned dark brown in color. The reaction was removed from the stir plate and allowed to cool to room temperature, which initiated crystallization of the formamidinium chloride salt. Anhydrous diethyl ether (200 mL) was added to the crude reaction, swirled vigorously, quickly transferred to a fritted glass funnel, and filtered under a cone of argon gas. The crystals were quickly transferred to a round bottom flask and dried overnight under vacuum to yield 60.3 g (88% yield) of **S28** as a tan solid. The product is *extremely* hygroscopic, thus it was stored in the glovebox away from ambient moisture.

Tris(dimethylamino)methane (S29)

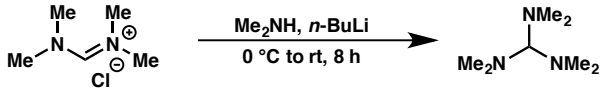

Similar to a procedure by Wasserman and coworkers,[82] anhydrous diethyl ether (500 mL) and dimethylamine (440 mL, 2 M in THF, 369 mmol, 2 equiv) were added under an inert atmosphere (N_2) to a flame-dried 2 L round bottom flask with a magnetic stir bar. The

reaction was cooled to –78 °C and *n*-butyllithium (*n*-BuLi, 210 mL, 2.5 M in hexane, 295 mmol, 1.2 equiv) was added via cannula under a stream of N_2, resulting in a pink homogenous solution. The reaction was warmed to room temperature and stirred for 30 min, forming a white slurry. The flask was cooled to 0 °C, **S28** (60.3 g, 246 mmol, 1 equiv) was quickly added, and the reaction was warmed to room temperature and stirred overnight for 8 h forming a light brown slurry. The flask was fitted with a distillation head and reflux condenser, and the solvent was distilled off into a 2 L receiving flask under ambient pressure. The flask was cooled and a new collection flask was added along with a vacuum regulator. The desired product was distilled out of the crude residue by slowly decreasing the pressure of the vacuum regulator to 1 mm Hg while increasing the oil bath temperature upwards of 100 °C. The liquid collected in the trap was THF, whereas the liquid collected in the receiving flask yielded 45.2 g (71% yield) of tris(dimethylamino)methane as a colorless oil. **^{1}H NMR (300 MHz, $CDCl_3$):** δ 3.02 (s, 1H), 2.29 (s, 18H). **^{13}C NMR (101 MHz, $CDCl_3$)**: δ 100.3, 41.3.

Tetrakis(dimethylamino)ethylene (TDAE)

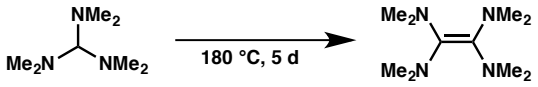

Similar to a procedure by Murphy and coworkers,[83] the tris(dimethylamino)methane was added to a 250 mL flame-dried round bottom flask fitted with a reflux condenser and a magnetic stir bar, and sparged with argon for 15 minutes. The reaction was heated to reflux for 5 days at 180 °C while being maintained under a steady stream of dry argon. The reaction was cooled to room temperature and remained under an argon atmosphere while

the flask was fitted with a distillation apparatus (also under an argon atmosphere). The product was purified via fractional distillation under reduced pressure with the aid of a Vigreux column. The remaining tris(dimethylamino)methane starting material was collected in the first fraction at 1 mm Hg and 30 °C as a colorless oil. When a yellow-green oil began to collect in the receiving flask, the fractions were exchanged and the desired product was collected at 1 mm Hg and 65 °C to yield 19.4 g (62% yield) of tetrakis(dimethylamino)ethylene as a yellow-green oil. Spectra matched those reported in literature[83] and also matched a sample of the commercially available material. The reagent was stored under inert atmosphere (N_2) in the glovebox. **^{1}H NMR (400 MHz, $C_6D_5CD_3$):** δ 2.57 (s, 24H). **^{13}C NMR (101 MHz, $C_6D_5CD_3$):** δ 131.5, 41.2.

3.6.4 Optimization of Reaction Parameters

On a bench-top to a 1 dram vial equipped with a stir bar was added alkenyl bromide **86** (43 mg, 0.2 mmol, 1 equiv), NHP ester **136** (59 mg, 0.2 mmol, 1 equiv), **L2**·$NiCl_2$ or **L2**·$NiBr_2$ (0.00–0.02 mmol, 0.00–0.10 equiv), reductant (if Mn or Zn, 0.6 mmol, 3 equiv), and sodium iodide (0.0–15.0 mg, 0.0–0.1 mmol, 0.0–0.5 equiv). Under an inert atmosphere in a glovebox, the vial was charged with DMA (0.2 mL, 1.0 M), the reagents were stirred until dissolved, and then cooled to the desired temperature. The reductant was then added (if tetrakis(dimethylamino)ethylene, TDAE, 0.3–0.6 mmol, 70–140 µl, 1.5–3 equiv). The reaction was stirred for 10 minutes before the trimethylsilyl chloride (TMSCl) or trimethylsilyl bromide (TMSBr) was added (0.0–0.2 mmol, 0–1 equiv). The vial was sealed with a screw cap and stirred for 16 hours. As the reaction proceeds, the TDAE salts begin

to precipitate, forming an orange slurry. The vial was removed from the glovebox and dibenzyl ether was added as an internal standard. The solution was quenched with aqueous HCl, extracted with Et_2O, dried with $MgSO_4$, and concentrated to afford the crude reaction mixture, which was analyzed by ^1H NMR and chiral phase SFC to provide the reaction yield and enantioselectivity of the desired product (**137**).

3.6.5 Substrate Preparation

General Procedure 1: NHP Ester Synthesis

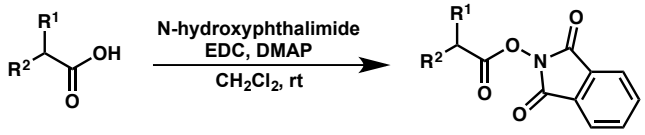

To a round bottom flask equipped with a magnetic stir bar was added the carboxylic acid (1.0 equiv), N-hydroxyphthalimide (1.0 equiv), and 4-dimethylaminopyridine (DMAP, 0.10 equiv). The reagents were dissolved in CH_2Cl_2 (0.2 M) and the N-(3-dimethylaminopropyl)-N-ethylcarbodiimide·HCl (EDC, 1.1 equiv) was added. The reaction continued to stir overnight at room temperature. The crude reaction was concentrated to afford a thick oil, which was purified by column chromatography (silica, EtOAc/hexane or CH_2Cl_2) to afford the desired product.

1,3-dioxoisoindolin-2-yl 2-phenylpropanoate (136)

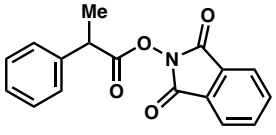

Prepared from 2-phenylpropanoic acid (5.0 g, 33.3 mmol) according to General Procedure 1. The crude residue was purified by filtering through a plug of silica with CH_2Cl_2 as the eluent to yield 8.7 g (88% yield) of **136** as a white solid. $\mathbf{R_f}$ = 0.28 (silica gel, 20% EtOAc/hexane, UV). **m.p.** = 62–64 °C. ^{1}**H**

NMR (400 MHz, $CDCl_3$): δ 7.85 (d, *J* = 5.5, 3.1 Hz, 2H), 7.76 (dd, *J* = 5.5, 3.1 Hz, 2H), 7.43 – 7.37 (m, 4H), 7.37 – 7.30 (m, 1H), 4.13 (q, *J* = 7.2 Hz, 1H), 1.68 (d, *J* = 7.2 Hz, 3H). **^{13}C NMR (101 MHz, $CDCl_3$):** δ 170.9, 161.9, 138.5, 134.9, 129.02, 128.98, 127.9, 127.7, 124.0, 43.1, 19.1. **FTIR (NaCl, thin film, cm^{-1}):** 1810, 1785, 1743, 1466, 1453, 1358, 1186, 1123, 1043, 1028, 877, 695. **HRMS (ESI-TOF, m/z):** calc'd for $C_{17}H_{13}NO_4$ $[M+H]^+$: 296.0923; found: 296.0903.

1,3-dioxoisoindolin-2-yl 2-(4-methoxyphenyl)propanoate (62a)

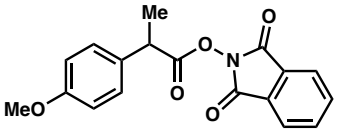

Prepared from 2-(4-methoxyphenyl)propanoic acid (500 mg, 2.77 mmol) according to General Procedure 1. The crude residue was purified by filtering through a plug of silica with 30% EtOAc/hexane as the eluent to yield 671 mg (74% yield) of **62a** as a white solid. **R_f** = 0.22 (silica gel, 20% EtOAc/hexane, UV). **m.p.** = 91–92 °C. **^{1}H NMR (400 MHz, $CDCl_3$):** δ 7.86 (dd, *J* = 5.5, 3.1 Hz, 2H), 7.77 (dd, 2H), 7.33 (d, *J* = 8.7 Hz, 2H), 6.92 (d, *J* = 8.8 Hz, 2H), 4.08 (q, *J* = 7.2 Hz, 1H), 3.81 (s, 3H), 1.65 (d, *J* = 7.2 Hz, 3H). **^{13}C NMR (101 MHz, $CDCl_3$):** δ 171.1, 162.0, 159.2, 134.9, 130.5, 129.0, 128.8, 124.0, 114.4, 55.4, 42.2, 19.2. **FTIR (NaCl, thin film, cm^{-1}):** 1810, 1784, 1743, 1611, 1513, 1467, 1371, 1249, 1185, 1123, 1045, 1033, 878, 832, 696. **HRMS (ESI-TOF, m/z):** calc'd for $C_{18}H_{15}NO_5$, $[M+H]^+$: 326.1028; found: 326.1022.

1,3-dioxoisoindolin-2-yl 2-(4-(trifluoromethyl)phenyl)propanoate (62b)

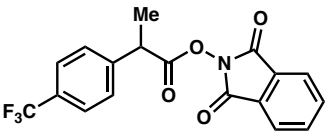

Prepared from 2-(4-(trifluoromethyl)phenyl)propanoic acid (200 mg, 0.92 mmol) according to General Procedure 1. The

crude residue was purified by filtering through a plug of silica with 30% EtOAc/hexane as the eluent to yield 290 mg (87% yield) of **62b** as a yellow solid. $\mathbf{R_f}$ = 0.28 (silica gel, 20% EtOAc/hexane, UV). **m.p.** = 76–77 °C. **^{1}H NMR (400 MHz, $CDCl_3$):** δ 7.87 (dd, *J* = 5.6, 3.2 Hz, 2H), 7.78 (dd, *J* = 5.5, 3.1 Hz, 2H), 7.66 (d, *J* = 7.8 Hz, 2H), 7.54 (d, *J* = 8.1 Hz, 2H), 4.19 (q, *J* = 7.2 Hz, 1H), 1.69 (d, *J* = 7.2 Hz, 3H). **^{13}C NMR (101 MHz, $CDCl_3$):** δ 170.3, 161.9, 142.4 (q, J_{C-F} = 1 Hz), 135.0, 130.2 (q, J_{C-F} = 33 Hz), 128.9, 128.2, 126.1 (q, J_{C-F} = 4 Hz). 124.14, 124.11 (q, J_{C-F} = 272 Hz), 43.0, 19.1. **^{19}F NMR (282 MHz, $CDCl_3$):** δ -65.8. **FTIR (NaCl, thin film, cm^{-1}):** 1813, 1788, 1746, 1620, 1468, 1421, 1359, 1326, 1186, 1168, 1125, 1079, 1067, 1048, 1017, 878, 842, 697. **HRMS (ESI-TOF, m/z):** calc'd for $C_{18}H_{12}F_3NO_4$ [M+H]+: 364.0797; found: 364.0815.

1,3-dioxoisoindolin-2-yl 2-(4-bromophenyl)propanoate (62c)

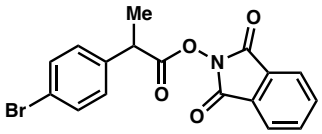

Prepared from 2-(4-bromophenyl)propanoic acid (1.0 g, 4.65 mmol) according to General Procedure 1. The crude residue was purified by filtering through a plug of silica with 20% EtOAc/hexane as the eluent to yield 511 mg (48% yield) of **62c** as a light yellow solid. $\mathbf{R_f}$ = 0.69 (silica gel, 20% EtOAc/hexane, UV). **m.p.** = 77–78 °C. **^{1}H NMR (400 MHz, $CDCl_3$):** δ 7.86 (dd, *J* = 5.5, 3.0 Hz, 2H), 7.80 – 7.75 (m, 2H), 7.52 (d, *J* = 8.5 Hz, 2H), 7.29 (d, *J* = 8.4 Hz, 2H), 4.08 (q, *J* = 7.2 Hz, 1H), 1.65 (d, *J* = 7.2 Hz, 3H). **^{13}C NMR (101 MHz, $CDCl_3$):** δ 170.5, 161.9, 137.4, 134.9, 132.2, 129.4, 129.0, 124.1, 122.0, 42.6, 19.0. **FTIR (NaCl, thin film, cm^{-1}):** 1811, 1786, 1742, 1489, 1467, 1369, 1186, 1133, 1078, 1046, 1010, 877, 696. **LRMS (API-ES, m/z):** calc'd for $C_{17}H_{12}BrNO_4$ $[M+H_2O]^+$: 391.0; found: 391.0.

1,3-dioxoisoindolin-2-yl 2-(4-fluorophenyl)propanoate (62d)

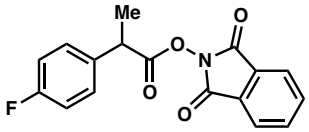

Prepared from 2-(4-fluorophenyl)propanoic acid (500 mg, 2.92 mmol) according to General Procedure 1. The crude residue was purified by filtering through a plug of silica with 20% EtOAc/hexane as the eluent to yield 590 mg (63% yield) of **62d** as a white solid. $\mathbf{R_f}$ = 0.35 (silica gel, 20% EtOAc/hexane, UV). **m.p.** = 108–110 °C. **^{1}H NMR (400 MHz, $CDCl_3$):** δ 7.86 (dd, *J* = 5.6, 3.1 Hz, 2H), 7.77 (dd, *J* = 5.5, 3.1 Hz, 2H), 7.41 – 7.35 (m, 2H), 7.12 – 7.05 (m, 2H), 4.11 (q, *J* = 7.2 Hz, 1H), 1.66 (d, *J* = 7.2 Hz, 3H). **^{13}C NMR (101 MHz, $CDCl_3$):** δ 170.78, 162.42 (d, $J_{C–F}$ = 246.4 Hz), 161.9, 134.9, 134.2 (d, $J_{C–F}$ = 3.3 Hz), 129.37 (d, $J_{C–F}$ = 8.3 Hz), 129.9, 124.1, 115.95 (d, $J_{C–F}$ = 21.5 Hz), 42.3, 19.2. **^{19}F NMR (282 MHz, $CDCl_3$):** δ -117.64 (tt, JF H = 8.4, 5.2 Hz). **FTIR (NaCl, thin film, cm^{-1}):** 1811, 1785, 1739, 1605, 1509, 1467, 1360, 1225, 1186, 1120, 1045, 1016, 959, 877, 837, 783, 696. **HRMS (FAB, m/z):** calc'd for $C_{17}H_{12}FNO_4$ $[M+H]^+$: 314.0823; found: 314.0859.

1,3-dioxoisoindolin-2-yl 2-(4-(dimethylamino)phenyl)propanoate (62e)

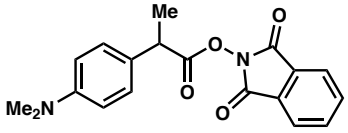

Prepared from 2-(4-(dimethylamino)phenyl)propanoic acid (392 mg, 2.02 mmol) according to General Procedure 1, with the exception of no DMAP. The crude residue was purified column chromatography (silica, 20 to 50% EtOAc/hexane) to yield 640 mg (94% yield) of **62e** as a yellow solid. $\mathbf{R_f}$ = 0.54 (silica gel, 50% EtOAc/hexane, UV). **m.p.** = 106–108 °C. **^{1}H NMR (400 MHz, $CDCl_3$):** δ 7.85 (dd, *J* = 5.6, 3.1 Hz, 2H), 7.76 (dd, *J* = 5.5, 3.1 Hz, 2H), 7.27 (d, *J* = 8.8 Hz, 2H), 6.75 (d, *J* = 8.8 Hz, 2H), 4.04 (q, *J* = 7.2 Hz, 1H), 2.95 (s, 6H), 1.64 (d, *J* = 7.2 Hz, 3H). **^{13}C NMR (101 MHz, $CDCl_3$):** δ 171.4, 162.1, 150.2, 134.8, 129.1, 128.3, 126.0, 124.0,

112.8, 42.1, 40.6, 19.2. **FTIR (NaCl, thin film, cm^{-1}):** 1809, 1784, 1743, 1615, 1523, 1467, 1356, 1186, 1134, 1081, 1044, 878, 819, 697. **HRMS (FAB, m/z):** calc'd for $C_{19}H_{18}N_2O_4$ $[M+\cdot]^+$: 338.1267; found: 338.1272.

1,3-dioxoisoindolin-2-yl 2-(3,4-dichlorophenyl)propanoate (62f)

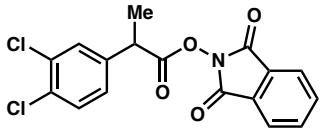

Prepared from 2-(3,4-dichlorophenyl)propanoic acid (231 mg, 1.05 mmol) according to General Procedure 1, with the exception of no DMAP. The crude residue was purified by column chromatography (silica, 0 to 15% EtOAc/hexane) to yield 241 mg (63% yield) of **62f** as a white solid. $\mathbf{R_f}$ = 0.35 (silica gel, 20% EtOAc/hexane, UV). **m.p.** = 103–105 °C. **^{1}H NMR (400 MHz, $CDCl_3$):** δ 7.87 (dd, *J* = 5.5, 3.1 Hz, 2H), 7.79 (dd, *J* = 5.5, 3.1 Hz, 2H), 7.52 (d, *J* = 2.2 Hz, 1H), 7.47 (d, *J* = 8.3 Hz, 1H), 7.26 (dd, *J* = 8.3, 2.2 Hz, 1H), 4.08 (q, *J* = 7.2 Hz, 1H), 1.66 (d, *J* = 7.2 Hz, 3H). **^{13}C NMR (101 MHz, $CDCl_3$):** δ 170.1, 161.9, 138.4, 135.0, 133.1, 132.2, 131.0, 129.9, 128.9, 127.1, 124.2, 42.3, 19.0. **FTIR (NaCl, thin film, cm^{-1}):** 2341, 2359, 1785, 1743, 1426, 1186, 1135, 1049, 962, 878, 696. **HRMS (FAB, m/z):** calc'd for $C_{17}H_{11}Cl_2NO_4$ $[M+H]^+$: 364.0143; found: 364.0131.

1,3-dioxoisoindolin-2-yl 2-phenylbutanoate (62g)

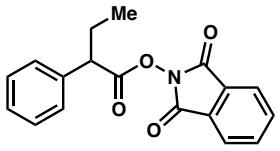

Prepared from 2-phenylbutanoic acid (5.0 g, 30.5 mmol) according to General Procedure 1. The crude residue was purified by column chromatography (silica, 20% EtOAc/hexane) to yield 8.1 g (86% yield) of **62g** as a white solid. $\mathbf{R_f}$ = 0.31 (silica gel, 20% EtOAc/hexane, UV). **m.p.** = 61–64 °C. **^{1}H NMR (400 MHz, $CDCl_3$):** δ 7.85 (dd, *J* = 5.6, 3.1 Hz, 2H), 7.76 (dd, *J* = 5.5, 3.1 Hz, 2H), 7.42

– 7.29 (m, 5H), 3.86 (t, J = 7.6 Hz, 1H), 2.31 – 2.18 (m, 1H), 2.03 – 1.90 (m, 1H), 1.04 (t, J = 7.4 Hz, 3H). **^{13}C NMR (101 MHz, $CDCl_3$):** δ 170.4, 162.0, 136.9, 134.8, 129.0, 128.9, 128.2, 128.0, 124.0, 50.5, 27.3, 12.0. **FTIR (NaCl, thin film, cm^{-1}):** 1811, 1786, 1744, 1467, 1455, 1360, 1186, 1128, 1080, 1058, 969, 877, 656. **HRMS (ESI-TOF, m/z):** calc'd for $C_{18}H_{15}NO_4$ $[M+H]^+$: 310.1079; found: 310.1061.

1,3-dioxoisoindolin-2-yl 2,3-diphenylpropanoate (62h)

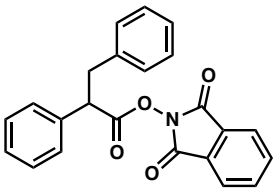

Prepared from 2,3-diphenylpropanoic acid (353 mg, 1.56 mmol) according to General Procedure 1. The crude residue was purified by column chromatography (silica, 20% EtOAc/hexane) to yield 542 mg (94% yield) of **62h** as a white solid. **R_f** = 0.28 (silica gel, 20% EtOAc/hexane, UV). **m.p.** = 116–119 °C. **^{1}H NMR (400 MHz, $CDCl_3$):** δ 7.85 (dd, J = 5.5, 3.0 Hz, 2H), 7.76 (dd, J = 5.5, 3.1 Hz, 2H), 7.41 – 7.20 (m, 8H), 7.15 – 7.10 (m, 2H), 4.23 (t, J = 7.6 Hz, 1H), 3.56 (dd, J = 13.9, 7.5 Hz, 1H), 3.19 (dd, J = 13.9, 7.8 Hz, 1H). **^{13}C NMR (101 MHz, $CDCl_3$):** δ 170.0, 161.8, 137.7, 136.4, 134.8, 129.2, 129.0, 128.9, 128.6, 128.3, 128.1, 126.9, 124.0, 50.9, 39.9. **FTIR (NaCl, thin film, cm^{-1}):** 3030, 1810, 1784, 1744, 1496, 1467, 1454, 1359, 1186, 1134, 1080, 1068, 972, 877, 736, 695. **HRMS (ESI-TOF, m/z):** calc'd for $C_{23}H_{17}NO_4$ $[M+H]^+$: 372.1236; found: 372.1236.

1,3-dioxoisoindolin-2-yl 3-methyl-2-phenylbutanoate (62i)

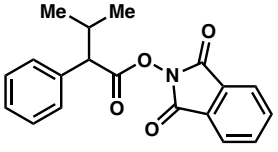

Prepared from 3-methyl-2-phenylbutanoic acid (300 mg, 1.68 mmol) according to General Procedure 1. The crude residue was purified by filtering through a plug of silica with 20% EtOAc/hexane as the eluent to yield

509 mg (93% yield) of **62i** as a white solid. $\mathbf{R_f}$ = 0.34 (silica gel, 20% EtOAc/hexane, UV). **m.p.** = 77–81 °C. **^{1}H NMR (400 MHz, $CDCl_3$):** δ 7.84 (dd, *J* = 5.6, 3.1 Hz, 2H), 7.76 (dd, *J* = 5.5, 3.1 Hz, 2H), 7.42 – 7.29 (m, 5H), 3.58 (d, *J* = 10.0 Hz, 1H), 2.51 – 2.37 (m, 1H), 1.23 (d, *J* = 6.6 Hz, 3H), 0.84 (d, *J* = 6.7 Hz, 3H). **^{13}C NMR (101 MHz, $CDCl_3$):** δ 170.2, 162.0, 136.1, 134.8, 129.0, 128.8, 128.7, 128.0, 124.0, 56.7, 32.6, 21.3, 20.3. **FTIR (NaCl, thin film, cm^{-1}):** 2966, 1811, 1786, 1745, 1468, 1455, 1375, 1311, 1186, 1132, 1080, 1060, 974, 889, 877, 786, 745, 696. **HRMS (ESI-TOF, m/z):** calc'd for $C_{19}H_{17}NO_4$ $[M+H]^+$: 324.1236; found: 324.1227.

1,3-dioxoisoindolin-2-yl 3-((*tert*-butyldimethylsilyl)oxy)-2-phenylpropanoate (62j)

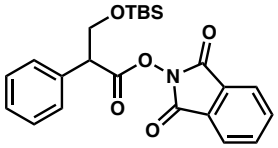

To a round bottom flask equipped with a stirring magnet was added tropic acid (830 mg, 5 mmol, 1 equiv), *tert*-butyldimethylsilyl chloride (1.1 g, 5.5 mmol, 1.1 equiv), dimethylaminopyridine (63 mg, 0.5 mmol, 0.1 equiv), and imidazole (682 mg, 10 mmol, 2 equiv). The reagents were dissolved in 15 mL of CH_2Cl_2 and stirred overnight at room temperature. The reaction was quenched with aq. NH_4Cl, extracted with Et_2O, dried with $MgSO_4$, filtered, and concentrated under reduced pressure to afford crude 3-((*tert*-butyldimethylsilyl)oxy)-2-phenylpropanoic acid. This crude material was used in the esterification step without purification, which was performed according to General Procedure 1. The crude residue was purified by column chromatography and dried under high vacuum (silica, 0 to 20% EtOAc/hexane) to yield 664 mg (31% yield) of **62j** as a colorless oil. $\mathbf{R_f}$ = 0.38 (silica gel, 20% EtOAc/hexane, UV). **^{1}H NMR (400 MHz, $CDCl_3$):** δ 7.86 (dd, *J* = 5.6, 3.1 Hz, 2H), 7.77 (dd, *J* = 5.5, 3.1 Hz, 2H), 7.43 – 7.31 (m, 5H), 4.28 – 4.18 (m, 2H), 3.93 (dd, *J* = 8.6,

4.4 Hz, 1H), 0.89 (s, 9H), 0.05 (s, 3H), 0.03 (s, 3H). **^{13}C NMR (101 MHz, $CDCl_3$):** δ 169.0, 161.8, 134.8, 134.1, 129.1, 129.0, 128.5, 128.3, 124.0, 65.3, 52.2, 25.9, 18.4, -5.4, -5.6. **FTIR (NaCl, thin film, cm^{-1}):** 2953, 2929, 2856, 1814, 1788, 1747, 1468, 1361, 1256, 1186, 1113, 1049, 1023, 877, 836, 780, 696. **HRMS (ESI-TOF, m/z):** calc'd for $C_{23}H_{27}NO_5Si$ $[M+H]^+$: 426.1737; found: 426.1708.

1,3-dioxoisoindolin-2-yl 2-phenylpent-4-enoate (62k)

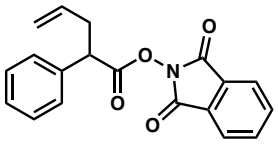

Prepared from 2-phenylpent-4-enoic acid (240 mg, 1.36 mmol) according to General Procedure 1. The crude residue was purified by column chromatography (silica, 0 to 20% EtOAc/hexane) to yield 295 mg (67% yield) of **62k** as a white solid. **R_f =** 0.31 (silica gel, 20% EtOAc/hexane, UV). **m.p. =** 68–69 °C. **^{1}H NMR (400 MHz, $CDCl_3$):** δ 7.85 (dd, *J* = 5.6, 3.1 Hz, 2H), 7.76 (dd, *J* = 5.5, 3.1 Hz, 2H), 7.42 – 7.31 (m, 5H), 5.81 (ddt, *J* = 17.1, 10.2, 6.9 Hz, 1H), 5.16 (dq, *J* = 17.1, 1.5 Hz, 1H), 5.14 – 5.09 (m, 1H), 4.04 (dd, *J* = 8.0, 7.2 Hz, 1H), 3.00 – 2.90 (m, 1H), 2.68 (dtt, *J* = 14.3, 7.1, 1.3 Hz, 1H). **^{13}C NMR (101 MHz, $CDCl_3$):** δ 169.9, 161.9, 136.4, 134.9, 134.0, 129.02, 128.99, 128.2, 128.1, 124.0, 118.3, 48.8, 37.9. **FTIR (NaCl, thin film, cm^{-1}):** 1811, 1785, 1743, 1467, 1359, 1186, 1133, 1080, 1068, 971, 877, 695. **HRMS (ESI-TOF, m/z):** calc'd for $C_{19}H_{15}NO_4$ $[M+H]^+$: 322.1079; found: 322.1063.

1,3-dioxoisoindolin-2-yl 5-chloro-2-phenylpentanoate (62l)

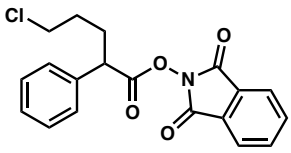

Prepared from 5-chloro-2-phenylpentanoic acid (1.01 g, 4.75 mmol) according to General Procedure 1. The crude residue was purified by filtering through a plug of silica with 20% EtOAc/hexane as the eluent to yield

977 mg (58% yield) of **62l** as a white solid. **R_f =** 0.25 (silica gel, 20% EtOAc/hexane, UV). **m.p. =** 96–99 °C. **^{1}H NMR (400 MHz, $CDCl_3$):** δ 7.85 (dd, *J* = 5.6, 3.1 Hz, 2H), 7.77 (dd, *J* = 5.5, 3.1 Hz, 2H), 7.42 – 7.31 (m, 5H), 3.97 (t, *J* = 7.7 Hz, 1H), 3.64 – 3.52 (m, 2H), 2.34 (dddd, *J* = 13.2, 10.4, 8.0, 5.1 Hz, 1H), 2.13 (dddd, *J* = 13.5, 10.3, 7.4, 5.5 Hz, 1H), 2.01 – 1.78 (m, 2H). **^{13}C NMR (101 MHz, $CDCl_3$):** δ 170.1, 161.9, 136.4, 134.9, 129.1, 129.0, 128.2, 128.1, 124.1, 48.2, 44.4, 31.2, 30.1. **FTIR (NaCl, thin film, cm^{-1}):** 2960, 1811, 1786, 1744, 1494, 1455, 1468, 1361, 1186, 1134, 1081, 1045, 965, 878, 697. **HRMS (FAB, m/z):** calc'd for $C_{19}H_{16}NO_4Cl$ $[M+H]^+$: 358.0846; found: 358.0872.

1,3-dioxoisoindolin-2-yl 2-methoxy-2-phenylacetate (145)

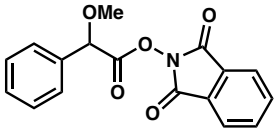

Prepared from 2-methoxy-2-phenylacetic acid (830 mg, 5.0 mmol) according to General Procedure 1. The crude residue was purified by column chromatography (silica, 10 to 30% EtOAc/hexane) to yield 1.16 g (74% yield) of **145** as a colorless oil. **Note:** This compound will slowly decompose (solidifies/hydrolyzes) under ambient conditions over extended periods (~1 month). **R_f =** 0.22 (silica gel, 20% EtOAc/hexane, UV). **^{1}H NMR (400 MHz, $CDCl_3$):** δ 7.83 (dd, *J* = 5.5, 3.1 Hz, 2H), 7.75 (dd, *J* = 5.5, 3.1 Hz, 2H), 7.60 – 7.52 (m, 2H), 7.50 – 7.37 (m, 3H), 5.19 (s, 1H), 3.56 (s, 3H). **^{13}C NMR (101 MHz, $CDCl_3$):** δ 167.4, 161.6, 134.9, 134.4, 129.6, 129.0, 128.8, 127.6, 124.1, 81.0, 58.0. **FTIR (NaCl, thin film, cm^{-1}):** 1818, 1789, 1745, 1468, 1359, 1186, 1079, 988, 969, 877, 696. **HRMS (ESI-TOF, m/z):** calc'd for $C_{17}H_{13}NO_5$ $[M+H]^+$: 312.0872; found: 312.0846.

1,3-dioxoisoindolin-2-yl 2-cyclopropyl-2-phenylacetate (160)

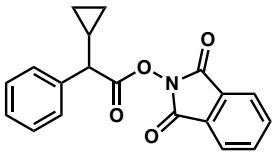

Prepared from 2-cyclopropyl-2-phenylacetic acid (50 mg, 0.28 mmol) according to General Procedure 1. The crude residue was purified by filtering through a plug of silica with 20% EtOAc/hexane as the eluent to yield 80 mg (89% yield) of **160** as a white solid. $\mathbf{R_f}$ **=** 0.39 (silica gel, 50% EtOAc/hexane, UV). **m.p. =** 92–93 °C. **^{1}H NMR (400 MHz, $CDCl_3$):** δ 7.87 (dd, *J* = 5.5, 3.0 Hz, 2H), 7.81 – 7.75 (m, 2H), 7.50 – 7.45 (m, 2H), 7.44 – 7.38 (m, 2H), 7.37 – 7.31 (m, 1H), 3.29 (d, *J* = 9.7 Hz, 1H), 1.53 (dtt, *J* = 9.7, 8.0, 4.9 Hz, 1H), 0.82 (dddd, *J* = 9.0, 8.1, 4.6, 2.9 Hz, 1H), 0.69 (dddd, *J* = 8.9, 8.0, 5.8, 4.8 Hz, 1H), 0.63 – 0.55 (m, 1H), 0.42 – 0.34 (m, 1H). **^{13}C NMR (101 MHz, $CDCl_3$):** δ 170.0, 162.0, 136.8, 134.9, 129.1, 128.9, 128.1, 128.0, 124.1, 53.4, 14.6, 4.91, 4.90. **FTIR (NaCl, thin film, cm^{-1}):** 1811, 1742, 1362, 1170, 1135, 1063, 974, 876. **HRMS (FAB, m/z):** calc'd for $C_{19}H_{15}NO_4$ $[M+H]^+$: 322.1079; found: 322.1065.

Alkenyl Bromide Synthesis

Alkenyl bromides **86**, **29a**, **29u**, **29j**, and **29i** were prepared according to procedures reported and referenced by Reisman and coworkers.[44]

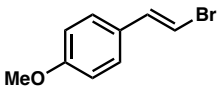

86

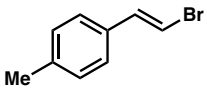

29a

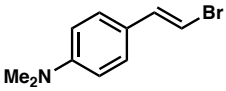

29u

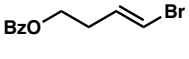

29j

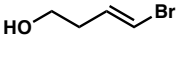

29i

Alkenyl bromides **29v**, **29w**, **29x**, **29y**, and **29k** were prepared according to General Procedure 2. Alkenyl bromides **29v** and **29x** were subjected to NaOH-mediated isomerization to afford geometrically pure *E*-isomer. Alkenyl bromides **29w**, **29y**, and **29k** were not subjected to NaOH-mediated isomerization;[84] alkenyl bromide **29w** decomposes

under these conditions therefore the substrate used in the cross-coupling reaction was a 93:7 E:Z ratio. The NMR spectra of **29v,**[44] **29w,**[85] and **29x**[86] matched those reported in literature. The characterization data for **29y** is reported below. For **29k**, see Chapter 2.

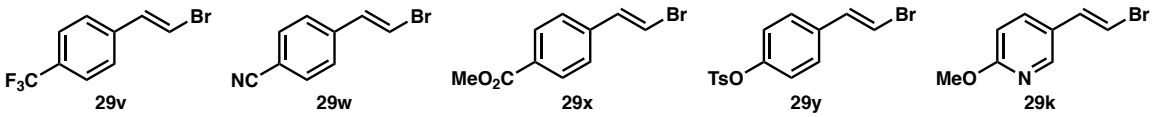

General Procedure 2: Alkenyl Bromides from Aldehydes

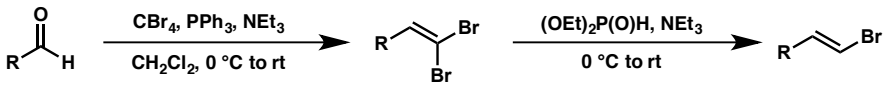

General Procedure 2, Part A: According to a procedure by Alexakis and coworkers,[84] a flame dried round bottom flask equipped with a magnetic stir bar was put under an inert atmosphere (N_2) and charged with the tetrabromomethane (20 mmol, 2 equiv) and triphenylphosphine (40 mmol, 4 equiv). The flask was cooled to 0 °C and then CH_2Cl_2 (30 mL) was added, followed by the triethylamine (10 mmol, 1 equiv). The aldehyde (10 mmol, 1 equiv) was dissolved in CH_2Cl_2 (5 mL) and added dropwise to the reaction mixture. The reaction was allowed to warm to room temperature and continued to stir for 90 minutes. The reaction was removed from the stir plate and slowly added to a vigorously stirring solution of Et_2O (150 mL) and hexane (150 mL), filtered through a plug of silica gel, and concentrated under reduced pressure to afford the desired dibromoalkene.

4-(2,2-dibromovinyl)phenyl 4-methylbenzenesulfonate (S30)

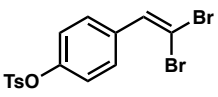

Prepared from 4-formylphenyl 4-methylbenzenesulfonate (5.14 g, 18.6 mmol) following General Procedure 2A. The crude residue was

purified by filtering through a plug of silica to yield 6.2 g (77% yield) of **S30** as a white solid. $\mathbf{R_f}$ = 0.38 (silica gel, 10% EtOAc/hexane). **m.p.** = 108–110 °C. **^{1}H NMR (400 MHz, $CDCl_3$):** δ 7.73 – 7.67 (m, 2H), 7.49 – 7.43 (m, 2H), 7.41 (s, 1H), 7.34 – 7.29 (m, 2H), 7.01 – 6.95 (m, 2H), 2.45 (s, 3H). **^{13}C NMR (101 MHz, $CDCl_3$):** δ 149.3, 145.7, 135.6, 134.2, 132.3, 129.9, 129.8, 128.6, 122.5, 90.8, 21.9. **FTIR (NaCl, thin film, cm^{-1})**: 3081, 3065, 1929, 1910, 1596, 1500, 1495, 1406, 1379, 1360, 1271, 1178, 1160, 1094, 1018, 877, 832, 914, 781, 732, 706, 698, 658. **HRMS (FAB, m/z)**: calc'd for $C_{15}H_{12}Br_2O_3S$ $[M+H]^+$: 432.8932; found: 432.8915.

General Procedure 2, Part B: The dibromoalkene (1.7 mmol, 1 equiv) and diethyl phosphite (5.1 mmol, 3 equiv) were added to a vial with a magnetic stirring rod and put under an inert atmosphere (N_2). The solution was cooled to 0 °C and the triethylamine (5.1 mmol, 3 equiv) was added dropwise. The reaction was warmed to room temperature and stirred overnight. The reaction was quenched with water (5 mL) and extracted with CH_2Cl_2 (20 mL). The organic layer was washed with brine (5 mL), dried with Na_2SO_4, filtered, and concentrated under reduced pressure. The crude residue was purified by column chromatography (silica, ether/hexanes) to afford the vinyl bromide.

(*E*)-4-(2-bromovinyl)phenyl 4-methylbenzenesulfonate (29y)

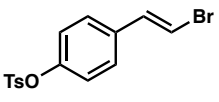

Prepared from **S30** (4.32 g, 10 mmol) following General Procedure 2B. The crude residue was purified by column chromatography (silica, 5% EtOAc/hexane to 20% EtOAc/hexane) to yield 2.75 g (78% yield, 90:10 E:Z) of **29y** as a white solid. $\mathbf{R_f}$ = 0.34 (silica gel, 10% EtOAc/hexane). **m.p.** = 90–93 °C. **^{1}H NMR (400**

MHz, $CDCl_3$): δ 7.72 – 7.67 (m, 2H), 7.34 – 7.28 (m, 2H), 7.23 – 7.17 (m, 2H), 7.03 (d, *J* = 14.0 Hz, 1H), 6.96 – 6.90 (m, 2H), 6.73 (d, *J* = 14.0 Hz, 1H), 2.44 (s, 3H). **^{13}C NMR (101 MHz, $CDCl_3$):** δ 149.3, 145.6, 135.9, 134.9, 132.3, 129.9, 128.6, 127.3, 122.9, 107.7, 21.9. **HRMS (FAB, m/z)**: calc'd for $C_{15}H_{13}BrO_3S$ $[M+\cdot]^+$: 353.9748; found: 353.9733.

Alkenyl bromide **29z** was prepared by a NaOH-mediated isomerization of commercially available β-bromostyrene as reported by Alexakis and coworkers.[84]

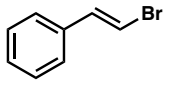

29z

Alkenyl bromide **S2** was prepared via a hydrozirconation/bromination sequence similar to a procedure reported by Zhou, Lin, and coworkers, which is reported in Chapter 2.[87] The NMR spectra matched those reported in literature.[88]

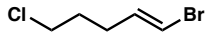

S2

Alkneyl bromide **29aa** was prepared according to a procedure reported by Wolfe and coworkers.[89]

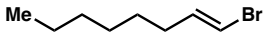

29aa

Alkneyl bromides **29ab** and **29o** were purchased from a commercial source (Sigma Aldrich).

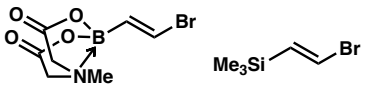

29ab **29o**

3.6.6 Enantioselective Reductive Cross-Couplings

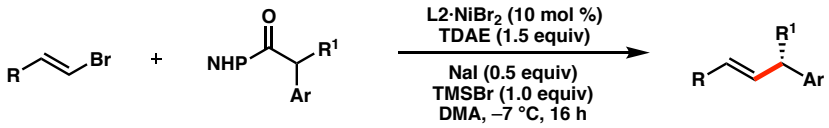

General Procedure 3: Reaction on 0.2 mmol scale.

On a bench-top, a 1 dram vial equipped with a stir bar was charged with the vinyl bromide (if air stable, 0.2 mmol, 1 equiv), NHP ester (0.2 mmol, 1 equiv), **L2**·$NiBr_2$ (11.5 mg, 0.02 mmol, 0.10 equiv), and sodium iodide (15.0 mg, 0.1 mmol, 0.5 equiv). The vial was then brought into the glovebox and charged with the vinyl bromide (if air sensitive, 0.2 mmol, 1 equiv) and DMA (0.2 mL, 1.0 M). The vial was then cooled to –7 °C and the reagents were stirred at 250 rpm until dissolved. **Note:** The recirculating Julabo LH45 chiller was set to –10 °C however an external thermometer in the glovebox read the temperature as –7 °C. The tetrakis(dimethylamino)ethylene (TDAE, 0.3 mmol, 70 μl, 1.5 equiv) was added and stirred for 10 minutes before the trimethylsilyl bromide (TMSBr, 0.2 mmol, 26 μL, 1 equiv) was added. The vial was sealed with a screw cap and stirred under nitrogen at –7 °C for 16 hours (overnight) in temperature controlled well plates in the glovebox. **Note:** Monitoring the reaction kinetics for product **137** revealed that the reaction went to >90% conversion after 1 hour, however we choose to run these reactions overnight to ensure full conversion. As the reaction proceeds, the TDAE salts begin to precipitate, forming an orange slurry. The crude reaction was quenched with 0.5 mL of 1 M HCl, diluted with water (5 mL), and extracted with diethyl ether (3 x 10 mL). **Note:** In order to efficiently remove all of the viscous reaction contents from the vial, we found it useful to fill the vial ¾ full with an extraction solvent (2.5 mL each time: first HCl/water, then Et_2O, water, Et_2O

3x), screw on a Teflon cap, and shake the vial vigorously with the stir bar still inside. The contents could then be easily poured into a separatory funnel. The combined organic layers were washed with brine (5 mL), dried with $MgSO_4$, filtered, and concentrated under reduced pressure. The crude residue was purified by column chromatography.

Assignment of Absolute Stereochemistry

The absolute stereochemistry of **137**, **140a**, and **140b** were assigned by comparing the optical rotation of the purified products to literature values. The optical rotation of products **137**, **140b–c**, **140i**, **141a**, **141c**, **141d**, **141g**, and **141h** correspond with those in reported in literature synthesized using the same chiral ligand **L2**.[44] Chiral products **140d–f**, **140h**, **140j–n**, **141b**, **141e**, **141f**, **141i–l**, and **146** were assigned by analogy.

Characterization of Reaction Products

(*S*,*E*)-1-methoxy-4-(3-phenylbut-1-en-1-yl)benzene (137)

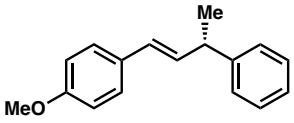

Prepared from (*E*)-1-(2-bromovinyl)-4-methoxybenzene (**86**, 43 mg, 0.2 mmol) and 1,3-dioxoisoindolin-2-yl 2-phenylpropanoate (**136**, 59 mg, 0.2 mmol) according to General Procedure 3. The crude residue was purified by column chromatography (silica gel, 10 to 20% toluene/hexane) to yield **137** (39 mg, 80% yield) in 96% ee as a colorless oil. Spectral data matched those reported in literature.[44] $\mathbf{R_f}$ = 0.59 (silica gel, 10% EtOAc/hexane, UV). **Chiral SFC**: (OB-H, 2.5 mL/min, 20% IPA in CO_2, λ = 254 nm): t_R (major) = 7.1 min, t_R (minor) = 8.4 min. $[\boldsymbol{\alpha}]_{\boldsymbol{D}}^{\mathbf{25}}$ = –34° (c = 1.0, $CHCl_3$). **^{1}H NMR (400 MHz, $CDCl_3$):** δ 7.37 – 7.27 (m, 6H), 7.25 – 7.20 (m, 1H), 6.85

(d, J = 8.8 Hz, 2H), 6.38 (d, J = 16.2 Hz, 1H), 6.27 (dd, J = 15.9, 6.7 Hz, 1H), 3.81 (s, 3H), 3.70 – 3.58 (m, 1H), 1.48 (d, J = 7.0 Hz, 3H). **^{13}C NMR (101 MHz, $CDCl_3$):** δ 158.9, 146.0, 133.3, 130.5, 128.6, 128.0, 127.42, 127.36, 126.3, 114.0, 55.4, 42.7, 21.5. The optical rotation of **137** generated in the presence of **L2**·$NiBr_2$ was measured as $[\boldsymbol{\alpha}]_{\boldsymbol{D}}^{\mathbf{25}}$ = –34° (c = 1.0, $CHCl_3$). Lit: $[\boldsymbol{\alpha}]_{\boldsymbol{D}}^{\mathbf{25}}$ = –16° (c = 1.28, $CHCl_3$, *S* enantiomer, 94% ee).[90] Based on the literature precedent, we assign our product as the *S* enantiomer.

Preparative Scale: Reaction on 5.0 mmol scale:

On a bench-top to a 25 mL round bottom flask equipped with a stir bar was added alkenyl bromide **86** (1.065 g, 5 mmol, 1 equiv), NHP ester **136** (1.476 g, 5 mmol, 1 equiv), **L2**·$NiBr_2$ (0.29 g, 0.5 mmol, 0.10 equiv), and sodium iodide (0.37 g, 2.5 mmol, 0.5 equiv). The flask was sealed with a rubber septum, purged with nitrogen, and the reagents were dissolved in DMA (5.0 mL, 1.0 M). The flask was cooled to –5 °C by submerging it in an isopropanol bath cooled with a Thermo Scientific EK90 Immersion Cooler. **Note:** TDAE will begin to freeze at temperatures below –8 °C with this setup. The TDAE (1.74 mL, 7.5 mmol, 1.5 equiv) was added and stirred for 10 minutes before the TMSBr (TMSBr, 0.66 mL, 5.0 mmol, 1 equiv) was added. The flask was stirred under a balloon of nitrogen at –5 °C for 16 hours. As the reaction proceeds, the TDAE salts begin to precipitate, forming an orange slurry. The crude reaction was quenched with 1 M HCl (30 mL), and extracted with diethyl ether (3 x 20 mL). The combined organic layers were washed with water (2 x 20 mL) and brine (20 mL), dried with $MgSO_4$, filtered, and concentrated under reduced pressure. The crude residue was purified by column chromatography (silica gel, 10 to 20% toluene/hexane) to yield **137** (918 mg, 77% yield) in 91% ee as a colorless oil.

(*S*,*E*)-1-methyl-4-(3-phenylbut-1-en-1-yl)benzene (140a)

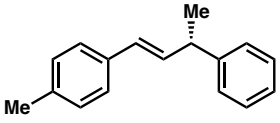

Prepared from (*E*)-1-(2-bromovinyl)-4-methylbenzene (**29a**, 39 mg, 0.2 mmol) and 1,3-dioxoisoindolin-2-yl 2-phenylpropanoate (**136**, 59 mg, 0.2 mmol) according to General Procedure 3. The crude residue was purified by column chromatography (10% $AgNO_3$ silica gel, 0 to 2% Et_2O/hexane) to yield **140a** (39 mg, 88% yield) in 95% ee as a colorless oil. Spectral data matched those reported in literature.[91] $\mathbf{R_f}$ = 0.26 (silica gel, hexane, UV). **Chiral SFC:** (OJ-H, 2.5 mL/min, 7% IPA in CO_2, λ = 254 nm): t_R (minor) = 8.0 min, t_R (major) = 10.0 min. $[\boldsymbol{\alpha}]_D^{25}$ = –41° (c = 1.0, $CHCl_3$). **^{1}H NMR (400 MHz, $CDCl_3$):** δ 7.41 – 7.30 (m, 6H), 7.30 – 7.24 (m, 1H), 7.16 (d, *J* = 8.0 Hz, 2H), 6.52 – 6.34 (m, 2H), 3.74 – 3.64 (m, 1H), 2.38 (s, 3H), 1.53 (d, *J* = 7.0 Hz, 3H). **^{13}C NMR (101 MHz, $CDCl_3$):** δ 145.9, 136.9, 134.9, 134.3, 129.3, 128.6, 128.5, 127.5, 126.3, 126.2, 42.7, 21.5, 21.3. The optical rotation of **140a** generated in the presence of **L2**·$NiBr_2$ was measured as $[\boldsymbol{\alpha}]_D^{25}$ = –41° (c = 1.0, $CHCl_3$). Lit: $[\boldsymbol{\alpha}]_D^{25}$ = +38.4° (c = 0.98, $CHCl_3$, *R* enantiomer, 91% ee).[90] Based on the literature precedent, we assign our product as the *S* enantiomer.

(*S*,*E*)-*N*,*N*-dimethyl-4-(3-phenylbut-1-en-1-yl)aniline (140b)

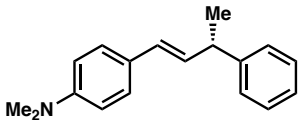

Prepared from (*E*)-4-(2-bromovinyl)-*N*,*N*-dimethylaniline (**29u**, 45 mg, 0.2 mmol) and 1,3-dioxoisoindolin-2-yl 2-phenyl-propanoate (**136**, 59 mg, 0.2 mmol) according to General Procedure 3. The crude residue was purified by column chromatography (silica gel, 5% Et_2O/hexane) to yield **140b** (38 mg, 76% yield) in 97% ee as a white solid. Spectral data matched those reported in literature.[44] $\mathbf{R_f}$ = 0.21 (silica gel, 5% Et_2O/hexane, UV). **m.p.** = 65–67 °C. **Chiral SFC:**

(OB-H, 2.5 mL/min, 35% IPA in CO_2, λ = 254 nm): t_R (major) = 6.0 min, t_R (minor) = 9.0 min. $[\boldsymbol{a}]_D^{25}$ = –56° (c = 1.0, $CHCl_3$). **^{1}H NMR (400 MHz, $CDCl_3$):** δ 7.40 – 7.29 (m, 6H), 7.29 – 7.23 (m, 1H), 6.73 (d, *J* = 8.8 Hz, 2H), 6.40 (d, *J* = 15.9 Hz, 1H), 6.24 (dd, *J* = 15.8, 6.8 Hz, 1H), 3.72 – 3.62 (m, 1H), 3.00 (s, 6H), 1.51 (d, *J* = 7.0 Hz, 3H). **^{13}C NMR (101 MHz, $CDCl_3$):** δ 149.9, 146.4, 131.2, 128.5, 128.4, 127.5, 127.1, 126.4, 126.1, 112.7, 42.7, 40.8, 21.6.

(*S*,*E*)-1-(3-phenylbut-1-en-1-yl)-4-(trifluoromethyl)benzene (140c)

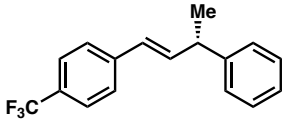

Prepared from (*E*)-1-(2-bromovinyl)-4-(trifluoromethyl)benzene (**29v**, 50 mg, 0.2 mmol) and 1,3-dioxoisoindolin-2-yl 2-phenylpropanoate (**136**, 59 mg, 0.2 mmol) according to General Procedure 3. The crude residue was purified by column chromatography (silica gel, hexane) to yield **140c** (48 mg, 87% yield) in 93% ee as a colorless oil. Spectral data matched those reported in literature.[44] **R_f** = 0.32 (silica gel, hexane, UV). **Chiral SFC:** (OJ-H, 2.5 mL/min, 3% IPA in CO_2, λ = 254 nm): t_R (minor) = 6.3 min, t_R (major) = 7.3 min. $[\boldsymbol{a}]_D^{25}$ = –27° (c = 1.0, $CHCl_3$). **^{1}H NMR (400 MHz, $CDCl_3$):** δ 7.56 (d, *J* = 8.6 Hz, 2H), 7.46 (d, *J* = 8.2 Hz, 2H), 7.40 – 7.33 (m, 2H), 7.33 – 7.23 (m, 3H), 6.52 (dd, *J* = 15.9, 6.2 Hz, 1H), 6.45 (d, *J* = 16.0 Hz, 1H), 3.74 – 3.64 (m, 1H), 1.51 (d, *J* = 7.0 Hz, 3H). **^{13}C NMR (101 MHz, $CDCl_3$):** δ 145.2, 141.2 (q, $J_{C\text{-}F}$ = 1 Hz), 138.1, 129.0 (q, $J_{C\text{-}F}$ = 32 Hz), 128.7, 127.5, 127.4, 126.6, 126.4, 125.6 (q, $J_{C\text{-}F}$ = 4 Hz), 124.4 (q, $J_{C\text{-}F}$ = 272 Hz), 42.8, 21.2. **^{19}F NMR (282 MHz, $CDCl_3$):** δ -65.6.

(*S*,*E*)-4-(3-phenylbut-1-en-1-yl)benzonitrile (140d)

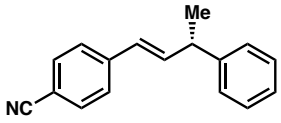

Prepared from methyl (*E*)-4-(2-bromovinyl)benzonitrile (**29w**, 42 mg, 0.2 mmol) and 1,3-dioxoisoindolin-2-yl 2-phenylpropanoate (**136**, 59 mg, 0.2 mmol) according to General Procedure 3. The crude residue was purified by column chromatography (silica gel, 0 to 3% Et_2O/hexane) to yield **140d** (42 mg, 91% yield) in 94% ee as a colorless oil. $\mathbf{R_f}$ = 0.42 (silica gel, 10% EtOAc/hexane, UV). **Chiral SFC**: (OB-H, 2.5 mL/min, 10% IPA in CO_2, λ = 254 nm): t_R (minor) = 9.5 min, t_R (major) = 10.1 min. $[\alpha]_D^{25}$ = –51° (c = 1.0, $CHCl_3$). **^{1}H NMR (400 MHz, $CDCl_3$):** δ 7.54 (d, *J* = 8.5 Hz, 2H), 7.40 (d, *J* = 8.3 Hz, 2H), 7.36 – 7.30 (m, 2H), 7.28 – 7.19 (m, 3H), 6.52 (dd, *J* = 15.9, 6.7 Hz, 1H), 6.40 (d, *J* = 16.0 Hz, 1H), 3.72 – 3.61 (m, 1H), 1.48 (d, *J* = 7.0 Hz, 3H). **^{13}C NMR (101 MHz, $CDCl_3$):** δ 144.7, 142.1, 139.5, 132.4, 128.7, 127.3, 127.2, 126.7, 126.6, 119.2, 110.2, 42.8, 21.0. **FTIR (NaCl, thin film, cm^{-1})**: 3027, 2967, 2872, 2225, 1646, 1604, 1504, 1493, 1452, 1412, 1176, 1013, 970, 866, 819, 763, 701. **HRMS (FAB, *m/z*)**: calc'd for $C_{17}H_{15}N$ $[M+H]^+$: 234.1283; found: 234.1265.

Methyl (*S*,*E*)-4-(3-phenylbut-1-en-1-yl)benzoate (140e)

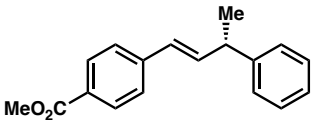

Prepared from methyl (*E*)-4-(2-bromovinyl)benzoate (**29x**, 48 mg, 0.2 mmol) and 1,3-dioxoisoindolin-2-yl 2-phenyl-propanoate (**136**, 59 mg, 0.2 mmol) according to General Procedure 3. The crude residue was purified by column chromatography (silica gel, 5% Et_2O/hexane) to yield **140e** (46 mg, 87% yield) in 95% ee as a colorless oil. $\mathbf{R_f}$ = 0.19 (silica gel, 5% Et_2O/hexane, UV). **Chiral SFC**: (OB-H, 2.5 mL/min, 20% IPA in CO_2, λ = 254 nm): t_R (minor) = 8.2 min, t_R (major) = 11.6 min. $[\alpha]_D^{25}$ = –44° (c = 1.0, $CHCl_3$). **^{1}H NMR (400 MHz, $CDCl_3$):** δ 7.96

(d, J = 8.4 Hz, 2H), 7.41 (d, J = 8.3 Hz, 2H), 7.37 – 7.30 (m, 2H), 7.30 – 7.20 (m, 3H), 6.53 (dd, J = 15.9, 6.5 Hz, 1H), 6.44 (d, J = 16.1 Hz, 1H), 3.91 (s, 3H), 3.72 – 3.62 (m, 1H), 1.49 (d, J = 7.0 Hz, 3H). **^{13}C NMR (101 MHz, $CDCl_3$):** δ 167.1, 145.2, 142.2, 138.2, 130.0, 128.7, 128.6, 127.9, 127.4, 126.5, 126.1, 52.2, 42.8, 21.2. **FTIR (NaCl, thin film, cm^{-1})**: 3025, 2963, 1718, 1605, 1492, 1433, 1411, 1276, 1177, 1108, 1015, 968, 759, 698. **LRMS (GC-MS, *m/z*)**: calc'd for $C_{18}H_{18}O_2$ $[M]^+$: 266.1; found: 266.1.

(*S*,*E*)-4-(3-phenylbut-1-en-1-yl)phenyl 4-methylbenzenesulfonate (140f)

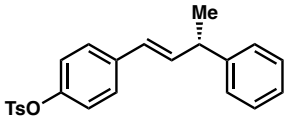

Prepared from (*E*)-4-(2-bromovinyl)phenyl 4-methyl-benzenesulfonate (**29y**, 71 mg, 0.2 mmol) and 1,3-dioxoisoindolin-2-yl 2-phenylpropanoate (**136**, 89 mg, 0.3 mmol) according to General Procedure 3 with the exception that 1.5 equiv NHP ester was used instead of 1.0 equiv. **Note:** The addition of excess NHP ester ensured full consumption of the vinyl bromide, which we found to be inseparable from the product when it remained in the crude reaction. The crude residue was purified by column chromatography (silica gel, hexane to 5% Et_2O/hexane) to yield **140f** (61 mg, 80% yield) in 94% ee as a colorless oil. $\mathbf{R_f}$ = 0.39 (silica gel, 10% EtOAc/hexane, UV). **Chiral SFC:** (OJ-H, 2.5 mL/min, 15% IPA in CO_2, λ = 254 nm): t_R (minor) = 12.2 min, t_R (major) = 13.7 min. $[\boldsymbol{\alpha}]_D^{25}$ = –24° (c = 1.0, $CHCl_3$). **^{1}H NMR (400 MHz, $CDCl_3$):** δ 7.70 (d, J = 8.4 Hz, 2H), 7.36 – 7.28 (m, 4H), 7.28 – 7.20 (m, 5H), 6.90 (d, J = 8.7 Hz, 2H), 6.39 – 6.30 (m, 2H), 3.69 – 3.58 (m, 1H), 2.45 (s, 3H), 1.46 (d, J = 7.0 Hz, 3H). **^{13}C NMR (101 MHz, $CDCl_3$):** δ 148.5, 145.4, 145.3, 136.7, 136.5, 132.4, 129.8, 128.6, 127.3, 127.2, 126.4, 122.5, 42.7, 21.8, 21.2. **FTIR (NaCl, thin film, cm^{-1})**: 3061, 3028, 2966, 2928, 2872, 1647, 1599, 1504, 1453, 1372, 1307, 1296, 1198, 1176,

1152, 1093, 1016, 969, 867, 841, 815, 763, 735, 700, 661. **HRMS (FAB, *m/z*)**: calc'd for $C_{23}H_{22}O_3S$ $[M+\cdot]^+$: 378.1290; found: 378.1283.

(*S*,*E*)-but-1-ene-1,3-diyldibenzene (140g)

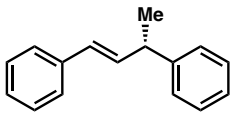

Prepared from (*E*)-(2-bromovinyl)benzene (**29z**, 37 mg, 0.2 mmol) and 1,3-dioxoisoindolin-2-yl 2-phenylpropanoate (**136**, 59 mg, 0.2 mmol) according to General Procedure 3. The crude residue was purified by column chromatography (silica gel, hexane) to yield **140g** (37 mg, 88% yield) in 96% ee as a colorless oil. $\mathbf{R_f}$ = 0.48 (silica gel, hexane, UV). **Chiral SFC**: (OJ-H, 2.5 mL/min, 5% IPA in CO_2, λ = 254 nm): t_R (minor) = 9.8 min, t_R (major) = 10.9 min. $[\boldsymbol{a}]_D^{25}$ = –35° (c = 1.0, $CHCl_3$). **^{1}H NMR (400 MHz, $CDCl_3$):** δ 7.43 – 7.29 (m, 8H), 7.29 – 7.21 (m, 2H), 6.51 – 6.38 (m, 2H), 3.73 – 3.65 (m, 1H), 1.52 (d, *J* = 7.0 Hz, 3H). **^{13}C NMR (101 MHz, $CDCl_3$):** δ 145.7, 137.7, 135.3, 128.6 (3C), 127.4, 127.2, 126.35, 126.27, 42.7, 21.4. **FTIR (NaCl, thin film, cm^{-1})**: 3080, 3058, 3024, 2964, 2928, 2871, 1599, 1492, 1448, 1371, 1010, 964, 742, 692. **HRMS (ESI-TOF, *m/z*)**: calc'd for $C_{16}H_{16}$ $[M–H_2+H]^+$: 207.1174; found: 207.1155. The optical rotation of **136** generated in the presence of **L2**·$NiBr_2$ was measured as $[\boldsymbol{a}]_D^{25}$ = –35° (c = 1.0, $CHCl_3$). Lit: $[\boldsymbol{a}]_D^{25}$ = –21.1° (c = 1.42, $CHCl_3$, *S* enantiomer, 95% ee).[92] Based on the literature precedent, we assign our product as the *S* enantiomer.

(*S*,*E*)-2-methoxy-5-(3-phenylbut-1-en-1-yl)pyridine (140h)

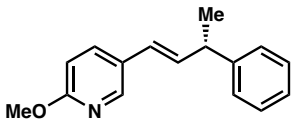

Prepared from (*E*)-5-(2-bromovinyl)-2-methoxypyridine (**29k**, 43 mg, 0.2 mmol) and 1,3-dioxoisoindolin-2-yl 2-phenyl-propanoate (**136**, 59 mg, 0.2 mmol) according to General Procedure 3. The crude residue

was purified by column chromatography (silica gel, 5% Et_2O/hexane) to yield **140h** (32 mg, 67% yield) in 95% ee as a colorless oil. $\mathbf{R_f}$ = 0.53 (silica gel, 10% EtOAc/hexane, UV). **Chiral SFC**: (OB-H, 2.5 mL/min, 15% IPA in CO_2, λ = 280 nm): t_R (major) = 5.0 min, t_R (minor) = 6.9 min. $[\alpha]_D^{25}$ = –33° (c = 1.0, $CHCl_3$). **^{1}H NMR (400 MHz, $CDCl_3$):** δ 8.06 (d, *J* = 2.4 Hz, 1H), 7.62 (dd, *J* = 8.7, 2.5 Hz, 1H), 7.35 – 7.28 (m, 2H), 7.28 – 7.18 (m, 3H), 6.67 (d, *J* = 8.6 Hz, 1H), 6.33 (d, *J* = 16.1 Hz, 1H), 6.26 (dd, *J* = 15.9, 6.3 Hz, 1H), 3.91 (s, 3H), 3.66 – 3.57 (m, 1H), 1.45 (d, *J* = 7.0 Hz, 3H). **^{13}C NMR (101 MHz, $CDCl_3$):** δ 163.4, 145.6, 145.3, 135.5, 134.7, 128.7, 127.4, 126.8, 126.4, 124.7, 110.9, 53.6, 42.8, 21.3. **FTIR (NaCl, thin film, cm^{-1})**: 2965, 1601, 1493, 1384, 1286, 1026, 962, 822, 762, 699. **HRMS (FAB, *m/z*)**: calc'd for $C_{16}H_{17}NO$ $[M+H]^+$: 240.1388; found: 240.1398.

(*S*,*E*)-5-phenylhex-3-en-1-yl benzoate (140i)

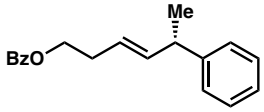

Prepared from (*E*)-4-bromobut-3-en-1-yl benzoate (**29j**, 51 mg, 0.2 mmol) and 1,3-dioxoisoindolin-2-yl 2-phenylpropanoate (**136**, 59 mg, 0.2 mmol) according to General Procedure 3. The crude residue was purified by column chromatography (silica gel, 5% Et_2O/hexane) to yield **140i** (49 mg, 88% yield) in 97% ee as a colorless oil. Spectral data matched those reported in literature.[44] $\mathbf{R_f}$ = 0.24 (silica gel, 5% Et_2O/hexane, UV). **Chiral SFC:** (OJ-H, 2.5 mL/min, 10% IPA in CO_2, λ = 254 nm): t_R (major) = 5.2 min, t_R (minor) = 6.1 min. $[\alpha]_D^{25}$ = +5° (c =1.0, $CHCl_3$). **^{1}H NMR (400 MHz, $CDCl_3$):** δ 8.04 – 8.00 (m, 2H), 7.59 – 7.53 (m, 1H), 7.46 – 7.40 (m, 2H), 7.29 – 7.23 (m, 2H), 7.22 – 7.15 (m, 3H), 5.77 (ddt, *J* = 15.4, 6.8, 1.3 Hz, 1H), 5.52 (dtd, *J* = 15.2, 6.8, 1.3 Hz, 1H), 4.36 (td, *J* = 6.7, 1.4 Hz, 2H), 3.50 – 3.42 (m, 1H), 2.54 – 2.46 (m, 2H), 1.35 (d, *J* = 7.0 Hz, 3H). **^{13}C NMR (101 MHz, $CDCl_3$):** δ 166.7, 146.0, 138.3, 133.0,

130.5, 129.7, 128.5, 128.4, 127.3, 126.2, 124.3, 64.4, 42.4, 32.2, 21.4.

(*S*,*E*)-(7-chlorohept-3-en-2-yl)benzene (140j)

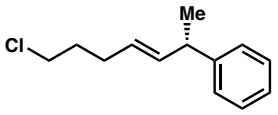

Prepared from (*E*)-1-bromo-5-chloropent-1-ene (**S2**, 37 mg, 0.2 mmol) and 1,3-dioxoisoindolin-2-yl 2-phenylpropanoate (**136**, 59 mg, 0.2 mmol) according to General Procedure 3. The crude residue was purified by column chromatography (silica gel, hexane) to yield **140j** (29 mg, 69% yield) in 91% ee as a colorless oil. $\mathbf{R}_f$ = 0.29 (silica gel, hexane, UV/CAM). **Chiral SFC:** (OD-H, 2.5 mL/min, 1% IPA in CO_2, λ = 210 nm): t_R (minor) = 5.4 min, t_R (major) = 6.0 min. $[\boldsymbol{\alpha}]_{\boldsymbol{D}}^{\mathbf{25}}$ = +9° (c =1.0, $CHCl_3$). **^{1}H NMR (400 MHz, $CDCl_3$):** δ 7.35 – 7.29 (m, 2H), 7.25 – 7.18 (m, 3H), 5.69 (ddt, *J* = 15.3, 6.8, 1.4 Hz, 1H), 5.43 (dtd, *J* = 15.1, 6.8, 1.1 Hz, 1H), 3.54 (t, *J* = 6.7 Hz, 2H), 3.50 – 3.40 (m, 1H), 2.23 – 2.16 (m, 2H), 1.90 – 1.82 (m, 2H), 1.36 (d, *J* = 7.0 Hz, 3H). **^{13}C NMR (101 MHz, $CDCl_3$):** δ 146.3, 136.7, 128.5, 127.24, 127.17, 126.1, 44.6, 42.4, 32.4, 29.7, 21.6. **FTIR (NaCl, thin film, cm^{-1})**: 3025, 2962, 2929, 2871, 1601, 1492, 1450, 1371, 1297, 1017, 969, 759, 698. **HRMS (FAB, *m/z*)**: calc'd for $C_{13}H_{17}Cl$ [M–H_2+H]$^+$: 207.0940; found: 207.0910.

(*S*,*E*)-dec-3-en-2-ylbenzene (140k)

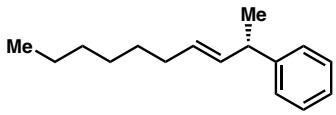

Prepared from (*E*)-1-bromooct-1-ene (**29aa**, 38 mg, 0.2 mmol) and 1,3-dioxoisoindolin-2-yl 2-phenylpropanoate (**136**, 59 mg, 0.2 mmol) according to General Procedure 3. The crude residue was purified by column chromatography (silica gel, hexane) to yield **140k** (31 mg, 72% yield) in 94% ee as a colorless oil. $\mathbf{R}_f$ = 0.59 (silica gel, hexane, UV/CAM). **Chiral SFC:** (OJ-H, 2.5 mL/min,

1% IPA in CO_2, λ = 210 nm): t_R (minor) = 3.9 min, t_R (major) = 4.5 min. $[\alpha]_D^{25}$ = +4° (c = 0.9, $CHCl_3$). **^{1}H NMR (400 MHz, $CDCl_3$):** δ 7.34 – 7.27 (m, 2H), 7.25 – 7.15 (m, 3H), 5.60 (ddt, *J* = 15.3, 6.6, 1.4 Hz, 1H), 5.46 (dtd, *J* = 15.1, 6.6, 1.2 Hz, 1H), 3.47 – 3.38 (m, 1H), 2.06 – 1.97 (m, 2H), 1.40 – 1.22 (m, 11H), 0.95 – 0.83 (m, 3H). **^{13}C NMR (101 MHz, $CDCl_3$):** δ 146.7, 135.0, 129.5, 128.4, 127.3, 126.0, 42.4, 32.7, 31.9, 29.6, 29.0, 22.8, 21.7, 14.3. **FTIR (NaCl, thin film, cm^{-1})**: 3025, 2959, 2925, 2854, 1492, 1451, 1371, 1016, 965, 758, 697. **LRMS (GC-MS, *m/z*)**: calc'd for $C_{16}H_{24}$ $[M]^+$: 216.2; found: 216.2.

(*S*,*E*)-trimethyl((5-phenylhex-3-en-1-yl)oxy)silane (140l)

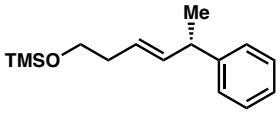

Prepared from (*E*)-4-bromobut-3-en-1-ol (**29i**, 30 mg, 0.2 mmol) and 1,3-dioxoisoindolin-2-yl 2-phenylpropanoate (**136**, 59 mg, 0.2 mmol) according to General Procedure 3 with the exception that 2.0 equiv TMSBr was used instead of 1.0 equiv. The reaction was quenched with water instead of 1 M HCl to prevent decomposition of the primary silyl ether. **Note:** An acidic workup yielded a mixture of the silyl ether and alcohol product, however the alcohol was inseparable from the phthalimide byproduct. The crude residue was purified by column chromatography (florisil, hexane to 1% Et_2O/hexane) to yield **140l** (33 mg, 66% yield) as a colorless oil. **Note:** The two enantiomers of the racemic silyl ether were inseparable by chiral SFC. **R_f** = 0.67 (silica gel, 10% EtOAc/hexane, UV/CAM). $[\alpha]_D^{25}$ = +6° (c = 1.0, $CHCl_3$). **^{1}H NMR (400 MHz, $CDCl_3$):** δ 7.35 – 7.28 (m, 2H), 7.25 – 7.17 (m, 3H), 5.69 (ddt, *J* = 15.4, 6.7, 1.3 Hz, 1H), 5.47 (dtd, *J* = 15.3, 6.9, 1.4 Hz, 1H), 3.61 (t, *J* = 7.0 Hz, 2H), 3.49 – 3.40 (m, 1H), 2.28 (qt, *J* = 7.0, 1.1 Hz, 2H), 1.36 (d, *J* = 7.1 Hz, 3H), 0.13 (s, 9H). **^{13}C NMR (101 MHz, $CDCl_3$):** δ 146.3, 137.3, 128.5, 127.3, 126.1, 125.4, 62.7, 42.5, 36.2, 21.5, -0.3.

FTIR (NaCl, thin film, cm^{-1}): 2961, 2930, 2902, 2863, 1602, 1493, 1452, 1382, 1251, 1094, 968, 940, 876, 841, 758, 748, 699. **HRMS (FAB, *m/z*)**: calc'd for $C_{15}H_{24}OSi$ $[M+H]^+$: 249.1675; found: 249.1684.

(*S*,*E*)-5-phenylhex-3-en-1-ol (S31)

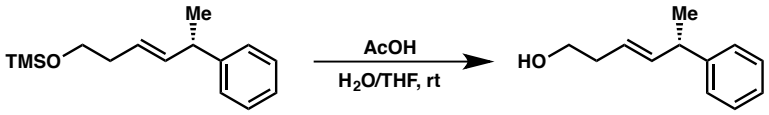

Deprotection of Silyl Ether: Silyl ether **140l** (33.0 mg, 0.132 mmol, 1 equiv) was dissolved in a solution of acetic acid (0.5 mL), water (0.5 mL), and THF (2.5 mL) in a 20 mL vial equipped with a magnetic stir bar and stirred at room temperature for 15 min. The reaction was slowly quenched with a solution of saturated $NaHCO_3$ until the pH was slightly basic (approx. 15 mL), extracted with Et_2O (3 x 10 mL), dried with $MgSO_4$, filtered, and concentrated under reduced pressure to yield **S31** (22.6 mg, 97% yield) in 89% ee as a colorless oil. Spectral data matched those reported in literature.[44] $\mathbf{R}_f$ = 0.11 (silica gel, 10% EtOAc/hexane, UV/CAM). **Chiral SFC:** (OB-H, 2.5 mL/min, 3% IPA in CO_2, λ = 210 nm): t_R (minor) = 6.9 min, t_R (major) = 7.5 min. $[\boldsymbol{a}]_{\boldsymbol{D}}^{\mathbf{25}}$ = +9° (c = 1.0, $CHCl_3$). **^{1}H NMR (400 MHz, $CDCl_3$):** δ 7.34 – 7.27 (m, 2H), 7.25 – 7.16 (m, 3H), 5.76 (ddt, *J* = 15.4, 6.7, 1.4 Hz, 1H), 5.45 (dtd, *J* = 15.3, 7.0, 1.4 Hz, 1H), 3.65 (t, *J* = 6.3 Hz, 2H), 3.52 – 3.42 (m, 1H), 2.30 (q, *J* = 6.3 Hz, 2H), 1.54 (s, 1H), 1.37 (d, *J* = 7.1 Hz, 3H). **^{13}C NMR (101 MHz, $CDCl_3$):** δ 146.1, 138.8, 128.6, 127.2, 126.2, 124.8, 62.2, 42.5, 36.0, 21.6.

(*S*,*E*)-6-methyl-2-(3-phenylbut-1-en-1-yl)-1,3,6,2-dioxazaborocane-4,8-dione (140m)

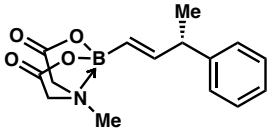

Prepared from *trans*-1-bromovinylboronic acid MIDA ester (**29ab**, 52 mg, 0.2 mmol) and 1,3-dioxoisoindolin-2-yl 2-phenylpropanoate (**136**, 59 mg, 0.2 mmol) according to General Procedure 3. The crude residue was purified by column chromatography (silica gel, 10% EtOAc/hexane to 100% EtOAc) to yield **140m** (25 mg, 43% yield) in 97% ee as a yellow solid. **Note:** The ^{1}H NMR contains two minor impurities that were identified as DMA and methyliminodiacetic acid. $\mathbf{R_f}$ = 0.35 (silica gel, EtOAc, UV/$KMnO_4$). **m.p.** = 144–146 °C. **Chiral SFC:** (OJ-H, 2.5 mL/min, 30% IPA in CO_2, λ = 210 nm): t_R (major) = 5.5 min, t_R (minor) = 10.2 min. $[\boldsymbol{\alpha}]_D^{25}$ = +0.5° ± 1.1° (c = 1.0, $CHCl_3$). **Note:** This compound shows low optical rotation. **^{1}H NMR (400 MHz, $CDCl_3$):** δ 7.32 – 7.23 (m, 2H), 7.21 – 7.13 (m, 3H), 6.32 (dd, *J* = 17.7, 6.4 Hz, 1H), 5.38 (dd, *J* = 17.7, 1.5 Hz, 1H), 3.92 (dd, *J* = 16.7, 4.5 Hz, 2H), 3.59 (dd, *J* = 16.8, 13.9 Hz, 2H), 3.54 – 3.46 (m, 1H), 2.69 (s, 3H), 1.36 (d, *J* = 7.0 Hz, 3H). **^{13}C NMR (101 MHz, $CDCl_3$):** δ 168.34, 168.27, 151.7, 145.3, 128.6, 127.4, 126.3, 61.53, 61.49, 47.0, 44.8, 20.8. **FTIR (NaCl, thin film, cm^{-1})**: 2963, 1762, 1636, 1492, 1338, 1290, 1246, 1193, 1154, 1126, 1090, 1025, 1007, 956, 867, 761, 702. **HRMS (FAB, *m/z*)**: calc'd for $C_{15}H_{18}BNO_4$ $[M+H]^+$: 288.1407; found: 288.1414.

(*S*,*E*)-trimethyl(3-phenylbut-1-en-1-yl)silane (140n)

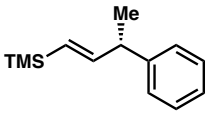

Prepared from (*E*)-(2-bromovinyl)trimethylsilane (**29o**, 36 mg, 0.2 mmol) and 1,3-dioxoisoindolin-2-yl 2-phenylpropanoate (**136**, 59 mg, 0.2 mmol) according to General Procedure 3. Alkenyl bromide **29o** is reported to be air

sensitive, and was added to the reaction while inside the glovebox. The crude residue was purified by column chromatography (silica gel, hexane) to yield **140n** (28 mg, 68% yield) in 97% ee as a colorless oil. $\mathbf{R_f}$ = 0.65 (silica gel, hexane, UV/CAM). **Chiral SFC:** (OJ-H, 2.5 mL/min, CO_2, λ = 210 nm): t_R (major) = 1.8 min, t_R (minor) = 2.0 min. $[\boldsymbol{a}]_D^{25}$ = –2.4° ± 0.2° (c = 0.9, $CHCl_3$). **^{1}H NMR (400 MHz, $CDCl_3$):** δ 7.35 – 7.28 (m, 2H), 7.24 – 7.18 (m, 3H), 6.19 (dd, *J* = 18.6, 5.9 Hz, 1H), 5.68 (dd, *J* = 18.6, 1.6 Hz, 1H), 3.52 – 3.44 (m, 1H), 1.36 (d, *J* = 7.0 Hz, 3H), 0.06 (s, 9H). **^{13}C NMR (101 MHz, $CDCl_3$):** δ 150.8, 145.8, 128.5, 128.1, 127.5, 126.2, 45.6, 20.9, -1.0. **FTIR (NaCl, thin film, cm^{-1})**: 3028, 2958, 1612, 1602, 1492, 1452, 1248, 1009, 987, 868, 837, 759, 698. **LRMS (GC-MS, *m/z*)**: calc'd for $C_{13}H_{20}Si$ $[M]^+$: 204.1; found: 204.1.

(*S*,*E*)-4,4'-(but-1-ene-1,3-diyl)bis(methoxybenzene) (141a)

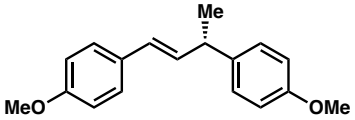

Prepared from (*E*)-1-(2-bromovinyl)-4-methoxybenzene (**86**, 43 mg, 0.2 mmol) and 1,3-dioxoisoindolin-2-yl 2-(4-methoxyphenyl)propanoate (**62a**, 65 mg, 0.2 mmol) according to General Procedure 3. The crude residue was purified by column chromatography (silica gel, 10% toluene/hexane then 10% Et_2O/hexane) to yield **141a** (42 mg, 78% yield) in 93% ee as a white solid. Spectral data matched those reported in literature.[44] $\mathbf{R_f}$ = 0.45 (silica gel, 10% EtOAc/hexane, UV). **m.p.** = 51–59 °C. **Chiral SFC**: (AD-H, 2.5 mL/min, 20% IPA in CO_2, λ = 235 nm): t_R (major) = 7.0 min, t_R (minor) = 8.5 min. $[\boldsymbol{a}]_D^{25}$ = –34° (c = 1.0, $CHCl_3$). **^{1}H NMR (400 MHz, $CDCl_3$)**: δ 7.32 (d, *J* = 8.7 Hz, 2H), 7.22 (d, *J* = 8.5 Hz, 2H), 6.89 (d, *J* = 8.8 Hz, 2H), 6.86 (d, *J* = 8.8 Hz, 2H), 6.37 (d, *J* = 16.0 Hz, 1H), 6.25 (dd, *J* = 15.9, 6.6 Hz, 1H), 3.82 (s, 3H), 3.81 (s, 3H), 3.65 – 3.55 (m, 1H), 1.46 (d, *J* = 7.0 Hz, 3H). **^{13}C NMR (101 MHz, $CDCl_3$):**

δ 158.9, 158.0, 138.1, 133.6, 130.5, 128.3, 127.7, 127.3, 114.0, 113.9, 55.4 (2C), 41.8, 21.6.

(*S*,*E*)-1-methoxy-4-(3-(4-(trifluoromethyl)phenyl)but-1-en-1-yl)benzene (141b)

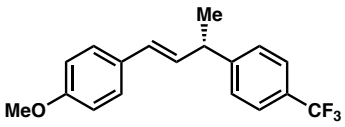

Prepared from (*E*)-1-(2-bromovinyl)-4-methoxybenzene (**86**, 43 mg, 0.2 mmol) and 1,3-dioxoisoindolin-2-yl 2-(4-(trifluoromethyl)phenyl)propanoate (**62b**, 73 mg, 0.2 mmol) according to General Procedure 3. The crude residue was purified by column chromatography (silica gel, 5% toluene/hexane) to yield **141b** (40 mg, 65% yield) in 88% ee as a white solid. $\mathbf{R_f}$ = 0.48 (silica gel, 10% EtOAc/hexane, UV). **m.p.** = 67–70 °C. **Chiral SFC**: (OB-H, 2.5 mL/min, 5% IPA in CO_2, λ = 254 nm): t_R (major) = 6.5 min, t_R (minor) = 7.5 min. $[\boldsymbol{\alpha}]_D^{25}$ = –39° (c = 1.0, $CHCl_3$). **^{1}H NMR (400 MHz, $CDCl_3$):** δ 7.58 (d, *J* = 8.1 Hz, 2H), 7.39 (d, *J* = 8.4 Hz, 2H), 7.30 (d, *J* = 8.7 Hz, 2H), 6.85 (d, *J* = 8.8 Hz, 2H), 6.38 (d, *J* = 16.0 Hz, 1H), 6.21 (dd, *J* = 15.9, 6.8 Hz, 1H), 3.81 (s, 3H), 3.73 – 3.64 (m, 1H), 1.48 (d, *J* = 7.0 Hz, 3H). **^{13}C NMR (101 MHz, $CDCl_3$):** δ 159.1, 150.1 (q, $J_{C\text{-}F}$ = 1.4 Hz), 132.0, 130.1, 128.8, 128.6 (q, $J_{C\text{-}F}$ = 32.3 Hz), 127.8, 127.4, 125.5 (q, $J_{C\text{-}F}$ = 3.8 Hz), 124.5 (q, $J_{C\text{-}F}$ = 271.9 Hz), 114.1, 55.4, 42.6, 21.3. **^{19}F NMR (282 MHz, $CDCl_3$):** δ -65.4. **FTIR (NaCl, thin film, cm^{-1})**: 2965, 1608, 1512, 1252, 1174, 1164, 1122, 1069, 1036, 1016, 967, 840, 818. **HRMS (EI, *m/z*)**: calc'd for $C_{18}H_{17}F_3O$ $[M+\cdot]^+$: 306.1232; found: 306.1241.

(*S*,*E*)-1-bromo-4-(4-(4-methoxyphenyl)but-3-en-2-yl)benzene (141c)

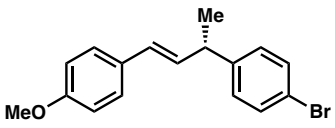

Prepared from (*E*)-1-(2-bromovinyl)-4-methoxybenzene (**86**, 43 mg, 0.2 mmol) and 1,3-dioxoisoindolin-2-yl 2-(4-

bromophenyl)propanoate (**62c**, 75 mg, 0.2 mmol) according to General Procedure 3. The crude residue was purified by column chromatography (silica gel, 5 to 10% toluene/hexane) to yield **141c** (51 mg, 80% yield) in 90% ee as a white solid. Spectral data matched those reported in literature.[44] $\mathbf{R_f}$ = 0.59 (silica gel, 10% EtOAc/hexane, UV). **m.p.** = 74–76 °C. **Chiral SFC**: (OB-H, 2.5 mL/min, 35% IPA in CO_2, λ = 254 nm): t_R (major) = 5.3 min, t_R (minor) = 8.5 min. $[\boldsymbol{a}]_D^{25}$ = –32° (c = 1.0, $CHCl_3$). **^{1}H NMR (400 MHz, $CDCl_3$):** δ 7.45 (d, *J* = 8.5 Hz, 2H), 7.30 (d, *J* = 8.6 Hz, 2H), 7.16 (d, *J* = 8.3 Hz, 2H), 6.86 (d, *J* = 8.8 Hz, 2H), 6.36 (d, *J* = 16.0 Hz, 1H), 6.20 (dd, *J* = 15.9, 6.7 Hz, 1H), 3.81 (s, 3H), 3.64 – 3.55 (m, 1H), 1.45 (d, *J* = 7.0 Hz, 3H). **^{13}C NMR (101 MHz, $CDCl_3$):** δ 159.0, 145.0, 132.5, 131.6, 130.2, 129.2, 128.4, 127.4, 120.0, 114.0, 55.4, 42.1, 21.3.

(*S*,*E*)-1-fluoro-4-(4-(4-methoxyphenyl)but-3-en-2-yl)benzene (141d)

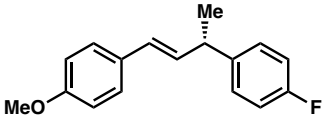

Prepared from (*E*)-1-(2-bromovinyl)-4-methoxybenzene (**86**, 43 mg, 0.2 mmol) and 1,3-dioxoisoindolin-2-yl 2-(4-fluorophenyl)propanoate (**62d**, 63 mg, 0.2 mmol) according to General Procedure 3. The crude residue was purified by column chromatography (silica gel, 5 to 30% toluene/hexane) to yield **141d** (44 mg, 85% yield) in 92% ee as a colorless oil. Spectral data matched those reported in literature.[44] $\mathbf{R_f}$ = 0.70 (silica gel, 10% EtOAc/hexane, UV). **Chiral SFC**: (OB-H, 2.5 mL/min, 15% IPA in CO_2, λ = 280 nm): t_R (major) = 5.9 min, t_R (minor) = 8.3 min. $[\boldsymbol{a}]_D^{25}$ = –29° (c = 1.0, $CHCl_3$). **^{1}H NMR (400 MHz, $CDCl_3$):** δ 7.34 – 7.28 (m, 2H), 7.28 – 7.20 (m, 2H), 7.06 – 6.98 (m, 2H), 6.89 – 6.83 (m, 2H), 6.40 – 6.32 (m, 1H), 6.23 (dd, *J* = 15.9, 6.7 Hz, 1H), 3.81 (s, 3H), 3.67 – 3.58 (m, 1H), 1.46 (d, *J* = 7.0 Hz, 3H). **^{13}C NMR (101 MHz, $CDCl_3$):** δ 161.5 (d, $J_{C\text{-}F}$ = 243.7 Hz), 159.0, 141.6 (d, $J_{C\text{-}F}$

= 3.1 Hz), 133.0, 130.3, 128.8 (d, $J_{C\text{-}F}$ = 7.8 Hz), 128.1, 127.4, 115.3 (d, $J_{C\text{-}F}$ = 21.2 Hz), 114.1, 55.4, 41.9, 21.6. **^{19}F NMR (282 MHz, $CDCl_3$):** δ -123.56 (tt, $J_{F\text{-}H}$ = 8.9, 5.4 Hz).

(*S*,*E*)-4-(4-(4-methoxyphenyl)but-3-en-2-yl)-*N*,*N*-dimethylaniline (141e)

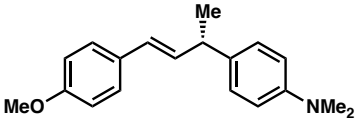

Prepared from (*E*)-1-(2-bromovinyl)-4-methoxybenzene (**89**, 43 mg, 0.2 mmol) and 1,3-dioxoisoindolin-2-yl 2-(4-(dimethylamino)phenyl)propanoate (**62e**, 68 mg, 0.2 mmol) according to General Procedure 3. The reaction was quenched with water instead of 1 M HCl. The crude residue was purified by column chromatography (silica gel, hexane to 10% Et_2O/hexane) to yield **141e** (37 mg, 66% yield) in 94% ee as a white solid. $\mathbf{R_f}$ = 0.28 (silica gel, 10% EtOAc/hexane, UV). **m.p.** = 72–75 °C. **Chiral SFC**: (AD-H, 2.5 mL/min, 20% IPA in CO_2, λ = 280 nm): t_R (major) = 8.2 min, t_R (minor) = 10.6 min. $[\boldsymbol{a}]_{\boldsymbol{D}}^{\mathbf{25}}$ = –29° (c = 1.1, $CHCl_3$). **^{1}H NMR (400 MHz, $CDCl_3$):** δ 7.29 (d, *J* = 8.7 Hz, 2H), 7.15 (d, *J* = 8.5 Hz, 2H), 6.83 (d, *J* = 8.8 Hz, 2H), 6.73 (d, *J* = 8.7 Hz, 2H), 6.34 (dd, *J* = 16.2, 0.8 Hz, 1H), 6.23 (dd, *J* = 15.9, 6.6 Hz, 1H), 3.80 (s, 3H), 3.58 – 3.50 (m, 1H), 2.93 (s, 6H), 1.42 (d, *J* = 7.1 Hz, 3H). **^{13}C NMR (101 MHz, $CDCl_3$):** δ 158.8, 149.3, 134.1, 130.7, 128.0, 127.3, 114.0, 113.1, 55.4, 41.6, 41.0, 21.5. **FTIR (NaCl, thin film, cm^{-1})**: 2958, 1608, 1518, 1509, 1456, 1341, 1249, 1173, 1034, 966, 948, 815. **HRMS (FAB, *m/z*)**: calc'd for $C_{19}H_{23}NO$ $[M+\cdot]^+$: 281.1780; found: 281.1774.

(*S*,*E*)-1,2-dichloro-4-(4-(4-methoxyphenyl)but-3-en-2-yl)benzene (141f)

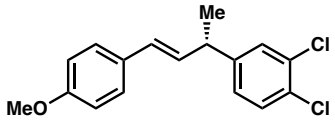

Prepared from (*E*)-1-(2-bromovinyl)-4-methoxybenzene (**86**, 43 mg, 0.2 mmol) and 1,3-dioxoisoindolin-2-yl 2-(3,4-

dichlorophenyl)propanoate (**62f**, 73 mg, 0.2 mmol) according to General Procedure 3. The crude residue was purified by column chromatography (silica gel, hexane to 5% Et_2O/hexane) to yield **141f** (48 mg, 77% yield) in 82% ee as a colorless oil. $\mathbf{R_f}$ = 0.51 (silica gel, 10% EtOAc/hexane, UV). **Chiral SFC**: (OB-H, 2.5 mL/min, 25% IPA in CO_2, λ = 280 nm): t_R (major) = 6.5 min, t_R (minor) = 9.0 min. $[\alpha]_D^{25}$ = –26° (c = 1.1, $CHCl_3$). **^{1}H NMR (400 MHz, $CDCl_3$):** δ 7.37 (d, *J* = 8.3 Hz, 1H), 7.35 (d, *J* = 2.1 Hz, 1H), 7.32 – 7.27 (m, 2H), 7.10 (ddd, *J* = 8.2, 2.1, 0.6 Hz, 1H), 6.87 – 6.82 (m, 2H), 6.35 (dd, *J* = 15.9, 1.3 Hz, 1H), 6.15 (dd, *J* = 15.9, 6.8 Hz, 1H), 3.81 (s, 3H), 3.62 – 3.53 (m, 1H), 1.43 (d, *J* = 7.0 Hz, 3H). **^{13}C NMR (101 MHz, $CDCl_3$):** δ 159.2, 146.3, 132.4, 131.7, 130.5, 130.1, 130.0, 129.4, 128.9, 127.4, 127.0, 114.1, 55.4, 41.9, 21.2. **FTIR (NaCl, thin film, cm^{-1})**: 2964, 1607, 1511, 1466, 1299, 1250, 1174, 1106, 1030, 967, 815. **HRMS (FAB, *m/z*)**: calc'd for $C_{17}H_{16}Cl_2O$ $[M+\cdot]^+$: 306.0578; found: 306.0582.

(*S*,*E*)-1-methoxy-4-(3-phenylpent-1-en-1-yl)benzene (141g)

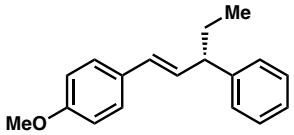

Prepared from (*E*)-1-(2-bromovinyl)-4-methoxybenzene (**86**, 43 mg, 0.2 mmol) and 1,3-dioxoisoindolin-2-yl 2-phenylbutanoate (**62g**, 62 mg, 0.2 mmol) according to General Procedure 3. The crude residue was purified by column chromatography (silica gel, 10 to 20% toluene/hexane) to yield **141g** (40 mg, 80% yield) in 97% ee as a colorless oil. Spectral data matched those reported in literature.[44] $\mathbf{R_f}$ = 0.59 (silica gel, 10% EtOAc/hexane, UV). **Chiral SFC:** (OB-H, 2.5 mL/min, 15% IPA in CO_2, λ = 254 nm): t_R (minor) = 8.0 min, t_R (major) = 9.9 min. $[\alpha]_D^{25}$ = –46° (c = 1.0, $CHCl_3$). **^{1}H NMR (400 MHz, $CDCl_3$):** δ 7.37 – 7.19 (m, 7H), 6.84 (d, *J* = 8.8 Hz, 2H), 6.37 (d, *J* = 15.8 Hz, 1H), 6.21 (dd, *J* = 15.8, 7.8 Hz, 1H), 3.80 (s, 3H), 3.35 – 3.26 (m,

1H), 1.90 – 1.78 (m, 2H), 0.93 (t, *J* = 7.4 Hz, 3H). **^{13}C NMR (101 MHz, $CDCl_3$):** δ 158.9, 144.9, 132.2, 130.6, 128.9, 128.6, 127.8, 127.3, 126.2, 114.0, 55.4, 51.1, 29.0, 12.5.

(*S*,*E*)-(4-(4-methoxyphenyl)but-3-ene-1,2-diyl)dibenzene (141h)

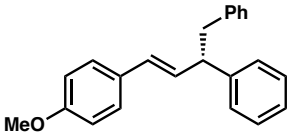

Prepared from (*E*)-1-(2-bromovinyl)-4-methoxybenzene (**86**, 43 mg, 0.2 mmol) and 1,3-dioxoisoindolin-2-yl 2,3-diphenylpropanoate (**62h**, 74 mg, 0.2 mmol) according to General Procedure 3. The crude residue was purified by column chromatography (silica gel, 10% toluene/hexane then 10% Et_2O/hexane) to yield **141h** (49 mg, 78% yield) in 95% ee as a white solid. Spectral data matched those reported in literature.[44] **R_f** = 0.48 (silica gel, 10% EtOAc/hexane, UV). **m.p.** = 72–73 °C. **Chiral SFC:** (AS-H, 2.5 mL/min, 10% IPA in CO_2, λ = 254 nm): t_R (minor) = 6.0 min, t_R (major) = 6.5 min. $[\alpha]_D^{25}$ = +19° (c = 1.0, $CHCl_3$). **^{1}H NMR (400 MHz, $CDCl_3$):** δ 7.34 – 7.13 (m, 10H), 7.10 (d, *J* = 8.8 Hz, 2H), 6.83 (d, *J* = 8.8 Hz, 2H), 6.30 (dd, *J* = 15.9, 6.3 Hz, 1H), 6.25 (d, *J* = 15.9 Hz, 1H), 3.80 (s, 3H), 3.78 – 3.67 (m, 1H), 3.19 – 3.06 (m, 2H). **^{13}C NMR (101 MHz, $CDCl_3$):** δ 158.9, 144.1, 140.2, 131.3, 130.4, 129.53, 129.49, 128.5, 128.2, 128.0, 127.4, 126.4, 126.0, 114.0, 55.4, 51.0, 42.9.

(*S*,*E*)-1-methoxy-4-(4-methyl-3-phenylpent-1-en-1-yl)benzene (141i)

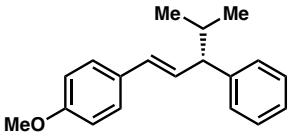

Prepared from (*E*)-1-(2-bromovinyl)-4-methoxybenzene (**86**, 43 mg, 0.2 mmol) and 1,3-dioxoisoindolin-2-yl 3-methyl-2-phenylbutanoate (**62i**, 65 mg, 0.2 mmol) according to General Procedure 3. The crude residue was purified by column chromatography (silica gel, 10 to 20% toluene/hexane) to yield **141i** (25 mg, 47% yield) in 97% ee as a white solid. **R_f** = 0.58 (silica gel, 10%

EtOAc/hexane, UV). **m.p.** = 67–68 °C. **Chiral SFC**: (AS-H, 2.5 mL/min, 10% IPA in CO_2, λ = 254 nm): t_R (minor) = 4.8 min, t_R (major) = 6.1 min. $[\boldsymbol{a}]_D^{25}$ = –39° (c = 1.0, $CHCl_3$). **^{1}H NMR (400 MHz, $CDCl_3$):** δ 7.34 – 7.28 (m, 4H), 7.26 – 7.17 (m, 3H), 6.84 (d, *J* = 8.8 Hz, 2H), 6.36 (d, *J* = 15.7 Hz, 1H), 6.26 (dd, *J* = 15.7, 8.8 Hz, 1H), 3.80 (s, 3H), 3.04 (t, *J* = 8.8 Hz, 1H), 2.14 – 1.96 (m, 1H), 1.02 (d, *J* = 6.7 Hz, 3H), 0.82 (d, *J* = 6.6 Hz, 3H). **^{13}C NMR (101 MHz, $CDCl_3$):** δ 158.9, 144.7, 131.2, 130.6, 129.8, 128.5, 128.1, 127.3, 126.1, 114.0, 57.8, 55.4, 33.4, 21.3, 21.1. **FTIR (NaCl, thin film, cm^{-1})**: 2953, 1600, 1509, 1450, 1251, 1027, 966, 838, 701. **LRMS (GC-MS, *m/z*)**: calc'd for $C_{19}H_{22}O$ $[M]^+$: 266.2; found: 266.1.

(*S*,*E*)-*tert*-butyl((4-(4-methoxyphenyl)-2-phenylbut-3-en-1-yl)oxy)dimethylsilane (141j)

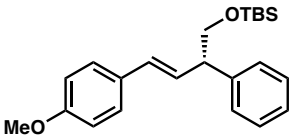

Prepared from (*E*)-1-(2-bromovinyl)-4-methoxybenzene (**86**, 43 mg, 0.2 mmol) and 1,3-dioxoisoindolin-2-yl 3-((*tert*-butyldimethylsilyl)oxy)-2-phenylpropanoate (**62j**, 74 mg, 0.2 mmol) according to General Procedure 3. The crude residue was purified by column chromatography (silica gel, 10% toluene/hexane then 10% Et_2O/hexane) to yield **141j** (43 mg, 58% yield) in 98% ee as a colorless oil. $\mathbf{R_f}$ = 0.55 (silica gel, 10% EtOAc/hexane, UV). **Chiral SFC**: (OJ-H, 2.5 mL/min, 10% IPA in CO_2, λ = 254 nm): t_R (major) = 3.4 min, t_R (minor) = 5.8 min. $[\boldsymbol{a}]_D^{25}$ = –14° (c = 1.0, $CHCl_3$). **^{1}H NMR (400 MHz, $CDCl_3$):** δ 7.39 – 7.29 (m, 6H), 7.28 – 7.23 (m, 1H), 6.87 (d, *J* = 8.8 Hz, 2H), 6.44 (d, *J* = 16.0 Hz, 1H), 6.34 (dd, *J* = 15.9, 7.2 Hz, 1H), 3.98 – 3.89 (m, 2H), 3.83 (s, 3H), 3.70 – 3.63 (m, 1H), 0.89 (s, 9H), 0.02 (s, 3H), 0.01 (s, 3H). **^{13}C NMR (101 MHz, $CDCl_3$):** δ 159.0, 142.3, 130.7, 130.5, 128.8, 128.45, 128.42,

127.4, 126.6, 114.0, 67.5, 55.4, 51.8, 26.0, 18.4, -5.2, -5.3. **FTIR (NaCl, thin film, cm^{-1})**: 2953, 2928, 2892, 2855, 1607, 1511, 1463, 1250, 1174, 1106, 1036, 836, 775, 699. **HRMS (FAB, *m/z*)**: calc'd for $C_{23}H_{32}O_2Si$ $[M–H_2+H]^+$: 367.2093; found: 367.2081.

(*S*,*E*)-1-methoxy-4-(3-phenylhexa-1,5-dien-1-yl)benzene (141k)

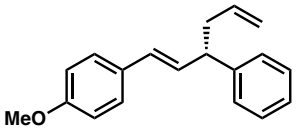

Prepared from (*E*)-1-(2-bromovinyl)-4-methoxybenzene (**86**, 43 mg, 0.2 mmol) and 1,3-dioxoisoindolin-2-yl 2-phenylpent-4-enoate (**62k**, 53 mg, 0.2 mmol) according to General Procedure 3. The crude residue was purified by column chromatography (silica gel, 5 to 20% toluene/hexane) to yield **141k** (42 mg, 79% yield) in 96% ee as a colorless oil. $\mathbf{R}_f$ = 0.55 (silica gel, 10% EtOAc/hexane, UV). **Chiral SFC**: (OJ-H, 2.5 mL/min, 10% IPA in CO_2, λ = 254 nm): t_R (minor) = 7.8 min, t_R (major) = 8.5 min. $[\alpha]_D^{25}$ = –19° (c =1.0, $CHCl_3$). **^{1}H NMR (400 MHz, $CDCl_3$):** δ 7.31 – 7.14 (m, 7H), 6.78 (d, *J* = 8.8 Hz, 2H), 6.30 (d, *J* = 15.9 Hz, 1H), 6.18 (dd, *J* = 15.8, 7.5 Hz, 1H), 5.73 (ddt, *J* = 17.1, 10.2, 6.9 Hz, 1H), 5.01 (ddt, *J* = 17.0, 2.0, 1.5 Hz, 1H), 4.95 (ddt, *J* = 10.2, 2.1, 1.0 Hz, 1H), 3.74 (s, 3H), 3.50 – 3.42 (m, 1H), 2.57 – 2.51 (m, 2H). **^{13}C NMR (101 MHz, $CDCl_3$):** δ 159.0, 144.2, 136.8, 131.5, 130.4, 129.2, 128.6, 127.8, 127.4, 126.4, 116.4, 114.0, 55.4, 49.1, 40.4. **FTIR (NaCl, thin film, cm^{-1})**: 3025, 2913, 2834, 1606, 1509, 1246, 1173, 1032, 963, 911, 756, 698. **HRMS (EI, *m/z*)**: calc'd for $C_{19}H_{20}O$ $[M+\cdot]^+$: 264.1514; found: 264.1521.

(*S*,*E*)-1-(6-chloro-3-phenylhex-1-en-1-yl)-4-methoxybenzene (141l)

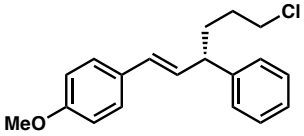

Prepared from (*E*)-1-(2-bromovinyl)-4-methoxybenzene (**86**, 43 mg, 0.2 mmol) and 1,3-dioxoisoindolin-2-yl 5-chloro-2-

phenylpentanoate (**62l**, 72 mg, 0.2 mmol) according to General Procedure 3. The crude residue was purified by column chromatography (silica gel, 5% Et_2O/hexane) to yield **141l** (52 mg, 87% yield) in 93% ee as a colorless oil. $\mathbf{R_f}$ = 0.53 (silica gel, 10% EtOAc/hexane, UV). **Chiral SFC**: (AS-H, 2.5 mL/min, 15% IPA in CO_2, λ = 254 nm): t_R (minor) = 3.7 min, t_R (major) = 4.7 min. $[\boldsymbol{a}]_D^{25}$ = –21° (c = 1.0, $CHCl_3$). **^{1}H NMR (400 MHz, $CDCl_3$):** δ 7.37 – 7.21 (m, 7H), 6.85 (d, *J* = 8.8 Hz, 2H), 6.38 (d, *J* = 15.8 Hz, 1H), 6.20 (dd, *J* = 15.8, 7.9 Hz, 1H), 3.81 (s, 3H), 3.56 (t, *J* = 6.5 Hz, 2H), 3.46 – 3.38 (m, 1H), 2.02 – 1.92 (m, 2H), 1.92 – 1.69 (m, 2H). **^{13}C NMR (101 MHz, $CDCl_3$):** δ 159.0, 144.2, 131.5, 130.2, 129.2, 128.7, 127.7, 127.4, 126.5, 114.0, 55.4, 48.7, 45.2, 33.2, 30.8. **FTIR (NaCl, thin film, cm^{-1})**: 2915, 1605, 1491, 1438, 1509, 1246, 1173, 1031, 964. **HRMS (FAB, *m/z*)**: calc'd for $C_{19}H_{21}ClO$ $[M+\cdot]^+$: 300.1281; found: 300.1274.

(*S*,*E*)-(3-methoxy-3-phenylprop-1-en-1-yl)trimethylsilane (146)

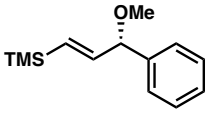

Prepared from (*E*)-(2-bromovinyl)trimethylsilane (**29o**, 36 mg, 0.2 mmol) and 1,3-dioxoisoindolin-2-yl 2-methoxy-2-phenylacetate (**145**, 62 mg, 0.2 mmol) according to General Procedure 3. The crude residue was purified by column chromatography (silica gel, 0 to 3% Et_2O/hexane) to yield **146** (26 mg, 59% yield) in 91% ee as a colorless oil. $\mathbf{R_f}$ = 0.62 (silica gel, 10% EtOAc/hexane, UV/CAM). **Chiral SFC:** (OD-H, 2.5 mL/min, 1% IPA in CO_2, λ = 210 nm): t_R (minor) = 2.6 min, t_R (major) = 5.9 min. $[\boldsymbol{a}]_D^{25}$ = +8° (c = 0.6, $CHCl_3$). **^{1}H NMR (400 MHz, $CDCl_3$):** δ 7.40 – 7.27 (m, 5H), 6.10 (dd, *J* = 18.6, 5.9 Hz, 1H), 5.93 (dd, *J* = 18.6, 1.2 Hz, 1H), 4.61 (d, *J* = 5.8 Hz, 1H), 3.32 (s, 3H), 0.07 (s, 9H). **^{13}C NMR (101 MHz, $CDCl_3$):** δ 145.7, 140.9, 131.9, 128.6, 127.7, 127.1, 86.6, 56.6, -1.2. **FTIR (NaCl, thin film, cm^{-1})**: 2955, 2820, 1453, 1248,

1100, 990, 863, 838, 760, 699. **HRMS (FAB, *m/z*)**: calc'd for $C_{13}H_{20}Osi$ $[M–H_2+H]^+$: 219.1205; found: 219.1191.

(*E*)-1-(3-cyclopropyl-3-phenylprop-1-en-1-yl)-4-methoxybenzene (161a)

1-methoxy-4-((1*E*,5*E*)-6-phenylhexa-1,5-dien-1-yl)benzene (161b)

1-methoxy-4-((1*E*,4*E*)-3-methyl-5-phenylpenta-1,4-dien-1-yl)benzene (161c)

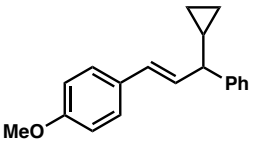

161a

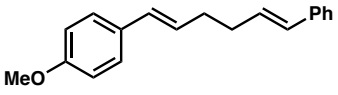

161b

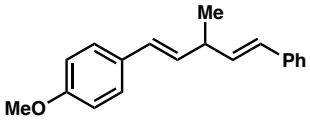

161c

Prepared from (*E*)-1-(2-bromovinyl)-4-methoxybenzene (**86**, 43 mg, 0.2 mmol) and 1,3-dioxoisoindolin-2-yl 2-cyclopropyl-2-phenylacetate (**160**, 64 mg, 0.2 mmol) according to General Procedure 3. The crude residue was purified by column chromatography (silica gel, hexane to 30% toluene/hexane) to yield a mixture of **161a–c** (22 mg, 42% yield) as a colorless oil. The reaction was repeated with 5 mol % and 20 mol % of **L2**·$NiBr_2$, yielding a mixture of **161a–c** in 44% and 49% yield, respectively. Three products are confirmed by GC-MS (extract ion *m/z* = 264). Distinct $^1H/^{13}C$ signals and coupling correlations are confirmed by ^1H, ^{13}C, COSY, HSQC, and HMBC NMR spectroscopy.

NMR data for **161a–c** with 20 mol % **L2**·$NiBr_2$:

^{1}H NMR (400 MHz, $CDCl_3$): δ 7.42 – 7.18 (m, 7H), 6.86 (dq, *J* = 8.9, 2.5 Hz, 2H), 6.49 – 6.36 (m, 1.8H), 6.34 – 6.08 (m, 1.82H), 3.81 (s, 3H), 3.20 (qt, *J* = 6.9, 1.3 Hz, 0.1H, *11c*), 2.76 (ddd, *J* = 8.6, 6.9, 1.2 Hz, 0.2H, *11a*), 2.49 – 2.31 (m, 2.8H, *11b*), 1.31 (d, *J* = 6.9 Hz, 0.3H, *11c*), 1.23 – 1.13 (m, 0.2H, *11a*), 0.68 (dddd, *J* = 9.1, 8.0, 5.3, 4.1 Hz, 0.2H, *11a*),

0.56 (dddd, J = 9.4, 8.0, 5.2, 4.1 Hz, 0.2H, *11a*), 0.40 – 0.31 (m, 0.2H, *11a*), 0.28 (dtd, J = 9.3, 5.2, 4.2 Hz, 0.2H, *11a*). **^{13}C NMR (101 MHz, $CDCl_3$):** δ 158.9, 158.8, 144.6, 137.9, 137.8, 134.7, 132.2, 131.2, 130.7, 130.5, 130.4, 130.3, 129.8, 129.0, 128.7, 128.6, 128.5, 128.3, 128.0, 127.9, 127.4, 127.3, 127.2, 127.1, 127.0, 126.4, 126.2, 126.1, 114.03, 114.02, 55.4, 53.2, 40.2, 33.2, 33.0, 20.5, 16.4, 4.9, 4.4. **FTIR (NaCl, thin film, cm^{-1})**: 3026, 2931, 2837, 1607, 1511, 1252, 1176, 1034, 966, 800, 692. **LRMS (GC-MS, *m/z*)**: calc'd for $C_{19}H_{20}O$ $[M]^+$: 264.2; found: 3 products, 264.1, 264.1, 264.2.

3.6.7 GC-MS Traces of Radical Clock Products

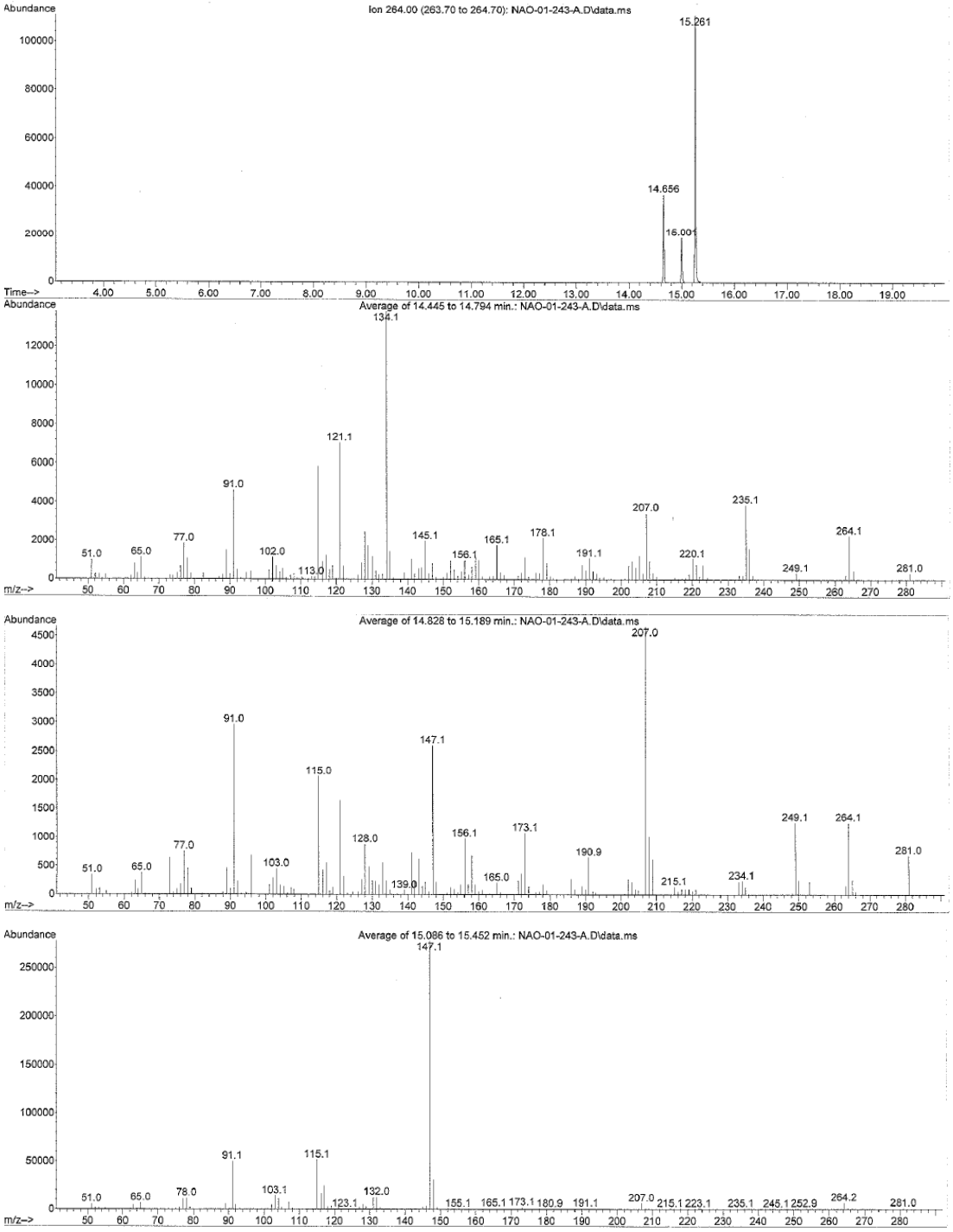

3.6.8 SFC and HPLC Traces of Racemic and Enantioenriched Products

137 (Figure 3.3): racemic

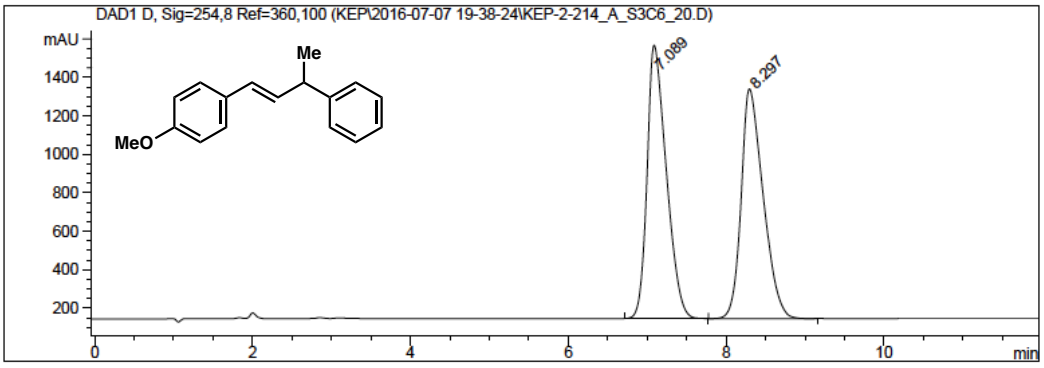

Peak #	RetTime [min]	Type	Width [min]	Area [mAU*s]	Height [mAU]	Area %
1	7.089	BV	0.2581	2.40965e4	1419.46216	50.9929
2	8.297	VB	0.2903	2.31582e4	1193.77161	49.0071

137 (Figure 3.3): enantioenriched, 96% ee

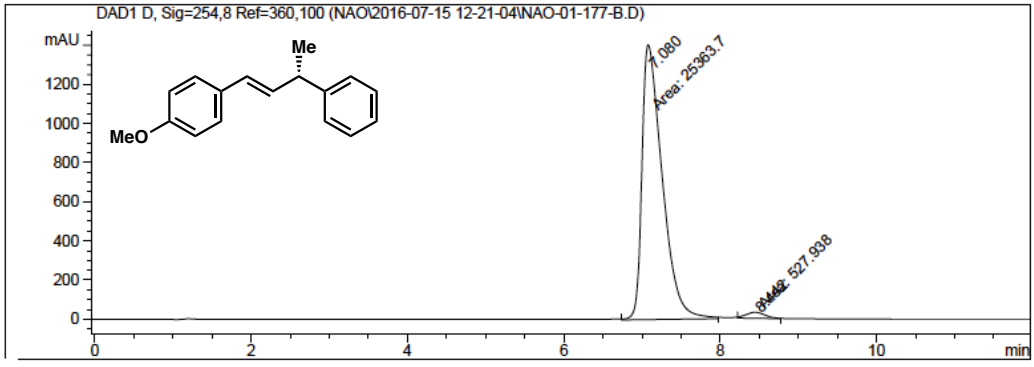

Peak #	RetTime [min]	Type	Width [min]	Area [mAU*s]	Height [mAU]	Area %
1	7.080	MM	0.3005	2.53637e4	1406.71533	97.9610
2	8.442	MM	0.2816	527.93842	31.25150	2.0390

140a (Figure 3.3): racemic

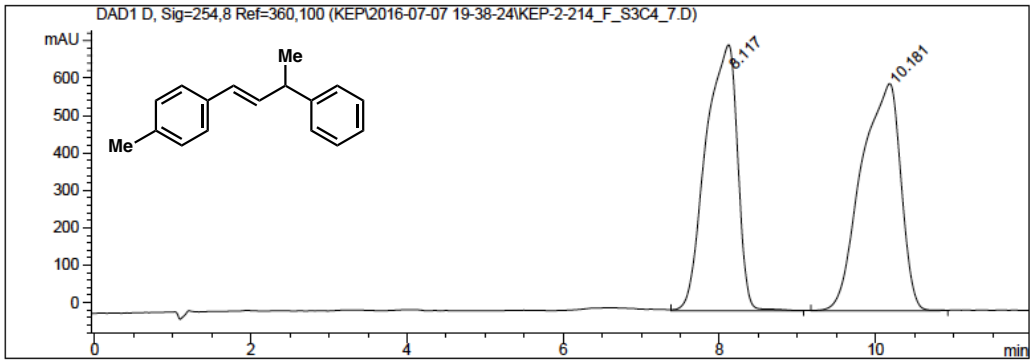

Peak #	RetTime [min]	Type	Width [min]	Area [mAU*s]	Height [mAU]	Area %
1	8.117	VB	0.3807	2.00095e4	710.31079	48.4555
2	10.181	BV	0.4692	2.12851e4	606.82129	51.5445

140a (Figure 3.3): enantioenriched, 95% ee

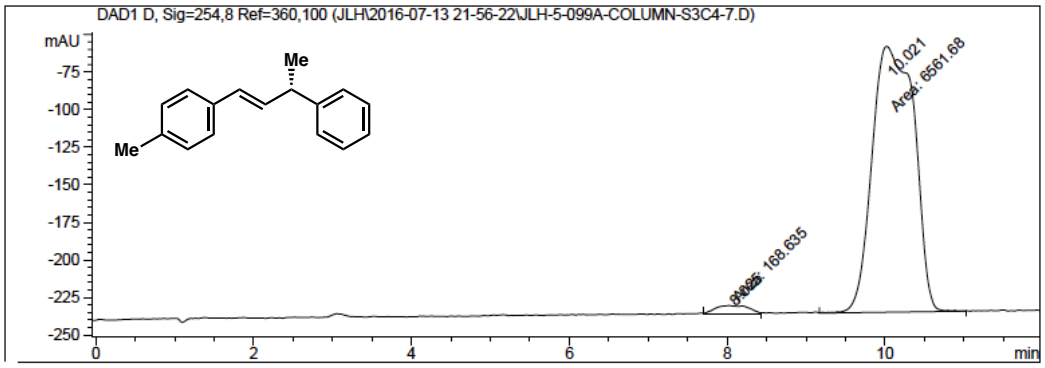

Peak #	RetTime [min]	Type	Width [min]	Area [mAU*s]	Height [mAU]	Area %
1	8.025	MM	0.4882	168.63531	5.75649	2.5056
2	10.021	MM	0.6182	6561.67920	176.91377	97.4944

140b (Figure 3.3): racemic

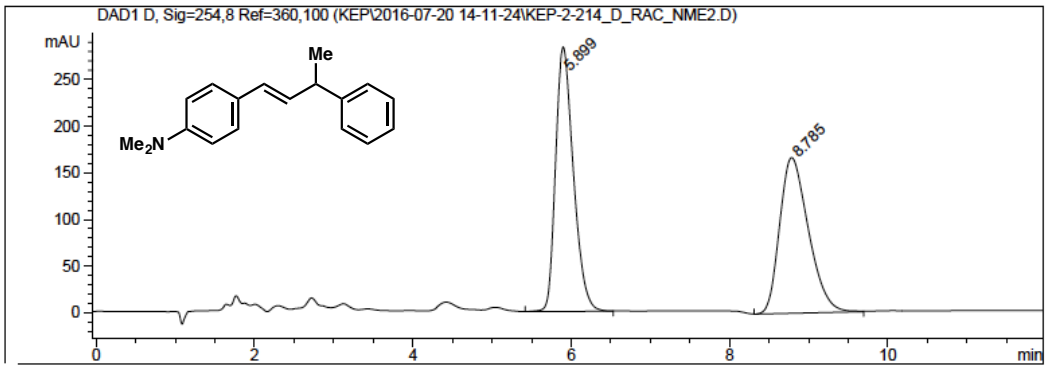

Peak #	RetTime [min]	Type	Width [min]	Area [mAU*s]	Height [mAU]	Area %
1	5.899	VB	0.2423	4429.97607	283.53226	51.2284
2	8.785	BB	0.3949	4217.52539	166.83267	48.7716

140b (Figure 3.3): enantioenriched, 97% ee

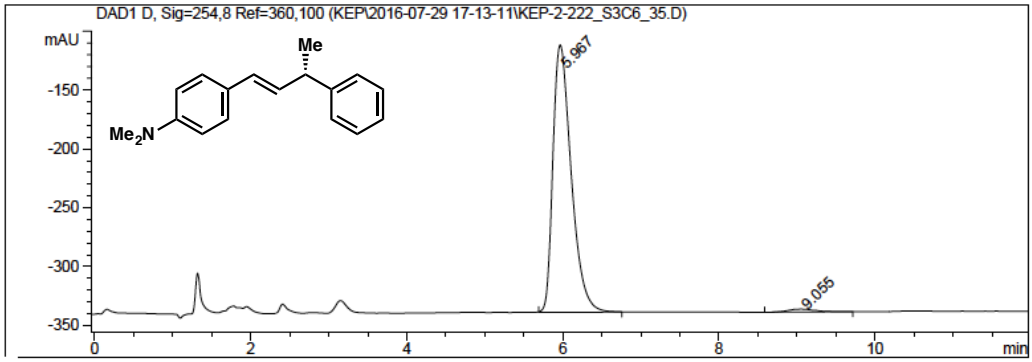

Peak #	RetTime [min]	Type	Width [min]	Area [mAU*s]	Height [mAU]	Area %
1	5.967	BB	0.2505	3707.96924	227.13380	98.4506
2	9.055	BB	0.2926	58.35402	2.46108	1.5494

140c (Figure 3.3): racemic

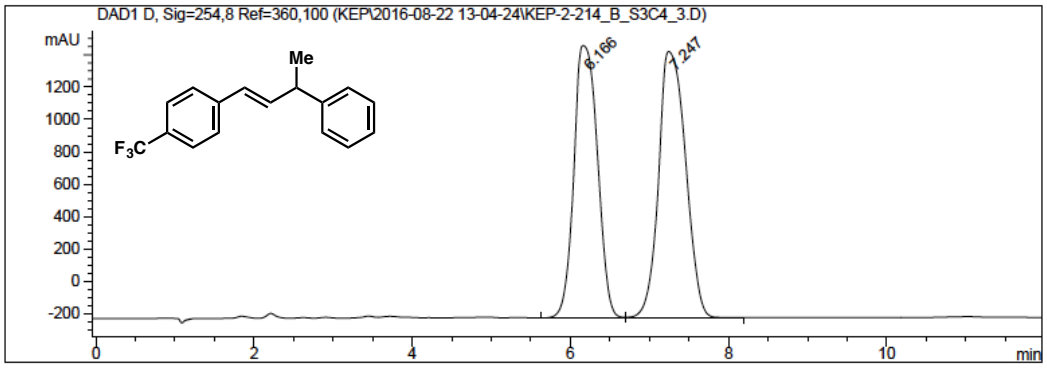

Peak #	RetTime [min]	Type	Width [min]	Area [mAU*s]	Height [mAU]	Area %
1	6.166	VV	0.3308	3.50747e4	1685.07422	47.1051
2	7.247	VB	0.3749	3.93858e4	1647.52795	52.8949

140c (Figure 3.3): enantioenriched, 93% ee

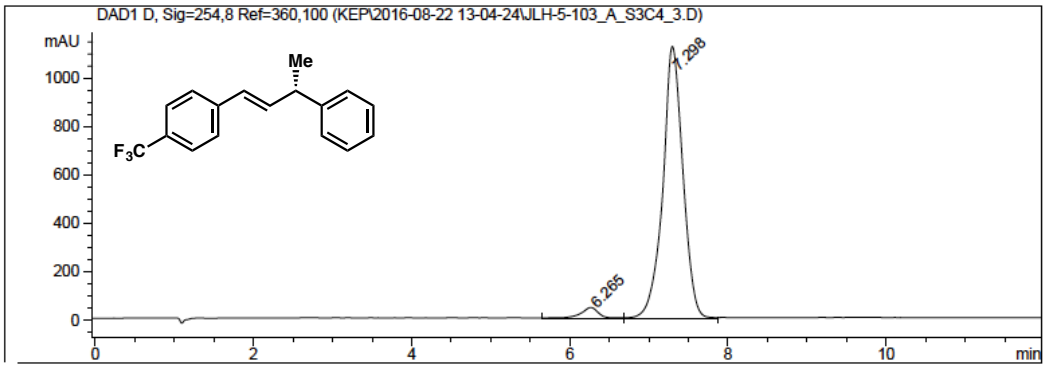

Peak #	RetTime [min]	Type	Width [min]	Area [mAU*s]	Height [mAU]	Area %
1	6.265	VV	0.2265	687.93018	43.98362	3.3472
2	7.298	VV	0.2624	1.98645e4	1122.81396	96.6528

140d (Figure 3.3): racemic

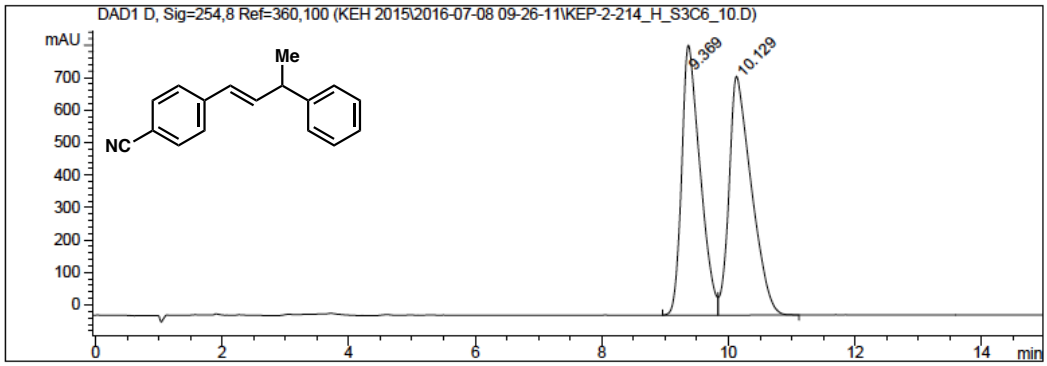

Peak #	RetTime [min]	Type	Width [min]	Area [mAU*s]	Height [mAU]	Area %
1	9.369	BV	0.2960	1.68057e4	830.62769	48.1897
2	10.129	VB	0.3508	1.80684e4	734.99915	51.8103

140d (Figure 3.3): enantioenriched, 94% ee

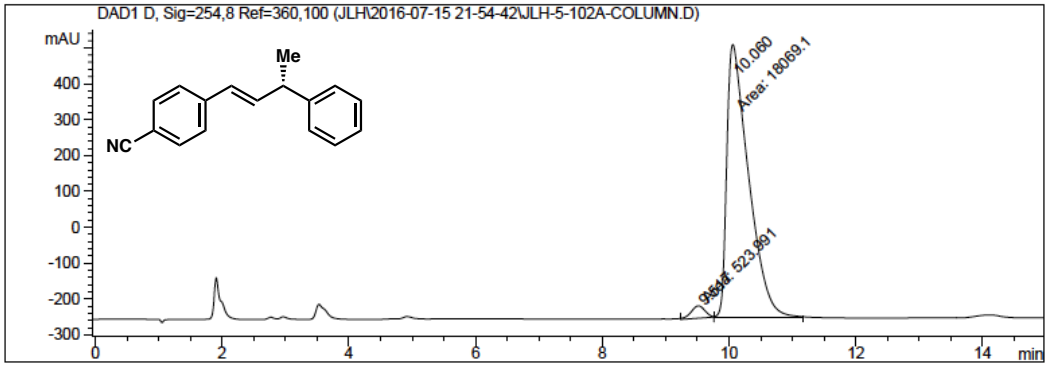

Peak #	RetTime [min]	Type	Width [min]	Area [mAU*s]	Height [mAU]	Area %
1	9.517	MM	0.2532	523.99091	34.49692	2.8182
2	10.060	MM	0.3962	1.80691e4	760.05249	97.1818

140e (Figure 3.3): racemic

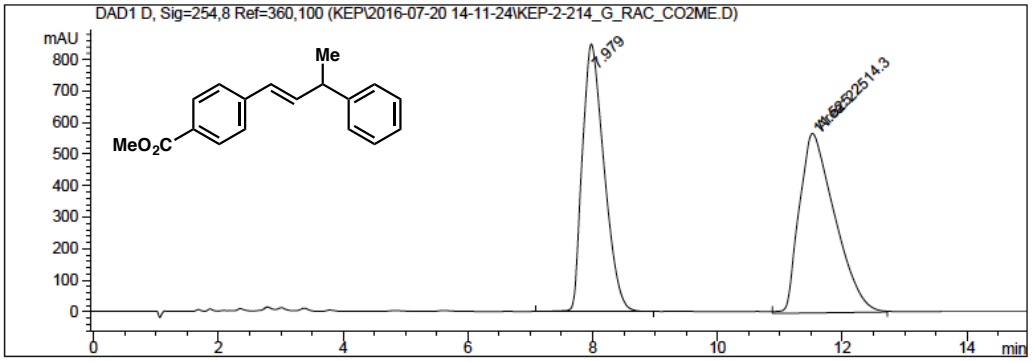

Peak #	RetTime [min]	Type	Width [min]	Area [mAU*s]	Height [mAU]	Area %
1	7.979	BB	0.3869	2.05724e4	848.34802	47.7466
2	11.525	MM	0.6592	2.25143e4	569.27423	52.2534

140e (Figure 3.3): enantioenriched, 95% ee

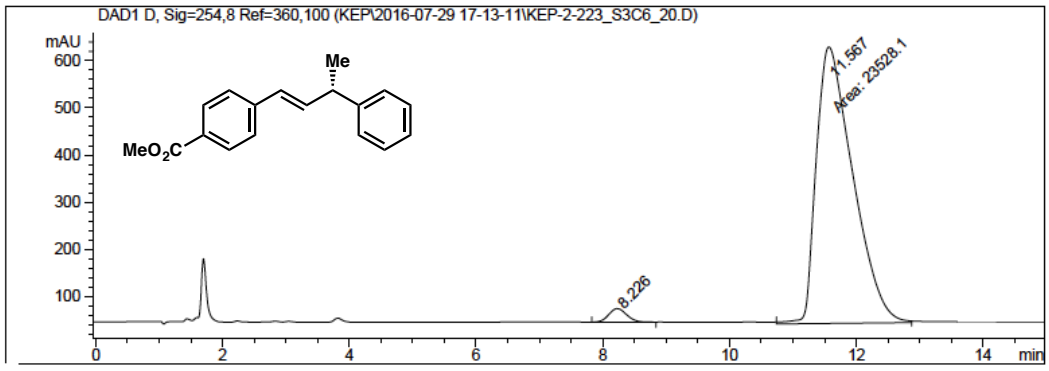

Peak #	RetTime [min]	Type	Width [min]	Area [mAU*s]	Height [mAU]	Area %
1	8.226	BB	0.3069	568.03058	28.69778	2.3574
2	11.567	MM	0.6679	2.35281e4	587.09686	97.6426

140f (Figure 3.3): racemic

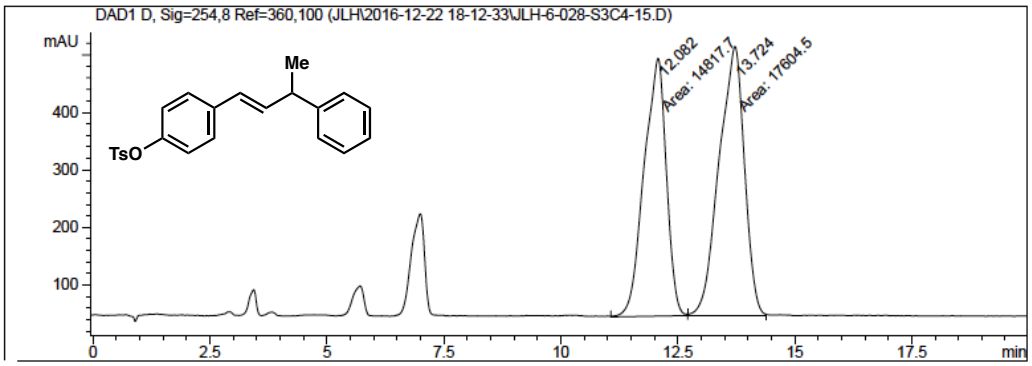

Peak #	RetTime [min]	Type	Width [min]	Area [mAU*s]	Height [mAU]	Area %
1	12.082	MM	0.5513	1.48177e4	447.97232	45.7023
2	13.724	MM	0.6275	1.76045e4	467.56030	54.2977

140f (Figure 3.3): enantioenriched, 94% ee

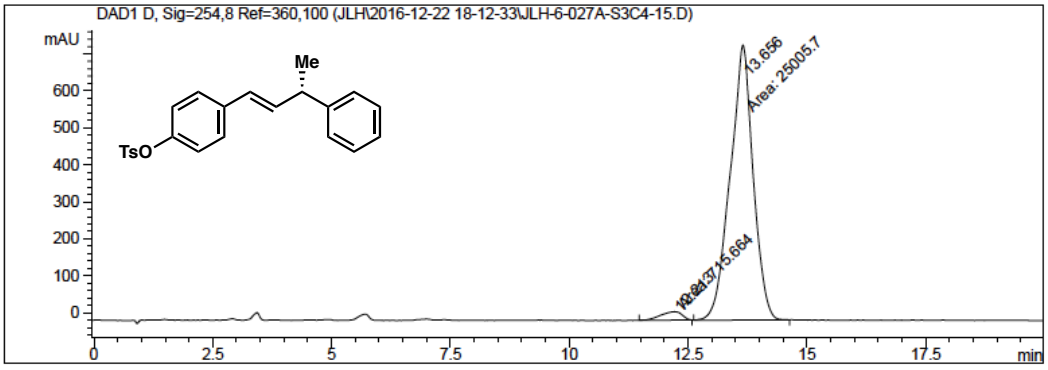

Peak #	RetTime [min]	Type	Width [min]	Area [mAU*s]	Height [mAU]	Area %
1	12.213	MM	0.5201	715.66412	22.93249	2.7824
2	13.656	MM	0.5598	2.50057e4	744.50916	97.2176

140g (Figure 3.3): racemic

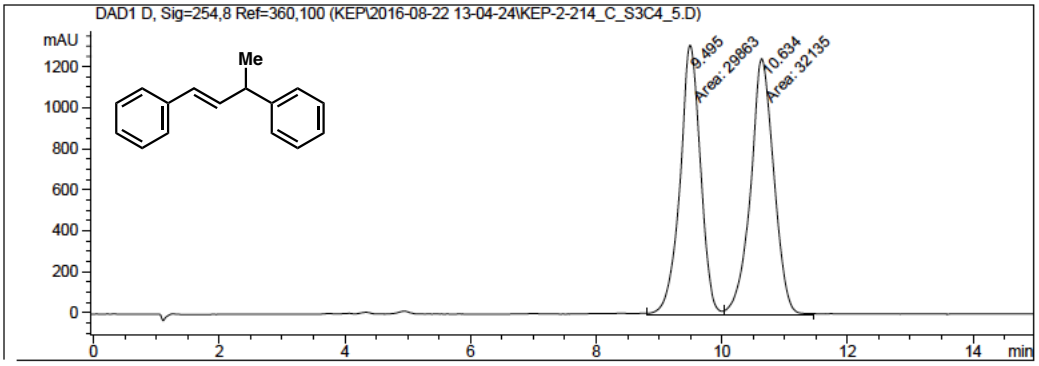

Peak #	RetTime [min]	Type	Width [min]	Area [mAU*s]	Height [mAU]	Area %
1	9.495	MM	0.3786	2.98630e4	1314.49744	48.1677
2	10.634	MM	0.4290	3.21350e4	1248.56421	51.8323

140g (Figure 3.3): enantioenriched, 96% ee

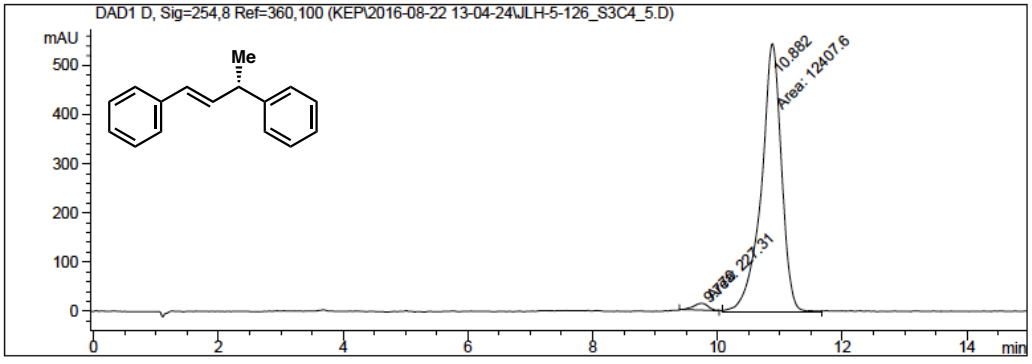

Peak #	RetTime [min]	Type	Width [min]	Area [mAU*s]	Height [mAU]	Area %
1	9.770	MM	0.2725	227.31046	13.90100	1.7991
2	10.882	MM	0.3782	1.24076e4	546.85577	98.2009

140h (Figure 3.3): racemic

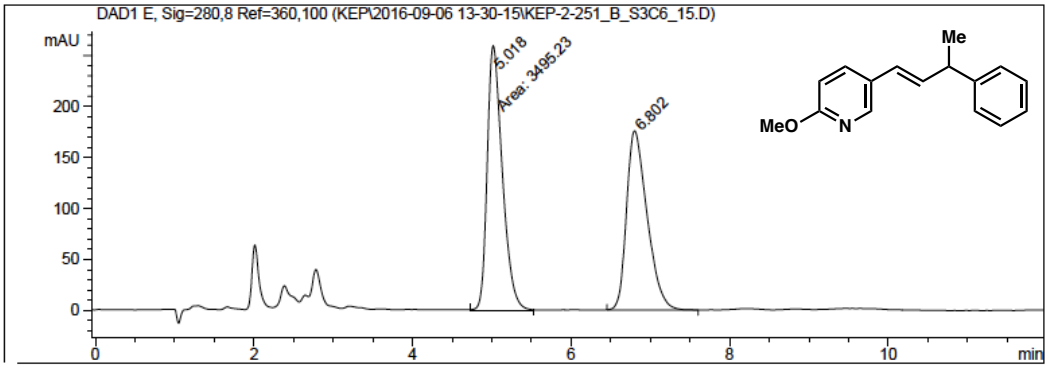

Peak #	RetTime [min]	Type	Width [min]	Area [mAU*s]	Height [mAU]	Area %
1	5.018	MM	0.2233	3495.22925	260.81982	52.4318
2	6.802	BB	0.2747	3171.01147	175.57878	47.5682

140h (Figure 3.3): enantioenriched, 95% ee

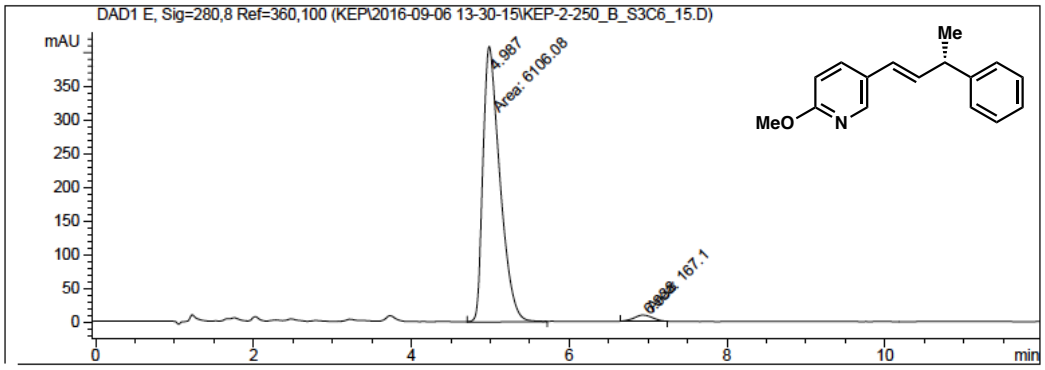

Peak #	RetTime [min]	Type	Width [min]	Area [mAU*s]	Height [mAU]	Area %
1	4.987	MM	0.2488	6106.07617	408.96854	97.3363
2	6.938	MM	0.2866	167.10007	9.71596	2.6637

140i (Figure 3.3): racemic

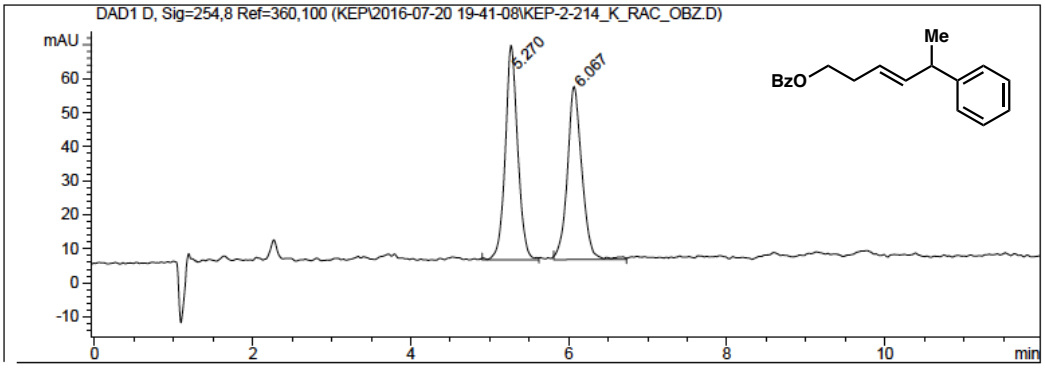

Peak #	RetTime [min]	Type	Width [min]	Area [mAU*s]	Height [mAU]	Area %
1	5.270	BB	0.1643	692.65100	62.99958	51.5795
2	6.067	BB	0.1892	650.22839	50.83070	48.4205

140i (Figure 3.3): enantioenriched, 97% ee

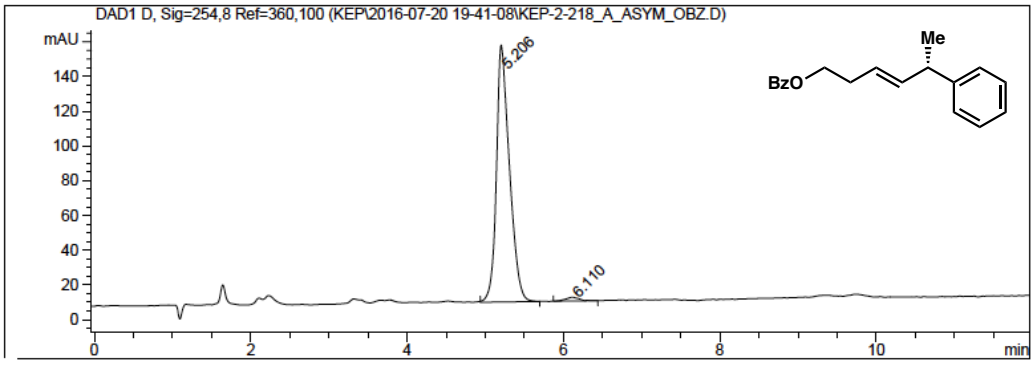

Peak #	RetTime [min]	Type	Width [min]	Area [mAU*s]	Height [mAU]	Area %
1	5.206	BB	0.1708	1710.15393	148.02460	98.4760
2	6.110	BB	0.1607	26.46575	2.19494	1.5240

140j (Figure 3.3): racemic

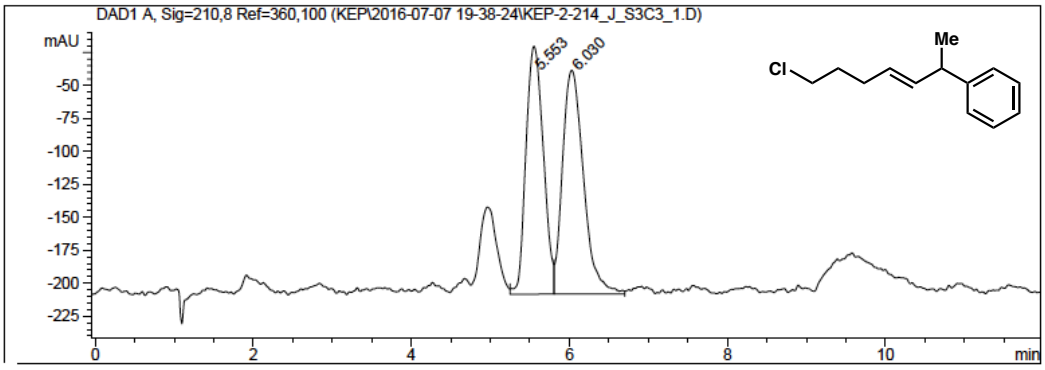

Peak #	RetTime [min]	Type	Width [min]	Area [mAU*s]	Height [mAU]	Area %
1	5.553	VV	0.2466	2879.10791	188.09062	47.7991
2	6.030	VV	0.2922	3144.24927	169.66949	52.2009

140j (Figure 3.3): enantioenriched, 91% ee

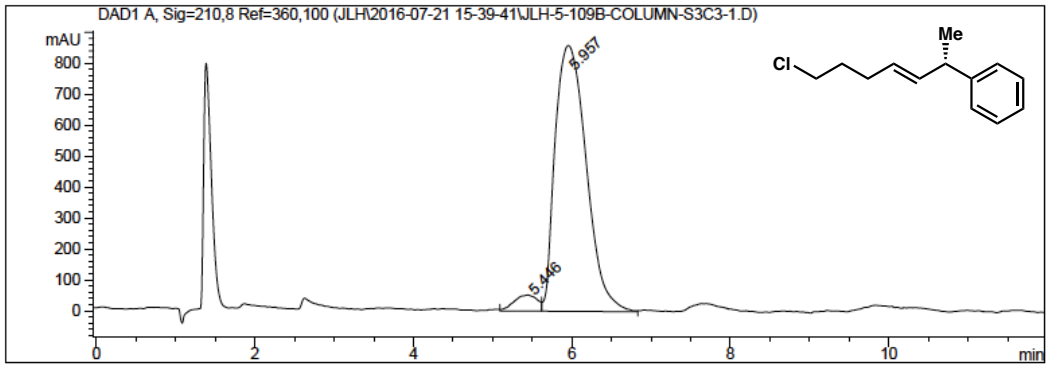

Peak #	RetTime [min]	Type	Width [min]	Area [mAU*s]	Height [mAU]	Area %
1	5.446	VV	0.2528	1053.08008	51.88251	4.2859
2	5.957	VV	0.4514	2.35179e4	858.91888	95.7141

140k (Figure 3.3): racemic

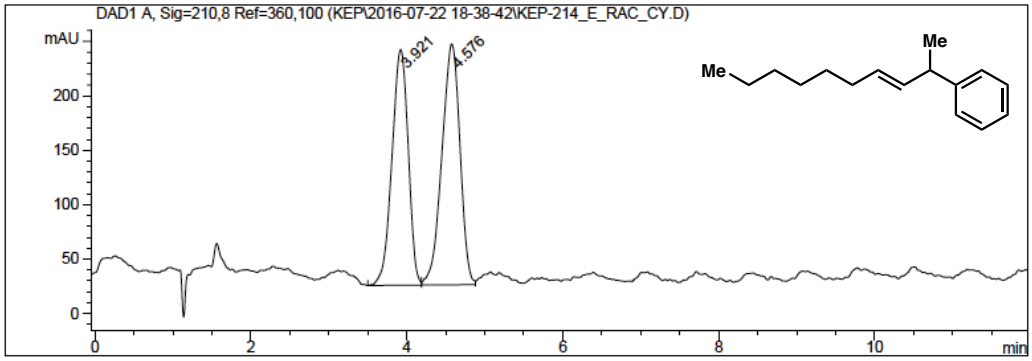

Peak #	RetTime [min]	Type	Width [min]	Area [mAU*s]	Height [mAU]	Area %
1	3.921	VV	0.2294	3145.27051	216.62386	46.8268
2	4.576	VV	0.2603	3571.54810	221.25337	53.1732

140k (Figure 3.3): enantioenriched, 94% ee

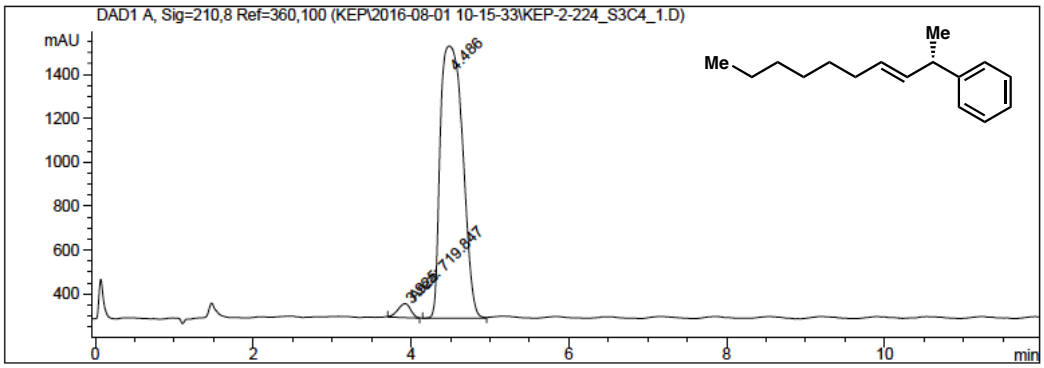

Peak #	RetTime [min]	Type	Width [min]	Area [mAU*s]	Height [mAU]	Area %
1	3.925	MM	0.1890	719.84717	63.47777	2.8630
2	4.486	VV	0.3261	2.44231e4	1238.09705	97.1370

S31 (de-silylated 140l, Figure 3.3): racemic

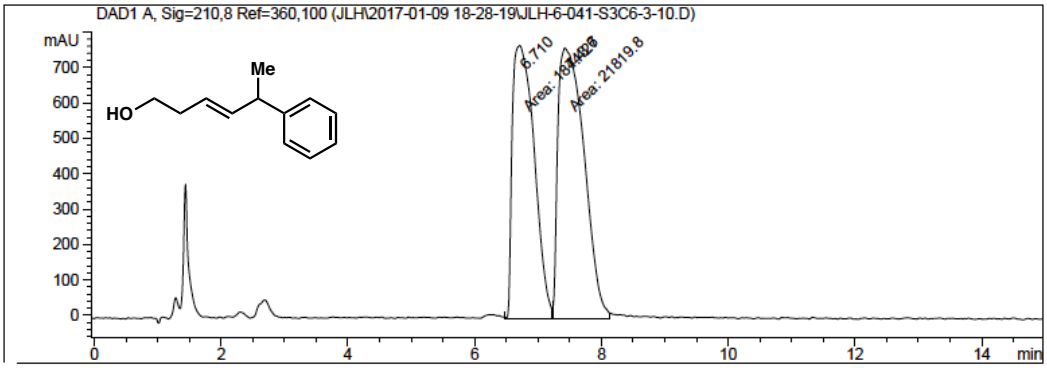

Peak #	RetTime [min]	Type	Width [min]	Area [mAU*s]	Height [mAU]	Area %
1	6.710	MM	0.3992	1.84436e4	770.06226	45.8074
2	7.427	MM	0.4761	2.18198e4	763.80591	54.1926

S31 (de-silylated 140l, Figure 3.3): enantioenriched, 89% ee

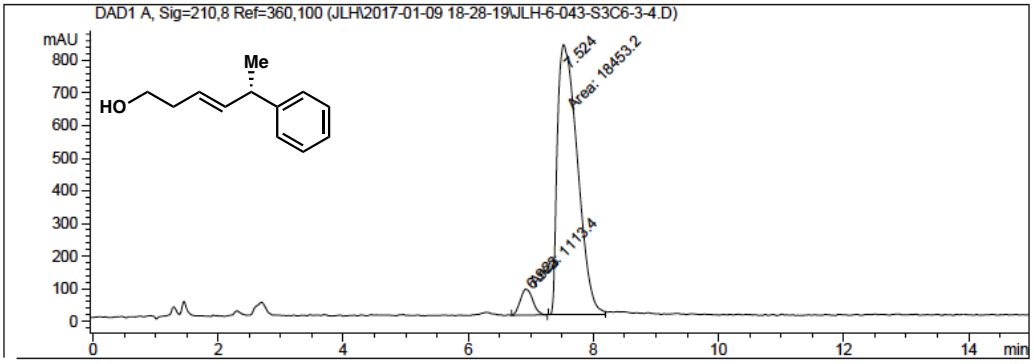

Peak #	RetTime [min]	Type	Width [min]	Area [mAU*s]	Height [mAU]	Area %
1	6.923	MM	0.2309	1113.40063	80.37251	5.6903
2	7.524	MM	0.3711	1.84532e4	828.86755	94.3097

140m (Figure 3.3): racemic

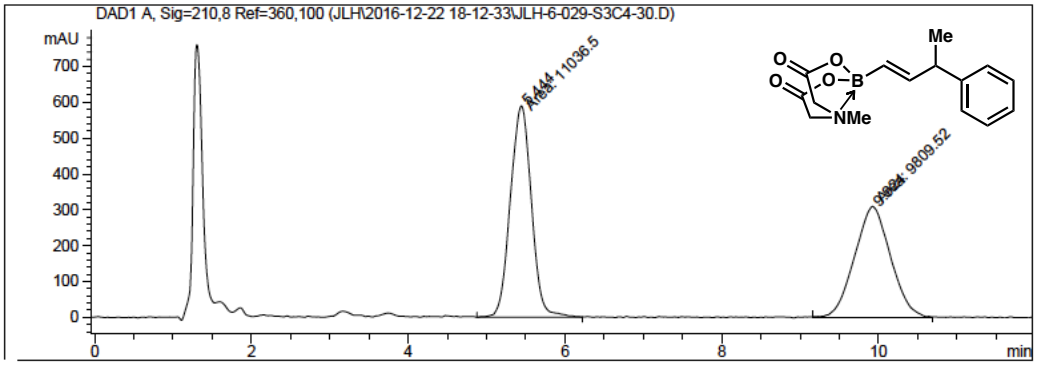

Peak #	RetTime [min]	Type	Width [min]	Area [mAU*s]	Height [mAU]	Area %
1	5.444	MM	0.3119	1.10365e4	589.78003	52.9429
2	9.924	MM	0.5290	9809.52246	309.03564	47.0571

140m (Figure 3.3): enantioenriched, 97% ee

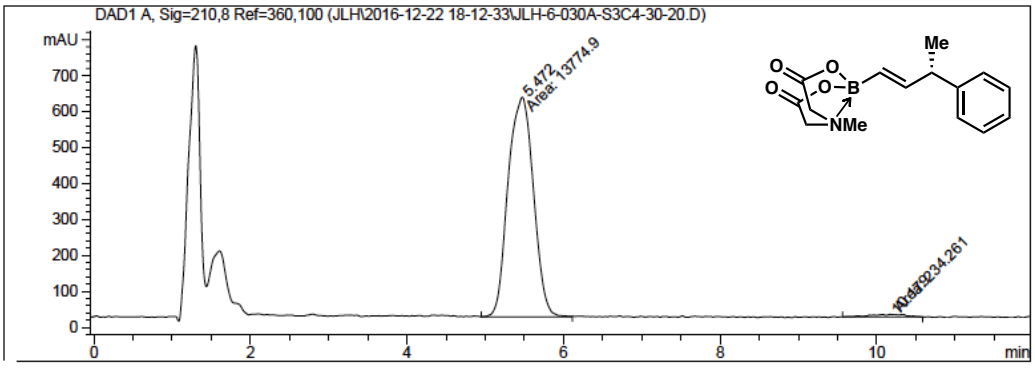

Peak #	RetTime [min]	Type	Width [min]	Area [mAU*s]	Height [mAU]	Area %
1	5.472	MM	0.3758	1.37749e4	610.96771	98.3278
2	10.179	MM	0.5146	234.26103	7.58734	1.6722

140n (Figure 3.3): racemic

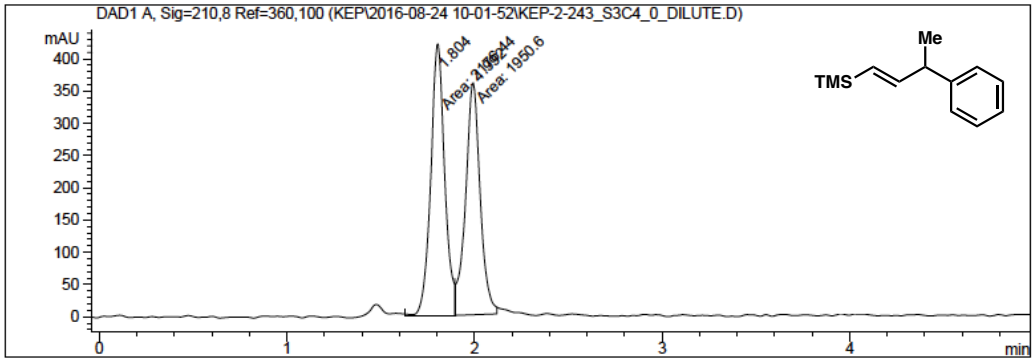

Peak #	RetTime [min]	Type	Width [min]	Area [mAU*s]	Height [mAU]	Area %
1	1.804	MM	0.0852	2176.43945	425.78909	52.7360
2	1.992	MM	0.0896	1950.60413	362.93353	47.2640

140n (Figure 3.3): enantioenriched, 97% ee

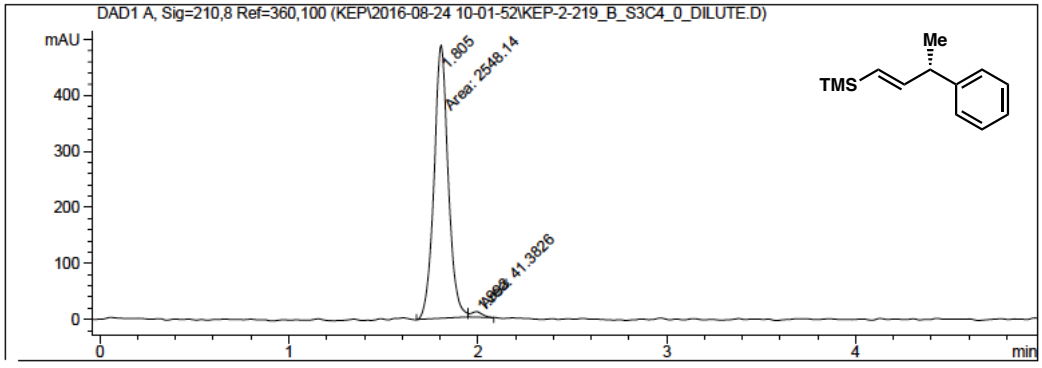

Peak #	RetTime [min]	Type	Width [min]	Area [mAU*s]	Height [mAU]	Area %
1	1.805	MM	0.0863	2548.14233	492.12225	98.4019
2	1.993	MM	0.0681	41.38256	10.12810	1.5981

141a (Figure 3.4): racemic

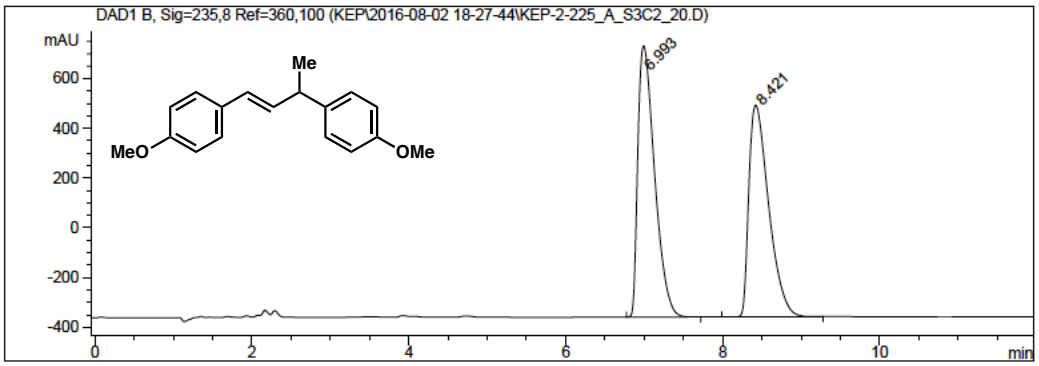

Peak #	RetTime [min]	Type	Width [min]	Area [mAU*s]	Height [mAU]	Area %
1	6.993	BB	0.2288	1.61745e4	1091.89661	51.9859
2	8.421	BB	0.2727	1.49387e4	851.43549	48.0141

141a (Figure 3.4): enantioenriched, 93% ee

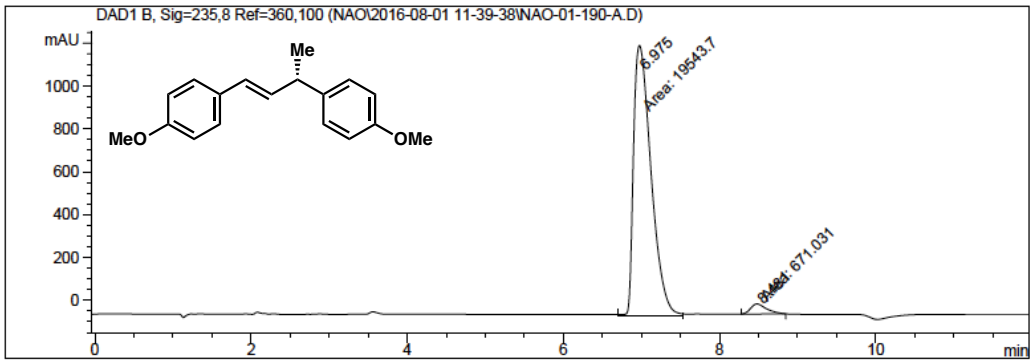

Peak #	RetTime [min]	Type	Width [min]	Area [mAU*s]	Height [mAU]	Area %
1	6.975	MM	0.2585	1.95437e4	1260.21631	96.6805
2	8.481	MM	0.2361	671.03094	47.35995	3.3195

141b (Figure 3.4): racemic

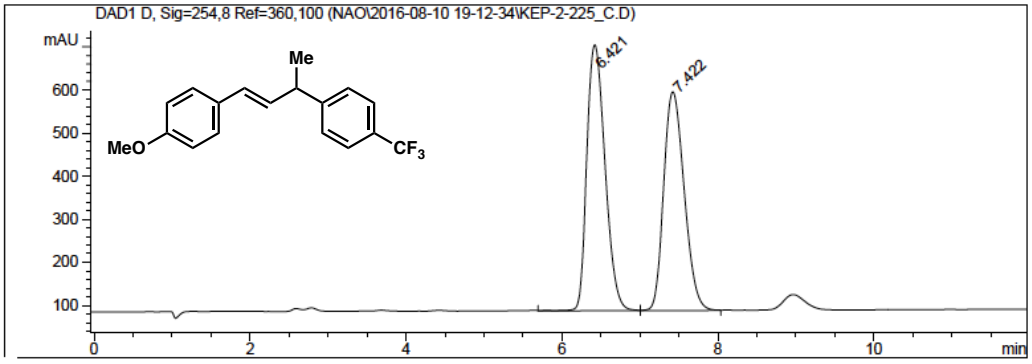

Peak #	RetTime [min]	Type	Width [min]	Area [mAU*s]	Height [mAU]	Area %
1	6.421	VV	0.2579	1.00441e4	616.96472	51.9654
2	7.422	VV	0.2894	9284.33398	507.48148	48.0346

141b (Figure 3.4): enantioenriched, 88% ee

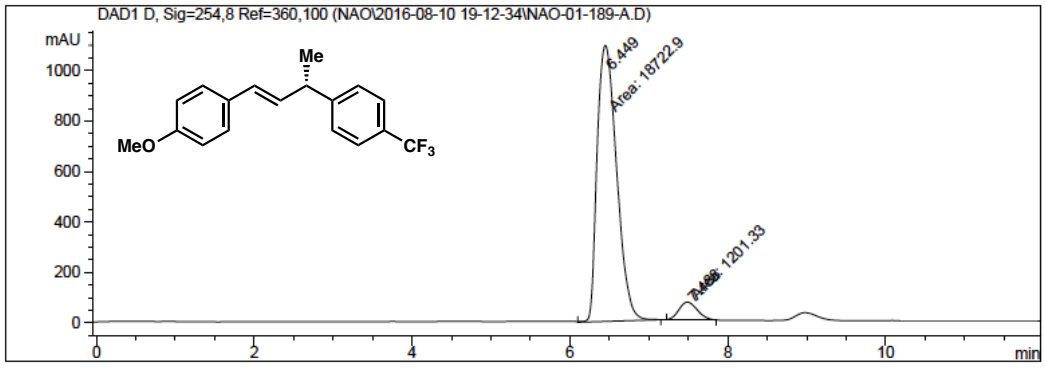

Peak #	RetTime [min]	Type	Width [min]	Area [mAU*s]	Height [mAU]	Area %
1	6.449	MM	0.2851	1.87229e4	1094.68372	93.9705
2	7.488	MM	0.2774	1201.33252	72.18948	6.0295

141c (Figure 3.4): racemic

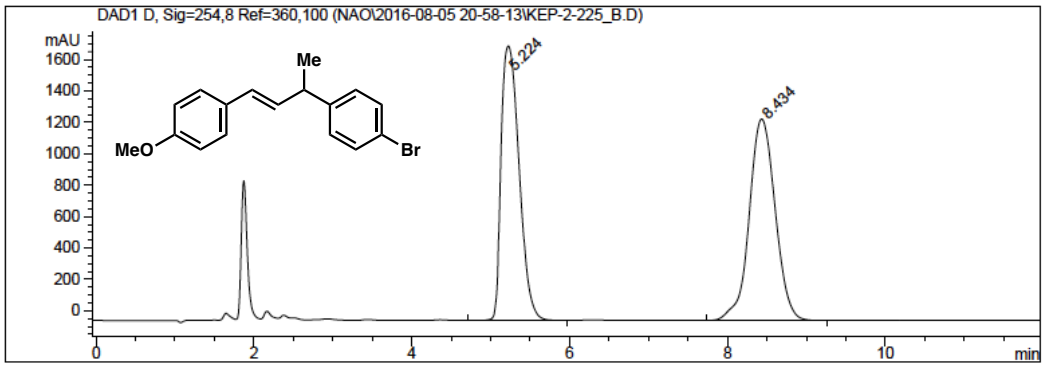

Peak #	RetTime [min]	Type	Width [min]	Area [mAU*s]	Height [mAU]	Area %
1	5.224	VV	0.2570	2.77188e4	1747.68750	48.5460
2	8.434	BB	0.3592	2.93793e4	1282.85803	51.4540

141c (Figure 3.4): enantioenriched, 90% ee

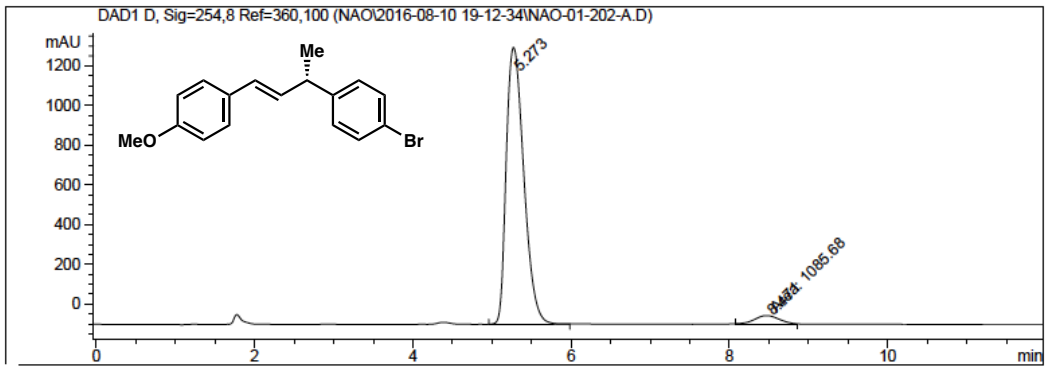

Peak #	RetTime [min]	Type	Width [min]	Area [mAU*s]	Height [mAU]	Area %
1	5.273	BB	0.2445	2.15843e4	1395.44788	95.2109
2	8.471	MM	0.3931	1085.67932	46.02574	4.7891

141d (Figure 3.4): racemic

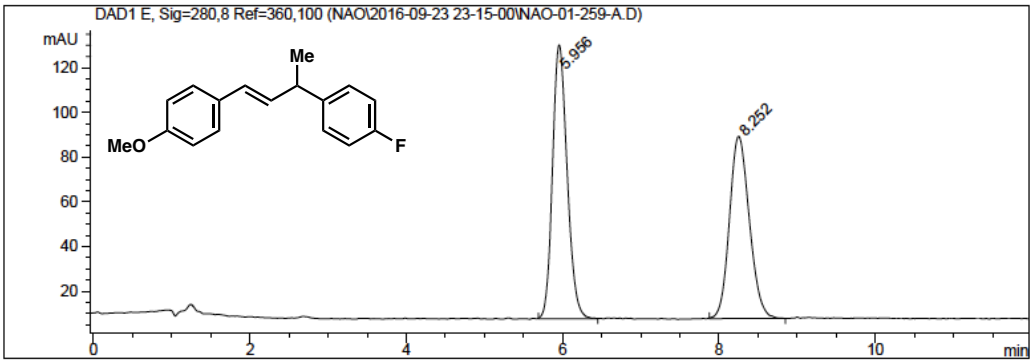

Peak #	RetTime [min]	Type	Width [min]	Area [mAU*s]	Height [mAU]	Area %
1	5.956	BB	0.2041	1597.30237	122.49622	52.5502
2	8.252	BB	0.2744	1442.27039	81.53059	47.4498

141d (Figure 3.4): enantioenriched, 92% ee

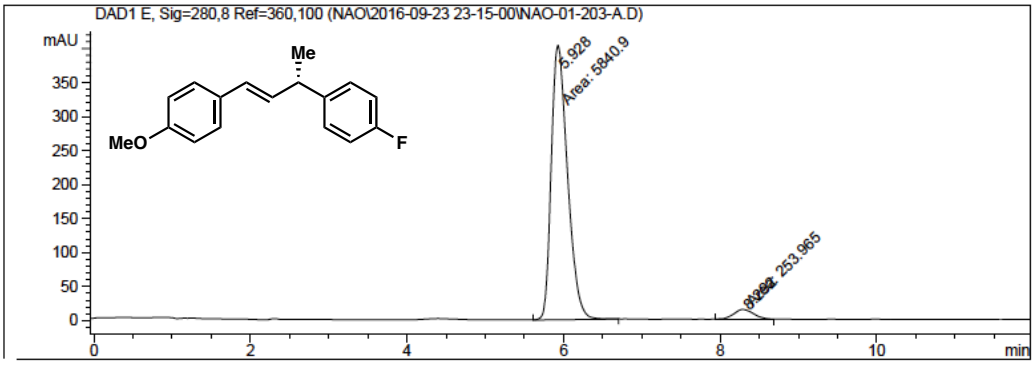

Peak #	RetTime [min]	Type	Width [min]	Area [mAU*s]	Height [mAU]	Area %
1	5.928	MM	0.2410	5840.89600	403.93130	95.8331
2	8.292	MM	0.2929	253.96486	14.45295	4.1669

141e (Figure 3.4): racemic

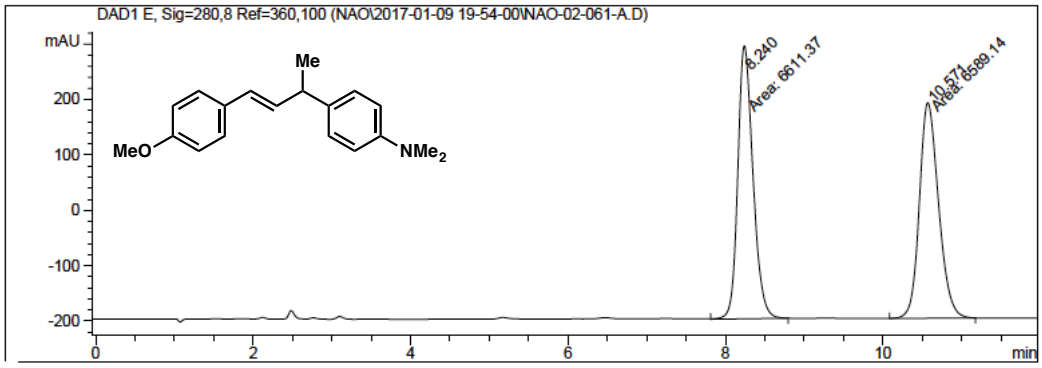

Peak #	RetTime [min]	Type	Width [min]	Area [mAU*s]	Height [mAU]	Area %
1	8.240	MM	0.2233	6611.36621	493.52872	50.0842
2	10.571	MM	0.2819	6589.13770	389.54446	49.9158

141e (Figure 3.4): enantioenriched, 94% ee

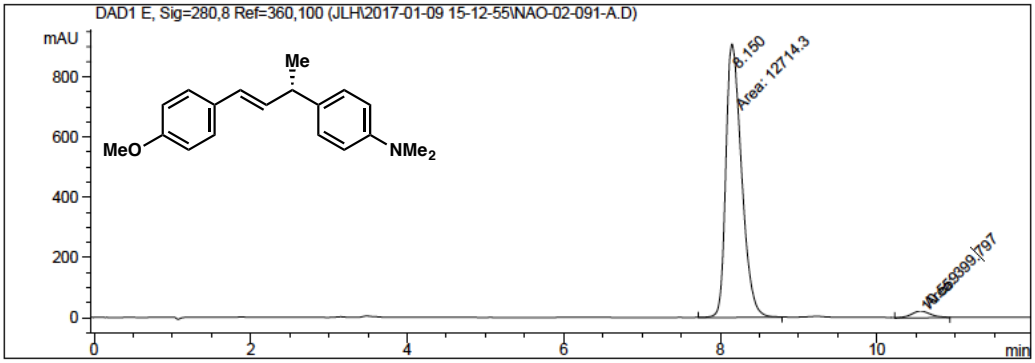

Peak #	RetTime [min]	Type	Width [min]	Area [mAU*s]	Height [mAU]	Area %
1	8.150	MM	0.2330	1.27143e4	909.57269	96.9514
2	10.559	MM	0.2917	399.79657	22.84231	3.0486

141f (Figure 3.4): racemic

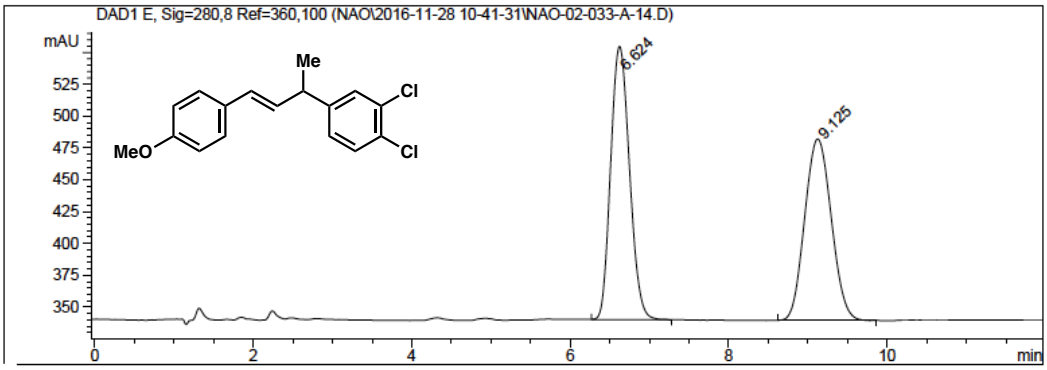

Peak #	RetTime [min]	Type	Width [min]	Area [mAU*s]	Height [mAU]	Area %
1	6.624	BB	0.2651	3551.33887	214.60269	51.6981
2	9.125	BB	0.3717	3318.03833	142.47495	48.3019

141f (Figure 3.4): enantioenriched, 82% ee

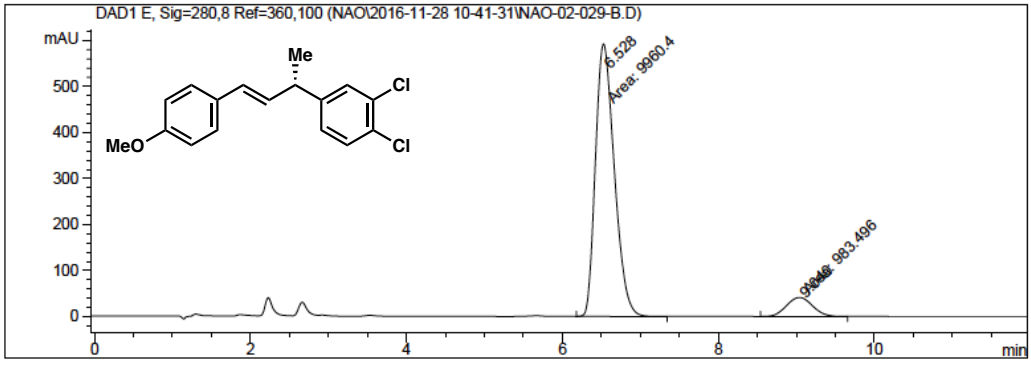

Peak #	RetTime [min]	Type	Width [min]	Area [mAU*s]	Height [mAU]	Area %
1	6.528	MM	0.2800	9960.39941	592.94763	91.0133
2	9.040	MM	0.3921	983.49628	41.80441	8.9867

141g (Figure 3.4): racemic

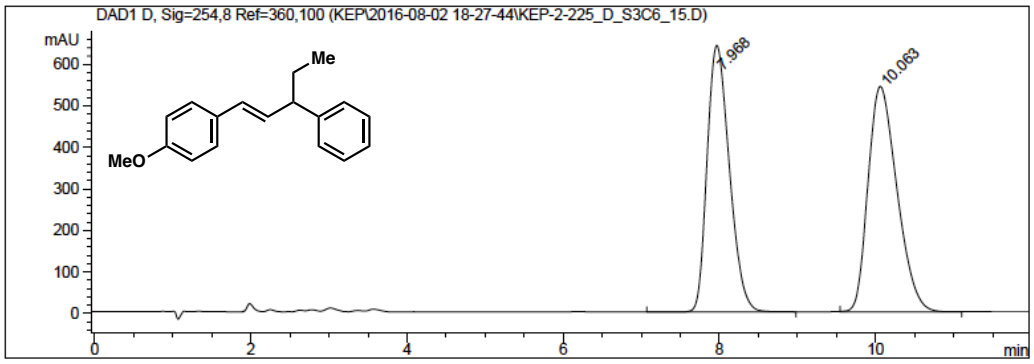

Peak #	RetTime [min]	Type	Width [min]	Area [mAU*s]	Height [mAU]	Area %
1	7.968	VB	0.3120	1.27647e4	642.02454	47.6750
2	10.063	BB	0.4049	1.40097e4	543.13721	52.3250

141g (Figure 3.4): enantioenriched, 97% ee

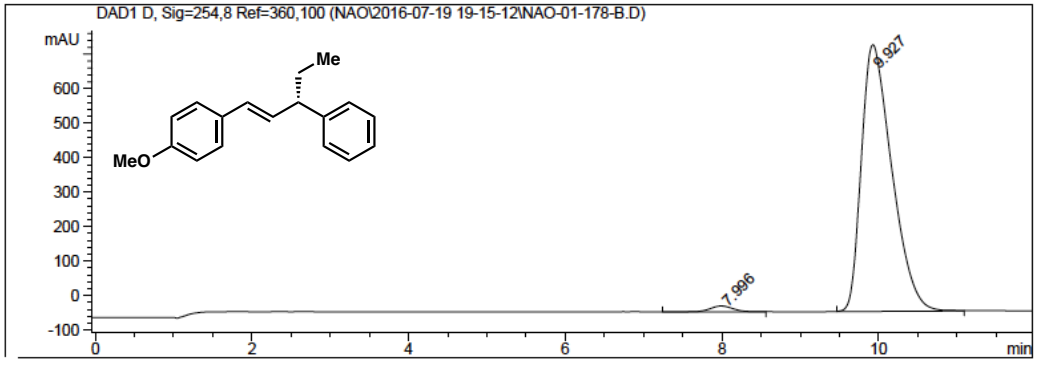

Peak #	RetTime [min]	Type	Width [min]	Area [mAU*s]	Height [mAU]	Area %
1	7.996	VB	0.3205	362.21658	17.28073	1.7024
2	9.927	BB	0.4153	2.09143e4	773.92688	98.2976

141h (Figure 3.4): racemic

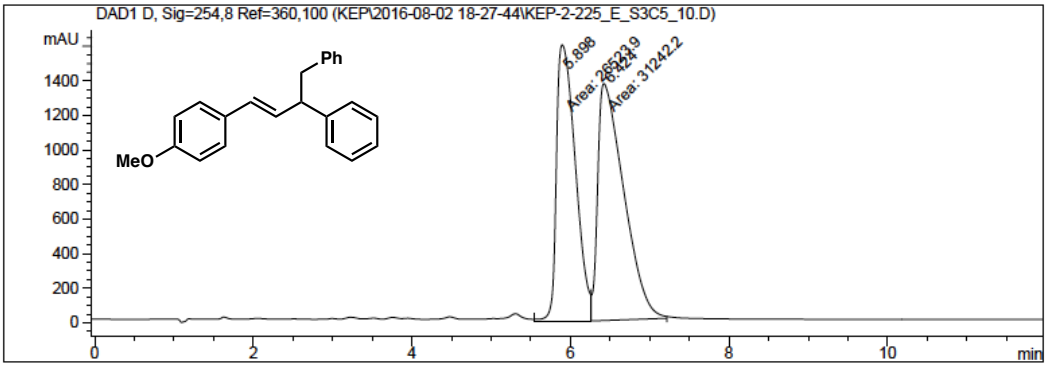

Peak #	RetTime [min]	Type	Width [min]	Area [mAU*s]	Height [mAU]	Area %
1	5.898	MM	0.2764	2.65239e4	1599.41284	45.9160
2	6.424	MM	0.3797	3.12422e4	1371.19714	54.0840

141h (Figure 3.4): enantioenriched, 95% ee

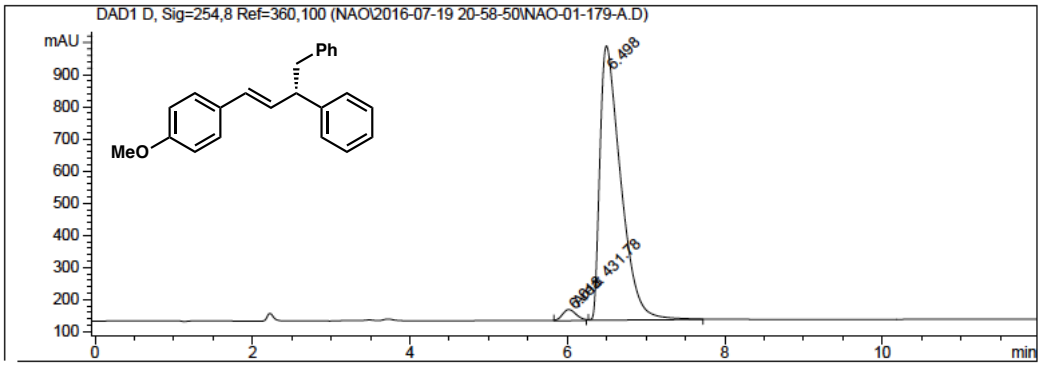

Peak #	RetTime [min]	Type	Width [min]	Area [mAU*s]	Height [mAU]	Area %
1	6.018	MM	0.2059	431.78006	34.94782	2.6714
2	6.498	VB	0.2791	1.57314e4	853.40881	97.3286

141i (Figure 3.4): racemic

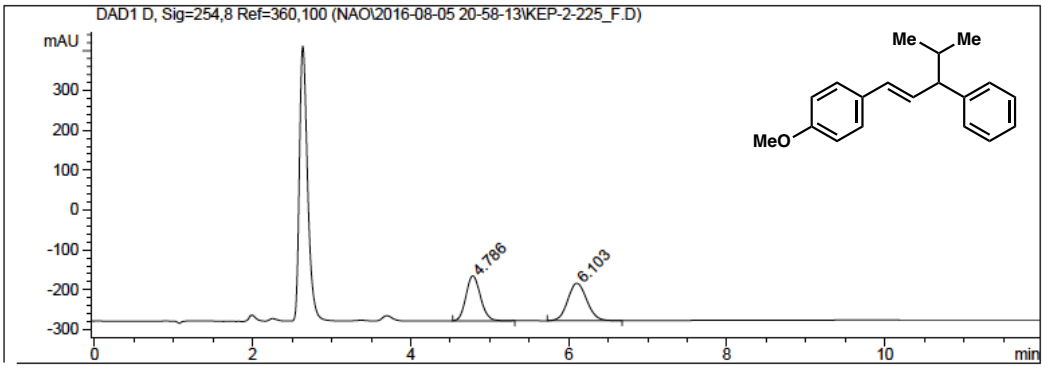

Peak #	RetTime [min]	Type	Width [min]	Area [mAU*s]	Height [mAU]	Area %
1	4.786	BB	0.2004	1430.79492	112.47615	47.8299
2	6.103	BB	0.2619	1560.63074	93.89527	52.1701

141i (Figure 3.4): enantioenriched, 97% ee

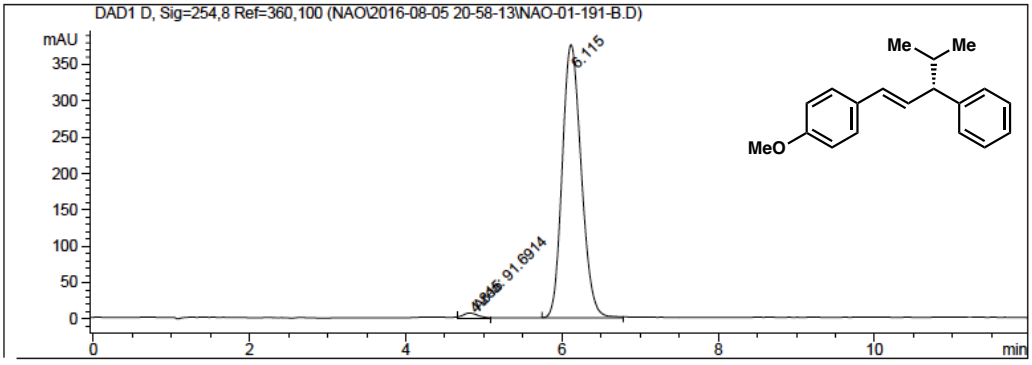

Peak #	RetTime [min]	Type	Width [min]	Area [mAU*s]	Height [mAU]	Area %
1	4.815	MM	0.2214	91.69138	6.90323	1.4194
2	6.115	BB	0.2659	6368.25781	375.46719	98.5806

141j (Figure 3.4): racemic

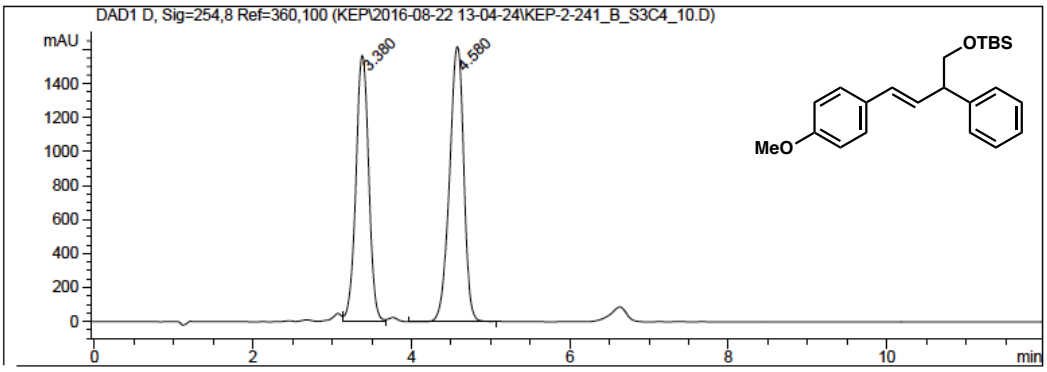

Peak #	RetTime [min]	Type	Width [min]	Area [mAU*s]	Height [mAU]	Area %
1	3.380	VV	0.1763	1.77440e4	1565.27930	46.6268
2	4.580	VB	0.1945	2.03113e4	1617.50305	53.3732

141j (Figure 3.4): enantioenriched, 98% ee

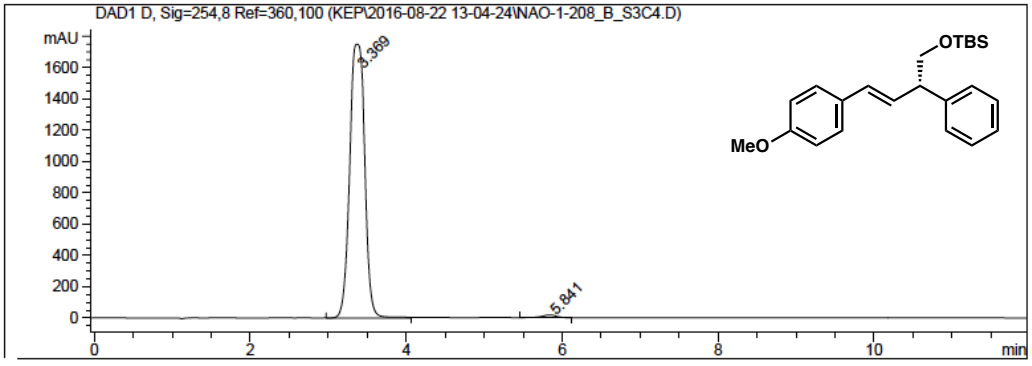

Peak #	RetTime [min]	Type	Width [min]	Area [mAU*s]	Height [mAU]	Area %
1	3.369	VV	0.2126	2.34730e4	1748.39075	98.8511
2	5.841	BV	0.2029	272.82288	19.07364	1.1489

141k (Figure 3.4): racemic

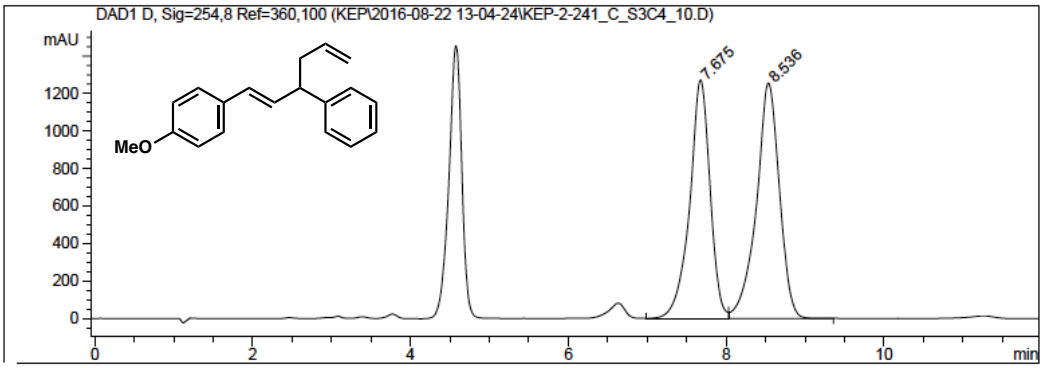

Peak #	RetTime [min]	Type	Width [min]	Area [mAU*s]	Height [mAU]	Area %
1	7.675	VV	0.2662	2.29359e4	1273.26990	47.2708
2	8.536	VB	0.3014	2.55844e4	1257.12512	52.7292

141k (Figure 3.4): enantioenriched, 96% ee

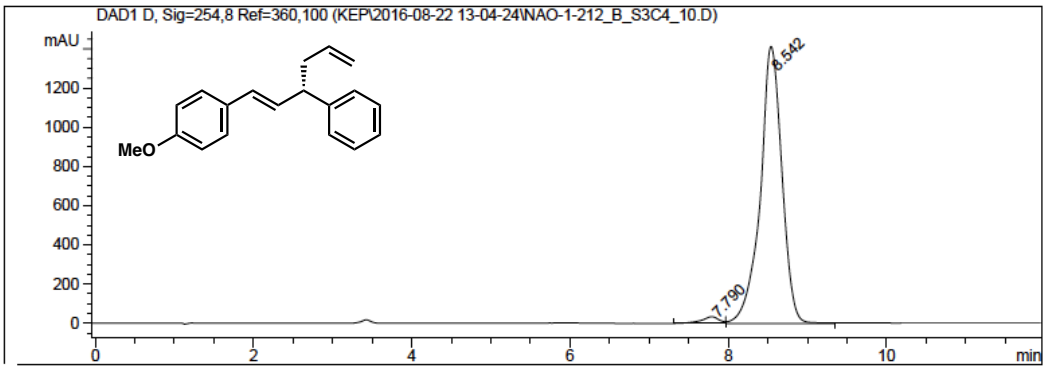

Peak #	RetTime [min]	Type	Width [min]	Area [mAU*s]	Height [mAU]	Area %
1	7.790	BV	0.2268	537.98590	34.33280	1.9596
2	8.542	VB	0.2824	2.69158e4	1411.98352	98.0404

141l (Figure 3.4): racemic

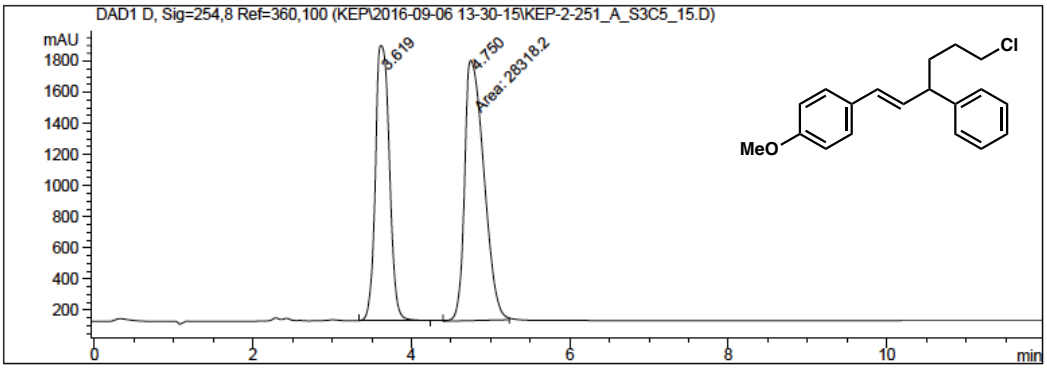

Peak #	RetTime [min]	Type	Width [min]	Area [mAU*s]	Height [mAU]	Area %
1	3.619	BV	0.1967	2.19414e4	1769.60486	43.6562
2	4.750	MM	0.2819	2.83182e4	1673.98267	56.3438

141l (Figure 3.4): enantioenriched, 93% ee

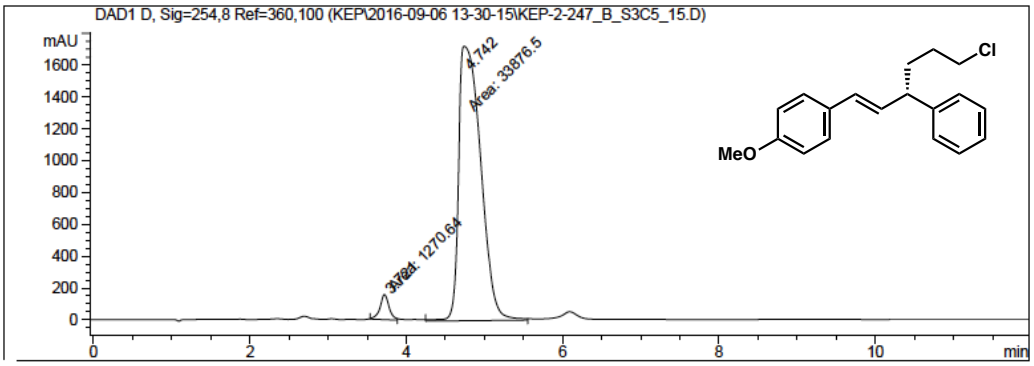

Peak #	RetTime [min]	Type	Width [min]	Area [mAU*s]	Height [mAU]	Area %
1	3.721	MM	0.1339	1270.64075	158.21689	3.6152
2	4.742	MM	0.3274	3.38765e4	1724.49841	96.3848

146 (Scheme 3.2): racemic

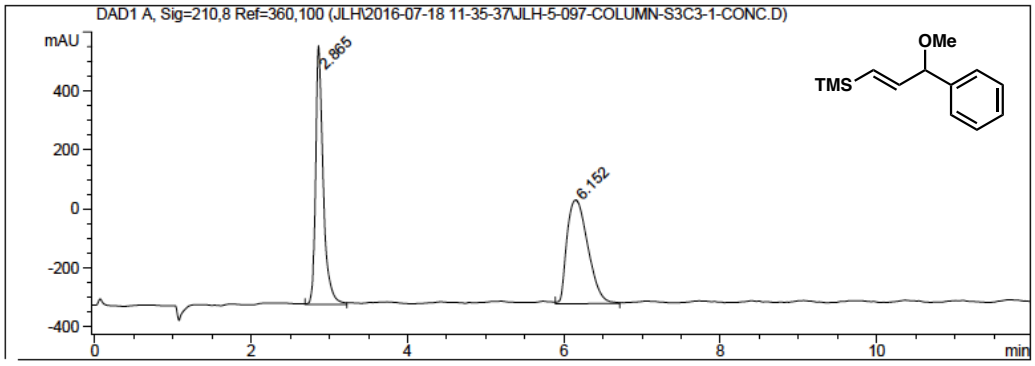

Peak #	RetTime [min]	Type	Width [min]	Area [mAU*s]	Height [mAU]	Area %
1	2.865	VV	0.1036	5942.20703	870.57599	47.5931
2	6.152	VV	0.2969	6543.22803	351.95050	52.4069

146 (Scheme 3.2): enantioenriched, 91% ee

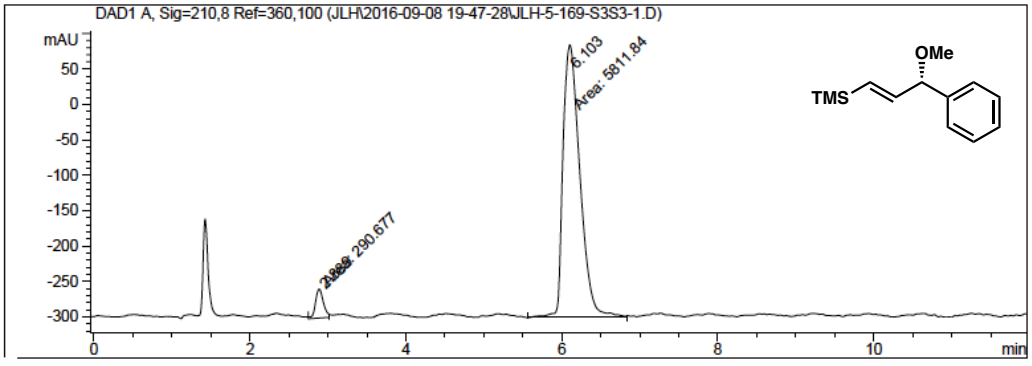

Peak #	RetTime [min]	Type	Width [min]	Area [mAU*s]	Height [mAU]	Area %
1	2.889	MM	0.1180	290.67731	41.05857	4.7632
2	6.103	MM	0.2515	5811.83789	385.08493	95.2368

3.7 REFERENCES

(1) Jana, R.; Pathak, T. P.; Sigman, M. S. *Chem. Rev.* **2011**, *111*, 1417.

(2) Hu, X. *Chem. Sci.* **2011**, *2*, 1867.

(3) Tasker, S. Z.; Standley, E. A.; Jamison, T. F. *Nature* **2014**, *509*, 299.

(4) Ananikov, V. P. *ACS Catal.* **2015**, *5*, 1964.

(5) Netherton, M. R.; Fu, G. C. *Adv. Synth. Catal.* **2004**, *346*, 1525.

(6) Park, K.; Yuan, K.; Scott, W. J. *J. Org. Chem.* **1993**, *58*, 4866.

(7) Devasagayaraj, A.; Stüdemann, T.; Knochel, P. *Angew. Chem. Int. Ed.* **1996**, *34*, 2723.

(8) Giovannini, R.; Stüdemann, T.; Dussin, G.; Knochel, P. *Angew. Chem. Int. Ed.* **1998**, *37*, 2387.

(9) Giovannini, R.; Knochel, P. *J. Am. Chem. Soc.* **1998**, *120*, 11186.

(10) Zhou, J.; Fu, G. C. *J. Am. Chem. Soc.* **2003**, *125*, 14726.

(11) Terao, J.; Todo, H.; Watanabe, H.; Ikumi, A.; Kambe, N. *Angew. Chem. Int. Ed.* **2004**, *43*, 6180.

(12) Fischer, C.; Fu, G. C. *J. Am. Chem. Soc.* **2005**, *127*, 4594.

(13) Arp, F. O.; Fu, G. C. *J. Am. Chem. Soc.* **2005**, *127*, 10482.

(14) Terao, J.; Watanabe, H.; Ikumi, A.; Kuniyasu, H.; Kambe, N. *J. Am. Chem. Soc.* **2002**, *124*, 4222.

(15) Terao, J.; Ikumi, A.; Kuniyasu, H.; Kambe, N. *J. Am. Chem. Soc.* **2003**, *125*, 5646.

(16) Vechorkin, O.; Hu, X. *Angew. Chem. Int. Ed.* **2009**, *48*, 2937.

(17) Vechorkin, O.; Proust, V.; Hu, X. *J. Am. Chem. Soc.* **2009**, *131*, 9756.

(18) Lou, S.; Fu, G. C. *J. Am. Chem. Soc.* **2010**, *132*, 1264.

(19) Zhou, J.; Fu, G. C. *J. Am. Chem. Soc.* **2004**, *126*, 1340.

(20) González-Bobes, F.; Fu, G. C. *J. Am. Chem. Soc.* **2006**, *128*, 5360.

(21) Saito, B.; Fu, G. C. *J. Am. Chem. Soc.* **2007**, *129*, 9602.

(22) Saito, B.; Fu, G. C. *J. Am. Chem. Soc.* **2008**, *130*, 6694.

(23) Lundin, P. M.; Fu, G. C. *J. Am. Chem. Soc.* **2010**, *132*, 11027.

(24) Durandetti, M.; Gosmini, C.; Périchon, J. *Tetrahedron* **2007**, *63*, 1146.

(25) Everson, D. A.; Shrestha, R.; Weix, D. J. *J. Am. Chem. Soc.* **2010**, *132*, 920.

(26) Yu, X.; Yang, T.; Wang, S.; Xu, H.; Gong, H. *Org. Lett.* **2011**, *13*, 2138.

(27) Everson, D. A.; Weix, D. J. *J. Org. Chem.* **2014**, *79*, 4793.

(28) Knappke, C. E. I.; Grupe, S.; Gärtner, D.; Corpet, M.; Gosmini, C.; Jacobi von Wangelin, A. *Chem. Eur. J.* **2014**, *20*, 6828.

(29) Moragas, T.; Correa, A.; Martin, R. *Chem. Eur. J.* **2014**, *20*, 8242.

(30) Weix, D. J. *Acc. Chem. Res.* **2015**, *48*, 1767.

(31) Gu, J.; Wang, X.; Xue, W.; Gong, H. *Org. Chem. Front.* **2015**, *2*, 1411.

(32) Wang, X.; Dai, Y.; Gong, H. *Top. Curr. Chem.* **2016**, *374*, 43.

(33) Tellis, J. C.; Primer, D. N.; Molander, G. A. *Science* **2014**, *345*, 433.

(34) Zuo, Z.; Ahneman, D. T.; Chu, L.; Terrett, J. A.; Doyle, A. G.; MacMillan, D. W. C. *Science* **2014**, *345*, 437.

(35) Noble, A.; McCarver, S. J.; MacMillan, D. W. C. *J. Am. Chem. Soc.* **2015**, *137*, 624.

(36) Primer, D. N.; Karakaya, I.; Tellis, J. C.; Molander, G. A. *J. Am. Chem. Soc.* **2015**, *137*, 2195.

(37) Jouffroy, M.; Primer, D. N.; Molander, G. A. *J. Am. Chem. Soc.* **2016**, *138*, 475.

(38) Joe, C. L.; Doyle, A. G. *Angew. Chem. Int. Ed.* **2016**, *55*, 4040.

(39) Zuo, Z.; Cong, H.; Li, W.; Choi, J.; Fu, G. C.; MacMillan, D. W. C. *J. Am. Chem. Soc.* **2016**, *138*, 1832.

(40) Cavalcanti, L. N.; Molander, G. A. *Top. Curr. Chem.* **2016**, *374*, 39.

(41) Swift, E. C.; Jarvo, E. R. *Tetrahedron* **2013**, *69*, 5799.

(42) Cherney, A. H.; Kadunce, N. T.; Reisman, S. E. *Chem. Rev.* **2015**, *115*, 9587.

(43) Cherney, A. H.; Kadunce, N. T.; Reisman, S. E. *J. Am. Chem. Soc.* **2013**, *135*, 7442.

(44) Cherney, A. H.; Reisman, S. E. *J. Am. Chem. Soc.* **2014**, *136*, 14365.

(45) Hofstra, J. L.; Cherney, A. H.; Ordner, C. M.; Reisman, S. E. *J. Am. Chem. Soc.* **2018**, *140*, 139.

(46) Kadunce, N. T.; Reisman, S. E. *J. Am. Chem. Soc.* **2015**, *137*, 10480.

(47) Okada, Keiji.; Okamoto, Kazushige.; Oda, Masaji. *J. Am. Chem. Soc.* **1988**, *110*, 8736.

(48) Okada, K.; Okamoto, K.; Morita, N.; Okubo, K.; Oda, M. *J. Am. Chem. Soc.* **1991**, *113*, 9401.

(49) Konev, M. O.; Jarvo, E. R. *Angew. Chem. Int. Ed.* **2016**, *55*, 11340.

(50) Murarka, S. *Adv. Synth. Catal.* **2018**, *360*, 1735.

(51) Qin, T.; Cornella, J.; Li, C.; Malins, L. R.; Edwards, J. T.; Kawamura, S.; Maxwell, B. D.; Eastgate, M. D.; Baran, P. S. *Science* **2016**, *352*, 801.

(52) Cornella, J.; Edwards, J. T.; Qin, T.; Kawamura, S.; Wang, J.; Pan, C.-M.; Gianatassio, R.; Schmidt, M.; Eastgate, M. D.; Baran, P. S. *J. Am. Chem. Soc.* **2016**, *138*, 2174.

(53) Edwards, J. T.; Merchant, R. R.; McClymont, K. S.; Knouse, K. W.; Qin, T.; Malins, L. R.; Vokits, B.; Shaw, S. A.; Bao, D.-H.; Wei, F.-L.; Zhou, T.; Eastgate, M. D.; Baran, P. S. *Nature* **2017**, *545*, 213.

(54) Smith, J. M.; Qin, T.; Merchant, R. R.; Edwards, J. T.; Malins, L. R.; Liu, Z.; Che, G.; Shen, Z.; Shaw, S. A.; Eastgate, M. D.; Baran, P. S. *Angew. Chem. Int. Ed.* **2017**, *56*, 11906.

(55) Sandfort, F.; O'Neill, M. J.; Cornella, J.; Wimmer, L.; Baran, P. S. *Angew. Chem. Int. Ed.* **2017**, *56*, 3319.

(56) Chen, T.-G.; Zhang, H.; Mykhailiuk, P. K.; Merchant, R. R.; Smith, C. A.; Qin, T.; Baran, P. S. *Angew. Chem. Int. Ed.* **2019**, *58*, 2454.

(57) deGruyter, J. N.; Malins, L. R.; Wimmer, L.; Clay, K. J.; Lopez-Ogalla, J.; Qin, T.; Cornella, J.; Liu, Z.; Che, G.; Bao, D.; Stevens, J. M.; Qiao, J. X.; Allen, M. P.; Poss, M. A.; Baran, P. S. *Org. Lett.* **2017**, *19*, 6196.

(58) Wang, J.; Qin, T.; Chen, T.-G.; Wimmer, L.; Edwards, J. T.; Cornella, J.; Vokits, B.; Shaw, S. A.; Baran, P. S. *Angew. Chem. Int. Ed.* **2016**, *55*, 9676.

(59) Huihui, K. M. M.; Caputo, J. A.; Melchor, Z.; Olivares, A. M.; Spiewak, A. M.; Johnson, K. A.; DiBenedetto, T. A.; Kim, S.; Ackerman, L. K. G.; Weix, D. J. *J. Am. Chem. Soc.* **2016**, *138*, 5016.

(60) Li, H.; Breen, C. P.; Seo, H.; Jamison, T. F.; Fang, Y.-Q.; Bio, M. M. *Org. Lett.* **2018**, *20*, 1338.

(61) Huang, L.; Olivares, A. M.; Weix, D. J. *Angew. Chem. Int. Ed.* **2017**, *56*, 11901.

(62) Koyanagi, T.; Herath, A.; Chong, A.; Ratnikov, M.; Valiere, A.; Chang, J.; Molteni, V.; Loren, J. *Org. Lett.* **2019**, *21*, 816.

(63) Qin, T.; Malins, L. R.; Edwards, J. T.; Merchant, R. R.; Novak, A. J. E.; Zhong, J. Z.; Mills, R. B.; Yan, M.; Yuan, C.; Eastgate, M. D.; Baran, P. S. *Angew. Chem. Int. Ed.* **2017**, *56*, 260.

(64) Ni, S.; Garrido-Castro, A. F.; Merchant, R. R.; de Gruyter, J. N.; Schmitt, D. C.; Mousseau, J. J.; Gallego, G. M.; Yang, S.; Collins, M. R.; Qiao, J. X.; Yeung, K.-S.; Langley, D. R.; Poss, M. A.; Scola, P. M.; Qin, T.; Baran, P. S. *Angew. Chem. Int. Ed.* **2018**, *57*, 14560.

(65) Lu, X.; Xiao, B.; Liu, L.; Fu, Y. *Chem. Eur. J.* **2016**, *22*, 11161.

(66) Li, C.; Wang, J.; Barton, L. M.; Yu, S.; Tian, M.; Peters, D. S.; Kumar, M.; Yu, A. W.; Johnson, K. A.; Chatterjee, A. K.; Yan, M.; Baran, P. S. *Science* **2017**, *356*, 7355.

(67) Everson, D. A.; Jones, B. A.; Weix, D. J. *J. Am. Chem. Soc.* **2012**, *134*, 6146.

(68) Johnson, K. A.; Biswas, S.; Weix, D. J. *Chem. Eur. J.* **2016**, *22*, 7399.

(69) Poremba, K. E.; Kadunce, N. T.; Suzuki, N.; Cherney, A. H.; Reisman, S. E. *J. Am. Chem. Soc.* **2017**, *139*, 5684.

(70) Biswas, S.; Weix, D. J. *J. Am. Chem. Soc.* **2013**, *135*, 16192.

(71) Broggi, J.; Terme, T.; Vanelle, P. *Angew. Chem. Int. Ed.* **2014**, *53*, 384.

(72) Anka-Lufford, L. L.; Huihui, K. M. M.; Gower, N. J.; Ackerman, L. K. G.; Weix, D. J. *Chem. Eur. J.* **2016**, *22*, 11564.

(73) Takagi, K.; Hayama, N.; Inokawa, S. *Chem. Lett.* **1978**, 1435.

(74) Tsou, T. T.; Kochi, J. K. *J. Org. Chem.* **1980**, *45*, 1930.

(75) Hofstra, J. L.; Cherney, A. H.; Ordner, C. M.; Reisman, S. E. *J. Am. Chem. Soc.* **2018**, *140*, 139.

(76) Beckwith, A. L. J.; Bowry, V. W. *J. Am. Chem. Soc.* **1994**, *116*, 2710.

(77) Halgren, T. A.; Roberts, J. D.; Horner, J. H.; Martinez, F. N.; Tronche, C.; Newcomb, M. *J. Am. Chem. Soc.* **2000**, *122*, 2988.

(78) Gutierrez, O.; Tellis, J. C.; Primer, D. N.; Molander, G. A.; Kozlowski, M. C. *J. Am. Chem. Soc.* **2015**, *137*, 4896.

(79) Still, W. C.; Kahn, M.; Mitra, A. *J. Org. Chem.* **1978**, *43*, 2923.

(80) Evans, D. A.; Downey, C. W.; Hubbs, J. L. *J. Am. Chem. Soc.* **2003**, *125*, 8706.

(81) Bestmann, H. J.; Schmid, G.; Oechsner, H.; Ermann, P. *Chem. Ber.* **1984**, *117*, 1561.

(82) Wasserman, H. H.; Ives, J. L. *J. Org. Chem.* **1985**, *50*, 3573.

(83) Mahesh, M.; Murphy, J. A.; LeStrat, F.; Wessel, H. P. *Beilstein J. Org. Chem.* **2009**, *5*, 1.

(84) Müller, D.; Alexakis, A. *Org. Lett.* **2012**, *14*, 1842.

(85) Qian, M.; Huang, Z.; Negishi, E. *Org. Lett.* **2004**, *6*, 1531.

(86) Kuang, C.; Senboku, H.; Tokuda, M. *Tetrahedron* **2005**, *61*, 637.

(87) Li, D.-R.; Zhang, D.-H.; Sun, C.-Y.; Zhang, J.-W.; Yang, L.; Chen, J.; Liu, B.; Su, C.; Zhou, W.-S.; Lin, G.-Q. *Chem. Eur. J.* **2006**, *12*, 1185.

(88) Brown, H. C.; Larock, R. C.; Gupta, S. K.; Rajagopalan, S.; Bhat, N. G. *J. Org. Chem.* **1989**, *54*, 6079.

(89) Ney, J. E.; Hay, M. B.; Yang, Q.; Wolfe, J. P. *Adv. Synth. Catal.* **2005**, *347*, 1614.

(90) Wu, H.-B.; Ma, X.-T.; Tian, S.-K. *Chem. Commun.* **2014**, *50*, 219.

(91) Ye, J.; Zhao, J.; Xu, J.; Mao, Y.; Zhang, Y. J. *Chem. Commun.* **2013**, *49*, 9761.

(92) Srinivas, H. D.; Zhou, Q.; Watson, M. P. *Org. Lett.* **2014**, *16*, 3596.